CHALMERS
UNIVERSITY OF TECHNOLOGY

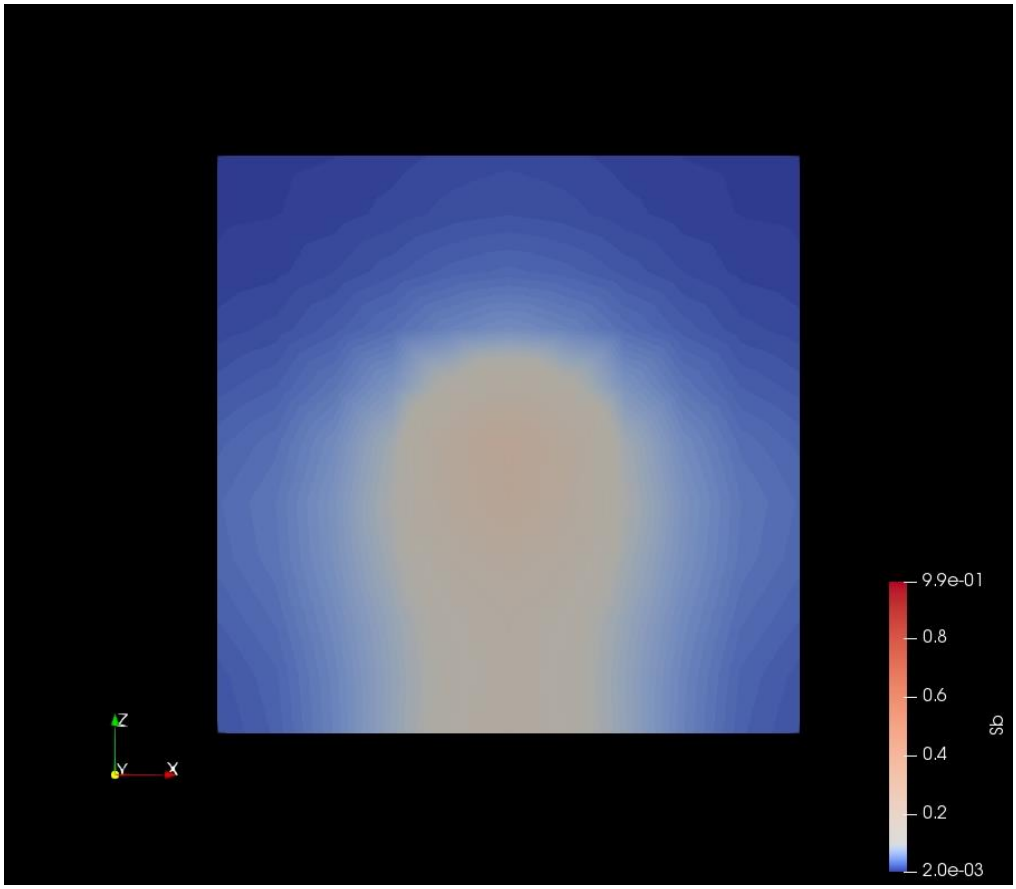

Multiphase Fluid Handling in Absorbing Materials

Simulating Porous Media Using OpenFoam

Master's thesis in Applied Mechanics

Dongyu Liu

Department of Mechanics and Maritime Sciences
CHALMERS UNIVERSITY OF TECHNOLOGY
Gothenburg, Sweden 2018

MASTER'S THESIS IN APPLIED MECHANICS

Multiphase Fluid Handling in Absorbing Materials

Simulating Porous Media Using OpenFoam

Dongyu Liu

Department of Mechanics and Maritime Sciences
Division of Fluid Mechanics

CHALMERS UNIVERSITY OF TECHNOLOGY
Göteborg, Sweden 2018

Multiphase Fluid Handling in Absorbing Materials
Simulating Porous Media Using OpenFoam
Dongyu Liu

Master's Thesis [Status]
Department of Mechanics and Maritime Sciences
Division of Fluid Mechanics
Chalmers University of Technology
SE-412 96 Göteborg
Sweden
Telephone: + 46 (0)31-772 1000

Cover:
When the wound is vertical, there will be more fluid at the direction gravity acts.

Name of the printers / Department of Mechanics and Maritime Sciences
Göteborg, Sweden 2018-09-01

Multiphase Fluid Handling in Absorbing Materials
Simulating Porous Media Using OpenFoam
Master's thesis in Applied Mechanics
Dongyu Liu
Department of Mechanics and Maritime Sciences
Division of Fluid Mechanics
Chalmers University of Technology

Abstract

Absorption takes place in many fields and applications, for instance, water absorption of soil and wicking of textiles. Computational models have been developed for many applications such as groundwater absorption and absorption of absorbents. The aim of this thesis is to establish computational models for absorbing materials and study absorption through modelling and experiments. The understanding of absorption is based on theories that two-phase fluids interact with a porous medium, which absorbing materials are regarded as. The modelling of this phenomenon can deepen the understanding and aid in further development of absorbing materials.

The experimental data can be understood by the help of modelling and the data can validate the model. In CFD simulation, the parameters of porous media including porosity, permeability and air entry pressure are included in the equations, stressing the importance of the experiments. There are existing capillary pressure models empirically developed in order to include the capillary pressure inside the porous media, and relative permeability models developed to introduce permeability in the porous media. OpenFoam is the open-source software that is used as a main simulation tool to model absorption in the work.

Absorption is modelled in macro scale which represents the general performances of absorbing materials. The initial case proved that the capillary forces were the driving force for the fluid flow inside the material. To further investigate absorbing materials, the effects of gravity and anisotropy were modelled. The capillary pressure models and relative permeability models were assessed to examine their performances in order to select corresponding models or modify the models based on selected models in different situations. Since boundary conditions are vital to simulations, a study of boundary conditions is done depending on different occasions of absorption in materials.

The permeability measurement and porosity measurement were performed to provide the model which models capillary forces with some input data. The fluid transport in experiments and simulations were compared. The fluid fronts and the saturation distributions show similar behaviours except the time which is longer in the simulations. Further research and development should be performed to improve the model.

Key words: porous medium, CFD, OpenFoam, Darcy’s law, capillary pressure model, relative permeability model, permeability, porosity

Preface

This study has been carried out from February 2018 to September 2018, aiming at modelling absorbing materials in a simplified way by using OpenFoam and performing corresponding experiments. This work was performed at Alten Sweden AB and Chalmers University of Technology. This project led to a considerable future of further development in absorbing materials.

I would like to thank my main supervisors Mikael Almquist and Océane Lançon to make this project possible. Many thanks as well to Daniel Grönberg at Alten for his help with simulations and his guidance on how to think and solve CFD problems. I also really appreciate the kind and constant support of Mattias Bryntesson at Alten, especially theoretical part of the project. I would like to thank Océane Lançon as my supervisor, for providing valuable information about experiments and reality to make this project valuable. Finally, I would like to give great thanks to my examiner Srdjan Sasic and my supervisor Henrik Ström at Chalmers, providing crucial help at all time in the course of thesis.

Göteborg 2018-09-01

Dongyu Liu

Contents

Notations

γ_{SV}	Interfacial tension between solid surface and vapor surface
γ_{SL}	Interfacial tension between solid surface and liquid surface
γ_{LV}	Interfacial tension between liquid surface and vapor surface
γ_{aL}	Interfacial tension between air surface and liquid surface
S_i	Saturation of phase i
$S_{i,eff}$	Effective saturation of phase i
$k_{ri}(S_i)$	Relative permeability as a function of saturation
$p_c(S_i)$	Capillary pressure as a function of saturation

1 Introduction

1.1 Background

Dressings have been applied to wounds for a long time to slow down bleeding, or even stop it. As society and technologies have developed, the use of wound dressings has been broadened and their performance has improved in healing, reducing pain, stopping bleeding and protecting wound from further infection. One of the most important functions of wound dressings is to absorb blood and other body fluids. The understanding of absorption in wound dressings is of importance when developing wound care products.

The word absorption has numerous meanings, all related to "something taken up by something else". It could be a gas taken by a liquid, a liquid taken up by a porous material, a dissolved drug taken up through human skin or by a human internal organ, sound or other mechanical energy taken up by solid material, to mention a few. In this thesis, the definition of absorption of a liquid (blood, plasma, water or similar) in a porous medium (a wound dressing, a dipper, a dishcloth) is narrowed down to water absorption in wound dressings.

There are several man-made absorbing materials, where absorption is driven by capillary forces, such as dishcloths absorbing water, diapers absorbing urine et cetera. Results from study of absorbing materials can not only be applied to wound dressings but help investigation of other man-made absorbing materials. In addition to man-made absorbing materials, nature also provides a lot of examples of absorption. Trees are able to absorb water from ground and transport water to leaves. Soil and some rocks have absorption as well driven by capillary forces. Although different materials behave differently, it shows the many areas that could be significant to investigate regarding capillary forces. The scope of present thesis is to study capillary forces in man-made materials, for instance, textile, foam and tissues through computational fluid dynamics (CFD) simulation and relevant experiments.

One of the important phenomena in absorbing materials is capillary force. Capillary force theory has been studied for many years in soil, plants, capillary tubes, oil industry, rocks, and in other absorbing materials in diverse fields. This thesis is focusing on the capillary forces as driving forces in absorbing materials that play an important role in daily life. Those man-made absorbing materials are usually composed of several layers with various materials. Each layer performs differently, meaning that there is a complex situation that has to be considered. The boundary conditions of each layer need to be considered carefully. Such multilayer dressings are beyond the scope of this thesis.

The absorbing materials are usually not uniform, homogeneous, mostly made of textiles and fibres. Some absorbing materials swell when put in contact with a liquid. Some have large capacity to absorb liquids, some not. To understand why it differs a lot, it is necessary to know the structure of absorbing material. The way of thinking is to regard absorbing materials as porous media, the theories of which can be applied in

absorbing materials. Porous media are materials containing pores. The pores can form a continuous pore space that span the material, or is can be dead-end pores or totally isolated pores or clusters of pores. Depending on the properties of the pore structure, its absorptive behavior will vary.

The pores of absorbing materials usually are of different sizes and shapes. Many pore structures have a random pore size distribution that can be described statistically. The nature of fluid absorption is replacement of one fluid by another fluid, in the case of medical dressings, typically that air is replaced by blood. The pore structure, including pore size, distribution of pore spaces, pore surface properties and contact angle, affects how materials absorb liquid and the process of imbibition. The liquid, usually blood, complex mixture whose different components influence the absorption process. Since blood is a complex mixture, water has been used as model liquid for both experiments and simulations in this work, because of its well-defined properties. Other model fluids could be introduced in the future.

CFD is increasingly applied to various fields, mechanics, vehicles, batteries, and life science. CFD aims to analyse fluid problems by using numerical analysis. CFD in life science is still developing, because of the complexity of many systems in life science. Plenty of researchers are working on life science to understand and improve it. CFD is an efficient way to develop and help understanding the theories. Moreover, CFD can be used to reduce materials consumption by simulating different conditions instead of doing experiments. It also can save time compared to experiments, which delays progress and costs money.

The porous media can be simulated in micro scale and macro scale. The geometric representation of the structure in micro scale can be simulated, but it is complex and would demand a lot of computational resources. Instead of modelling it in a complex way, this thesis focuses on simplified way in macro scale.

Figure 1 one of example of absorbing materials used in wound care

While there are some methods applied in porous media, they need to be tested and adjusted to be applied to absorbing materials in this work. The simulation methods will also be investigated to seek for optimizing solutions.

There is some alternative software to simulate it, for example, Ansys, Flow-3D. Since commercial software is expensive on licenses and has some limitations of developing further, an open-source software - OpenFoam is used, which might have the disadvantage to be less user-friendly than commercial software, but is suitable in research to develop models.

OpenFoam is an open-source software that is used as a main simulation tool to model absorption in this work. There is a code package for porous media containing fundamental solvers and libraries. Compared to Ansys Fluent, a commercial software, the capabilities to modify the models are larger in OpenFoam. ANSA, computational aided engineering (CAE) software, is a pre-processor that was used for geometry construction and mesh generation to improve the efficiency.

1.2 Objectives

The objective is to increase the understanding of absorbing materials using CFD. In the future, computational models could evaluate and facilitate the development of new high performance medical dressings.

Although there are many interesting perspectives that one can look into in simulations, considering limited time, the scope of thesis is to study one layer of material, ignoring the effect of swelling. The fluids modeled are air and water to simplify the problem. The input values of absorbing materials in the models are based on literature data except verification which used data from experiments. Both isotropy and anisotropy are to be considered. The former gives relative short time of calculation, and the latter is likely to be more realistic because the manufacture of porous sheets (woven, non-woven or foam) may yield a pore structure that is different in different directions. Based on results of experiments, corresponding simulations shall be performed.

Experiments should be simplified and clear about the aims which have been illustrated in this chapter.

Evaporation shall be considered as mass loss at the surface of materials. The rate of mass loss shall be modelled separately.

The main objectives are:

1. Assessing the model of absorbing materials in OpenFoam with
    a. Different capillary pressure models
    b. Different relative permeability models
    c. Different boundary conditions
    d. Different geometries corresponding to the physical samples of materials
    e. The effects of gravity for different orientations of materials

    f. Anisotropic materials versus isotropic materials
2. Performing experiments to provide parameters for the models.
    a. Porosity measurement
    b. Permeability measurement in three different orientations
3. Establishing parameter values for capillary pressure model and relative permeability model
4. Comparing CFD simulation and experiments, validating the method.
5. Implementing evaporation in the model to make it more realistic.

2 Theory

Porous materials contain relatively small spaces called pores. Pores are free of solid. The pore structure of porous materials determines the properties of porous materials, porosity and pore size, etc. Anisotropy is one of the characteristics of most of porous materials, which means that the properties are different in different orientations, due to not uniform distribution of pore spaces.

Pore size is also a crucial feature of porous materials, which could affect permeability, porosity and structure of porous media. Nevertheless, it is difficult to determine pore size because of variations of pore structure, surface properties of solid material and interconnection of pores.

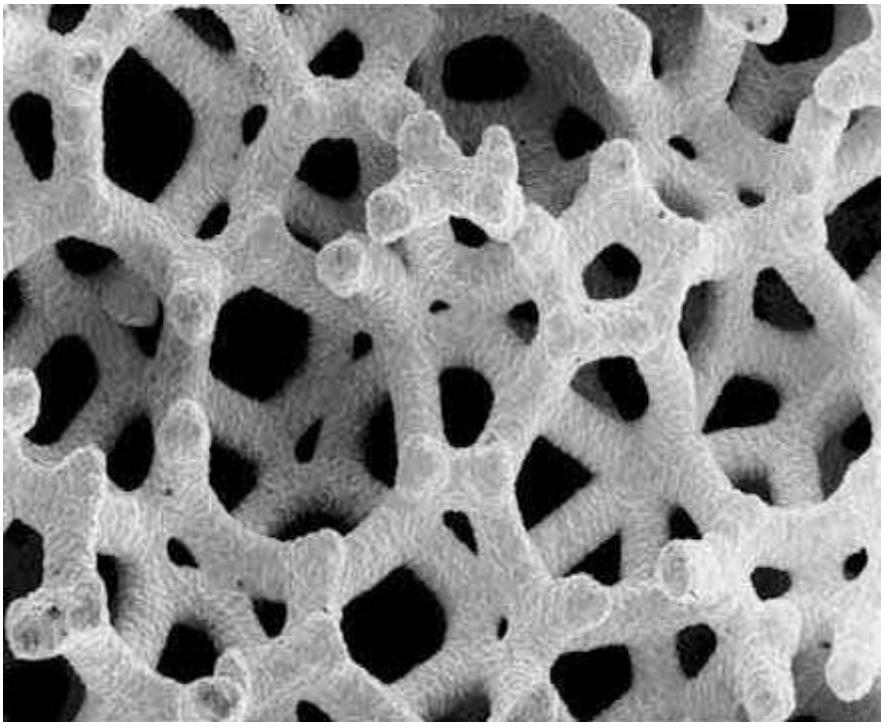

Figure 2 The structure of a porous medium in micro scale

Pore size distribution can be approximated by mercury porosimetry or image analysis of pore structure to get pore size distribution from microscopy. There are many ways to define pore size. One of used radius of pore size is the hydraulic radius, a measure of pore throats. Pore throats are the channels connecting the part where most of the porosity resides (Sahimi, 2011). Having been introduced in pore scale, porous media will be described in visible (macro) scale instead.

Liquid enters into a pore space. The air is replaced by liquid, which increases liquid-solid interfacial area, called wetting. Once the material is wetted, capillary forces can develop, further saturating the material with liquid, the process called wicking. Wicking and wetting happen inside porous medium, leading to absorption. Wicking appears after wetting, which indicates that wetting is the necessary condition of wicking. Therefore, various fluids are able to penetrate the effective voids in porous materials.

The wettability, defined as the interaction between liquid phase and porous materials, plays an important role in the physical phenomenon. (Kissa, 1996)

2.1 Capillary rise in a single capillary

The Young-Dupré equation (Kissa, 1996) describes the equilibrium of solid-liquid boundary using contact angle of liquid and solid phase.

$$\gamma_{SV} - \gamma_{SL} = \gamma_{LV} cos\theta \tag{2-1}$$

Where γ represents an interfacial tension, which describes the work which need to be expended to increase the interface between two adjacent phases which are not mixed (Ref); the subscripts S, L, and V denote solid, liquid and vapor surfaces respectively, θ is contact angle. $\gamma_{LV} cos\theta$ Is called adhesion tension or specific wettability. The contact angle is described as the angle between solid-liquid interface and liquid-air interface shown below. γ_{LV} can also be called the surface tension of the liquid-air interface.

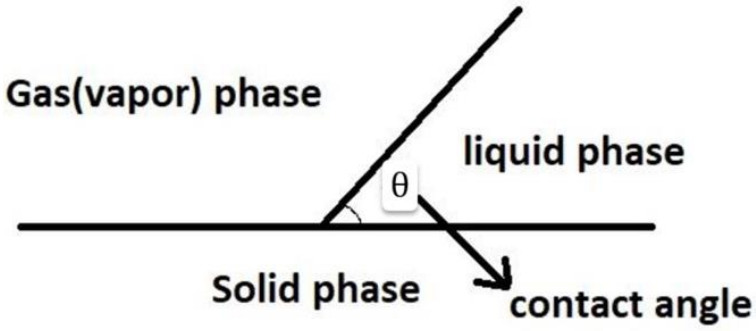

Figure 3 Contact angle

The surface tension that is one type of interfacial tension between liquid and gas is introduced to explain capillary pressure more specifically. The interface among fluids and solid phase is the essential to obtain the relationship between three phases. In a thin tube, the surface tension is caused by the molecules of the wetting fluid attracted by tube wall, resulting in meniscus (curved interface) between liquid and air. Young-Laplace equation is derived from the Young-Dupré equation to calculate the pressure difference between the air and liquid phases.

$$\Delta p = p_c = p_a - p_L = \frac{2\gamma_{aL} cos\theta}{r_c} \tag{2-2}$$

Where r_c is the thin tube radius, p_a and p_L are the pressure of air and liquid phase (at the interface) respectively.

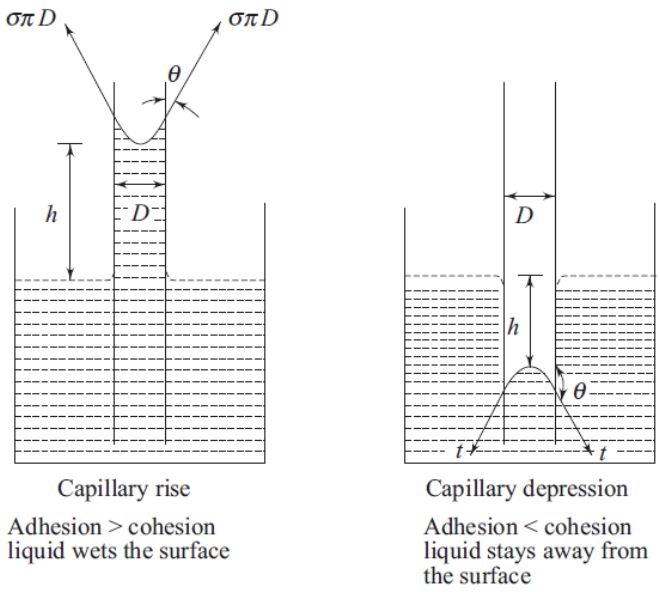

Figure 4 Capillary rise and depression in a tube

Hence, the capillary force that causes absorption can be defined that a liquid meniscus between two lyophilic (dispersed phase with a high affinity for the continuous phase) solid surfaces causes an attractive force (Butt, H. J., & Kappl, M, 2009).

From Young-Laplace equation, the height of capillary rise, h in the figure, can be calculated as

$$\rho g h = \Delta p \tag{2-3}$$

2.2 Continuous model of porous media

Porous media can be regarded as many thin tubes inside the solid so that those basic principles of capillary pressure in a single tube can be applied in porous medium. In the following, the properties of porous media described are averages of corresponding microscopic quantities, for example, the porosity and permeability, on the so-called Darcy scale or macro scale (visible scale). Due to large computational power and time required for micro scale (pore scale), the governing equations and modelling in this work are based on Darcy scale.

The volume fraction θ_i of phase a and phase b is defined below. Phase a and phase b are air and water respectively in the following simulations and experiments. (Dullien, 1992)

$$\theta_i = \frac{|V_i|}{|V|} \tag{2-4}$$

Where V is the bulk volume of the porous medium, V_i is the volume of phase $\boldsymbol{i}$ (a or b) in the porous medium.

The porosity is used to describe the pore space, expressed by the sum of the volume fractions of the two fluids.

$$\varepsilon = \theta_a + \theta_b \tag{2-5}$$

The saturation of phase a and phase b is determined as

$$S_i = \frac{\theta_i}{\varepsilon} \tag{2-6}$$

For practical reason, the effective (normalized) saturation is defined as:

$$S_{i,eff} = \frac{S_i - S_i^{min}}{S_i^{max} - S_i^{min}} \tag{2-7}$$

Where S_i^{max} and S_i^{min} are the maximum and minimum saturation of phase $\boldsymbol{i}$ (a or b) in the porous media.

Permeability K, one of core parameters of porous media, describes the ability of porous media to allow fluids to pass through.

$$\boldsymbol{K} = -\frac{\boldsymbol{U}_i * \mu_i}{\nabla p_i} \tag{2-8}$$

It depends on the geometry of porous media, pore structures and distributions. Capillary pressure is the difference between the pressures of two phases at the interface. The expression is shown below:

$$p_c = p_a - p_b \tag{2-9}$$

Where p_c is capillary pressure, p_a and p_b are the pressure of phase a and phase b respectively.

2.3 Governing equations

Derived from mass conservation, the equation of saturation is described below:

$$\varepsilon \frac{\partial S_i}{\partial t} + \nabla \cdot \boldsymbol{U}_i = q_i \tag{2-10}$$

Where $\boldsymbol{U}_i$ is superficial velocity that describes flow velocity is calculated for given phase in a given cross sectional area, q_i is source term for injection or extraction. (Szymkiewicz, A., & SpringerLink (e-book collection)., 2013)
Darcy law, determined by Darcy through experiments, describes how fluid flows through porous media. The superficial velocity can be calculated from Darcy's law. According to Navier-Stokes equations, the momentum conservation equation can be represented as the equation below. Due to the assumptions that only capillary forces and gravity account, laminar incompressible flow phase i can be expressed in a simplified equation- Poiseuille equation. The superficial fluid velocity of phase i can be calculated as:

$$\boldsymbol{U}_i = -\frac{\boldsymbol{K}}{\mu_i}(\nabla p_i - \rho_i \boldsymbol{g}) \tag{2-11}$$

Where $\boldsymbol{K}$ is permeability tensor, p_i is fluid pressure, ρ_i is fluid density, **g** is gravity vector, μ_i is dynamic viscosity. It can be seen from the equation (2.10) when capillary

forces are equal to gravity, the velocity will be zero, indicating that the capillary-gravity equilibrium is reached.

In addition, two-phase equations are discussed in this work which also focuses on two phases. Washburn's equation is most commonly applied to describe flow from saturated reservoirs into textiles driven by capillary forces, which also regards porous media as a lot of parallel tubes. (LANDERYOU, 2005)The permeability would be described as the saturated permeability in Washburn model. Washburn model suggests the geometrical interpretation of capillary radius expressed in the model, which is hard to be defined and obtained. More importantly, Washburn's model is constricted to describe spreading in two or three dimensions without introducing some form of analogy. Due to its characteristics, it is limited to apply. (Landeryou, M., Eames, I., Frampton, A., & Cottenden, A, 2004)

Richard equation is a commonly used equation that can describe partially saturated flow. The equation has been applied for fibrous materials and three-dimensional model. Richard equation only can be used with the increase of saturation instead of draining flows. (Landeryou, M., Eames, I., Frampton, A., & Cottenden, A, 2004)The Richard equation in the form below does not consider gravity and source term,

$$\frac{\partial S_i}{\partial t} = \nabla \cdot [K(S_i)\nabla p\,] \tag{2-12}$$

Richard equation could be a better option in this work. To close unknown terms in equations, two models are required as an input that are relative permeability and capillary pressure. Those two more models are based on features of materials.

2.3.1 Capillary pressure model

The capillary pressure models studied gives the capillary pressure as a function of saturation, an essential part in the model, depending on properties of materials.

$$p_c(S_b) = p_a - p_b \tag{2-13}$$

There are several typical models that are used to describe the capillary pressure. One parameter, the air entry pressure, a characteristic of a porous medium is defined as follows when the porous medium is fully saturated by fluids (water in this work), air might invade the water-filled pores, provided the air pressure exceeds the water pressure by a certain value. That value is the air entry pressure or bubbling pressure.

Linear model is a simplified model (Horgue, P., Soulaine, C., Franc, J., Guibert, R., & Debenest, G, 2015). Brooks and Corey model is used for porous media that have a uniform structure and a distinct air entry pressure. Van Genuchten model need to introduce air entry pressure as a parameter in the function. (Szymkiewicz, A., & SpringerLink (e-book collection)., 2013) Those models are explained in the following description. Leverett J-Function predicts capillary pressure depending on the porosity, interfacial tension, mean pore radius, this dimensionless function of saturation defined as J-function (Leverett, 1941). Skjaeveland model introduces a developed correlation

covering primary drainage, imbibition and secondary drainage (Skjaeveland, S.M., Siqveland, L.M., Kjosavik, A., Hammervold Thomas,W.L., Virnovsky, G.A., 2000).

In the simulations, some of them are used. All the parameters mentioned later, including entry pressure, residual saturation and power coefficient, are material specific.

Linear model:

$$p_c = p_{c0} + \left(1 - S_{b,eff}\right) * (p_{cMax} - p_{c0}) \tag{2-14}$$

Where p_{cMax} is the maximum capillary pressure that depends on materials, p_{c0} is air entry pressure.

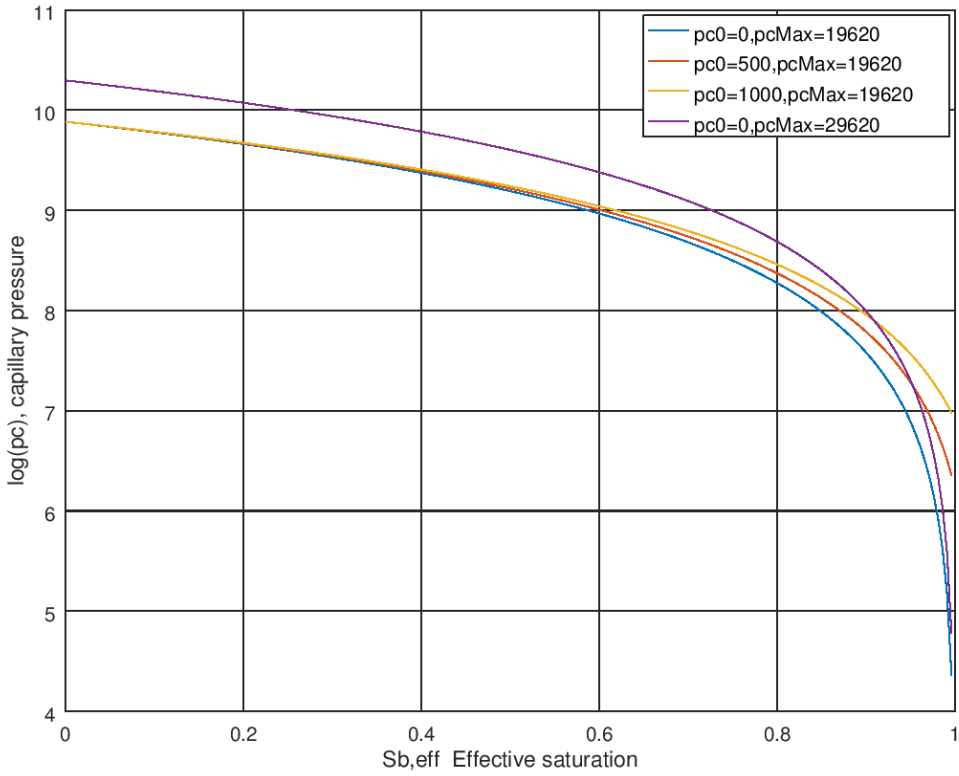

Figure 5 Capillary pressure model - Linear model

It can be seen that higher maximum capillary pressure and higher air entry pressure will result in higher capillary pressure at the same effective saturation of phase b.

Brooks and Corey Model:

$$p_c = p_{c0}(S_{b,eff})^{-1/n_b} \tag{2-15}$$

Where p_{c0} the air entry is pressure and n_b is power coefficient that is related to the pore size distribution, generally the range from 0.2 to 5. Larger power coefficient is typical for uniform pore structure (Szymkiewicz, A., & SpringerLink (e-book collection)., 2013). It can be seen from equation that the capillary pressure tends to

infinity when $S_{b,eff}$ tends to zero (S_b approaches minimum saturation), which should be avoided in the simulations.

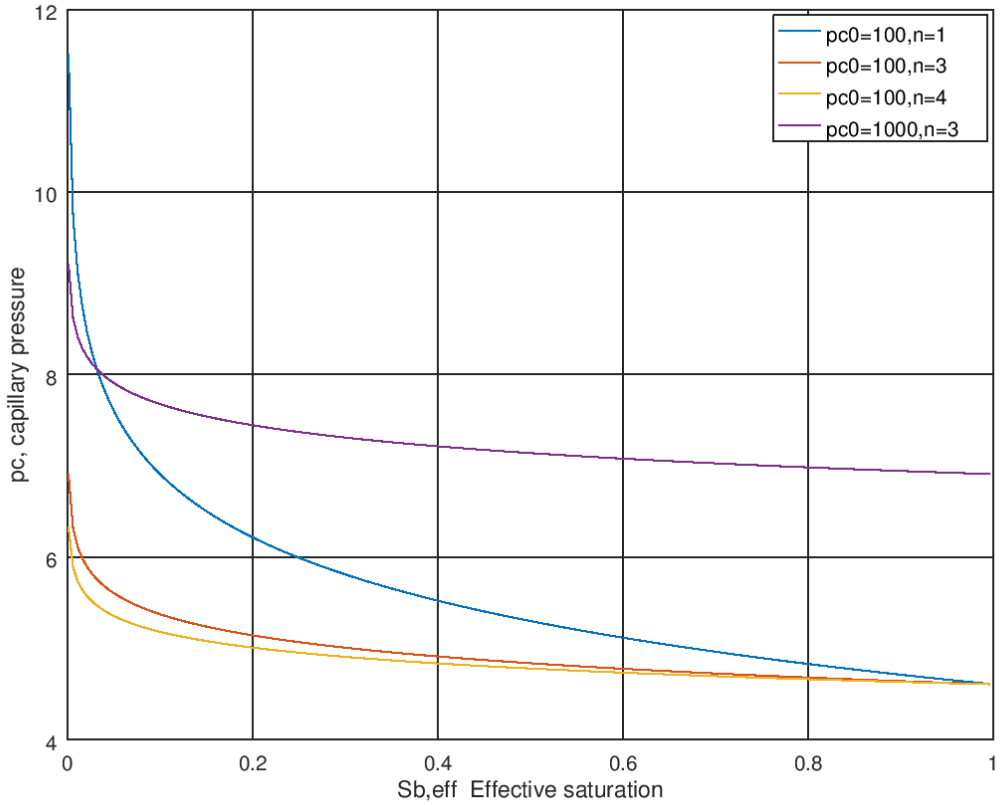

Figure 6 Capillary pressure model - Brooks and Corey model

As it is shown in the graph, higher entry pressure and lower power coefficient n can lead to higher capillary pressure at the same effective saturation of phase b.

Van Genuchten Model:

$$p_c = p_g[(S_{b,eff})^{-1/m} - 1]^{1/n} \quad (2\text{-}16)$$

$$\frac{1}{n} = 1 - m \quad (2\text{-}17)$$

Where p_g is a pressure scaling parameter, whose value is approximately the inflection point at capillary curve. In the simulation, p_{c0} is used to replace p_g to do calculations. The power coefficients n and m are related to pore size distribution. Besides, there is also another way to express the relationship between n and m, $\frac{2}{n} = 1 - m$. It can be seen from equation that the capillary pressure tends to infinity when $S_{b,eff}$ tends to zero (S_b approaches minimum saturation), which should be avoided in the simulations.

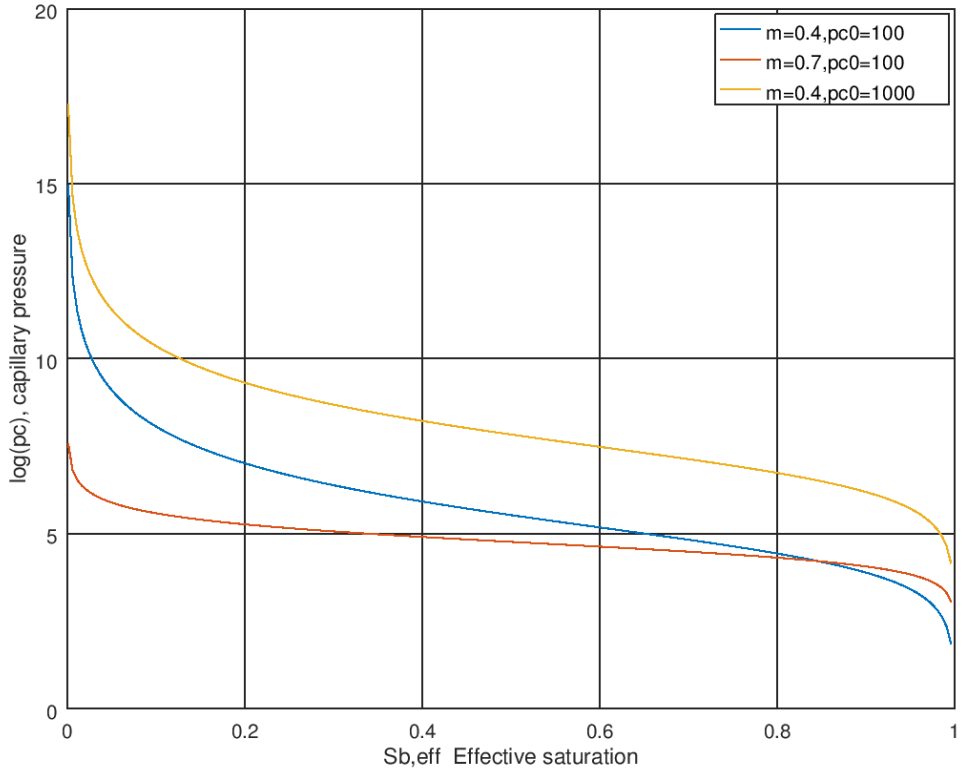

Figure 7 Capillary pressure model - Van Genuchten model

As it is shown in the graph, higher air entry pressure and lower power coefficient n can lead to higher capillary pressure at the same effective saturation of phase *b*.

Other important parameters are investigated in the model that how maximum saturation and minimum saturation of materials will influence the capillary pressure. Brooks and Corey model is taken as an example.

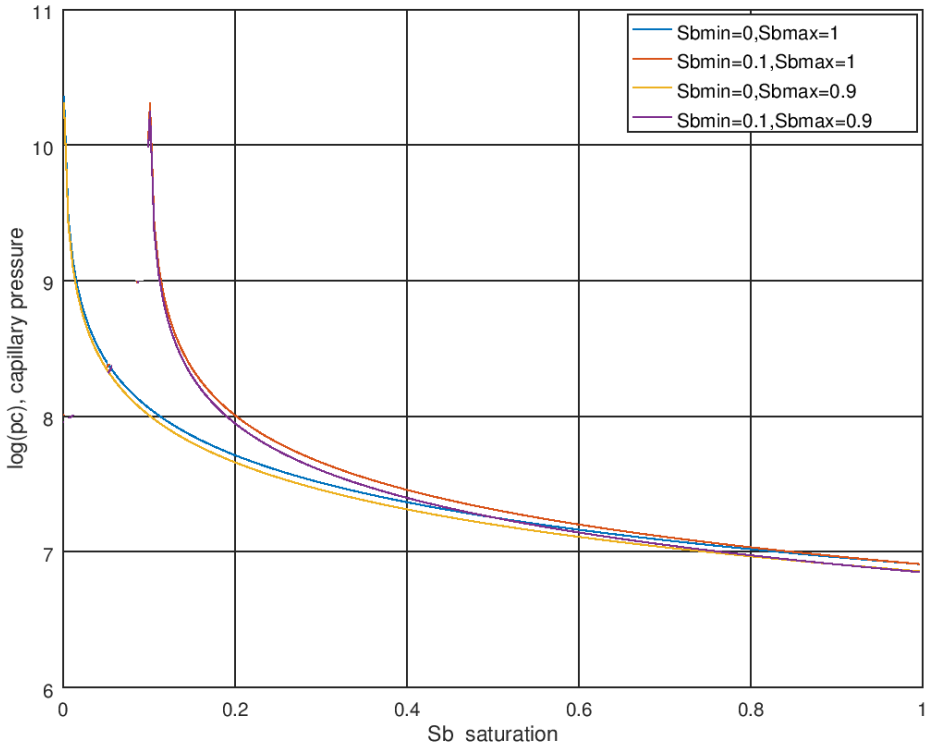

Figure 8 Capillary pressure model affected by minimum and maximum saturation

In this graph, the capillary pressure is not affected explicitly by minimum saturation and maximum saturation of materials with saturation increasing. When it comes to a lower saturation level, the minimum saturation has impact on capillary pressure. The lower minimum saturation it is, the lower capillary pressure it will be.

2.3.2 Relative permeability model

The permeability is one of the important properties of porous media, since it has an impact on fluid transport through porous media.

For multiphase fluids, it is necessary to distinguish intrinsic permeability and relative permeability. The intrinsic permeability is the permeability described as a property of porous media, only depending on the structure of porous media. Relative permeability in the mass conservation equation depends not only on geometry of porous media, but on saturation of phase $\boldsymbol{i}$. The relationship is shown below:

$$K_i(S_i) = K k_{ri}(S_i) \tag{2-18}$$

Where K is intrinsic permeability, $k_{ri}(S_i)$ is the relative permeability that is modelled as a function of saturation.

Relative permeability represents the ability of each fluid to flow with the presence of other fluids in the system. For anisotropic materials, permeability will be different at different orientations. In order not to be confused, only simplified form of

permeability – scalar permeability (meaning same permeability in all directions) will be involved to investigate on relative permeability models.

The models of relative permeability function vary from simple power-type relationship to sophisticated models, including Brooks and Corey model, Van Genuchten model, Brooks-Corey-Burdine model and Van Genuchten-Mualem model. Brooks-Corey-Burdine model and Van Genuchten-Mualem model are typical for sand and clay. Most commonly used models are Brooks and Corey model and Van Genuchten model, which are widely applied to petroleum industry. In those models, two main models are discussed and utilized in the simulations, which are Brooks and Corey model and Van Genuchten Model.

Brooks and Corey Model:

$$k_{ra} = K_{ra,max} * (1 - S_{b,eff})^n \tag{2-19}$$

$$k_{rb} = K_{rb,max} * S_{b.eff}^n \tag{2-20}$$

Where $S_{b,eff}$ is effective saturation of phase b, n is the power coefficient relying on the properties of materials, $K_{ra,max}$ and $K_{rb,max}$ are the maximal relative permeability, set to unity in Figure 9.

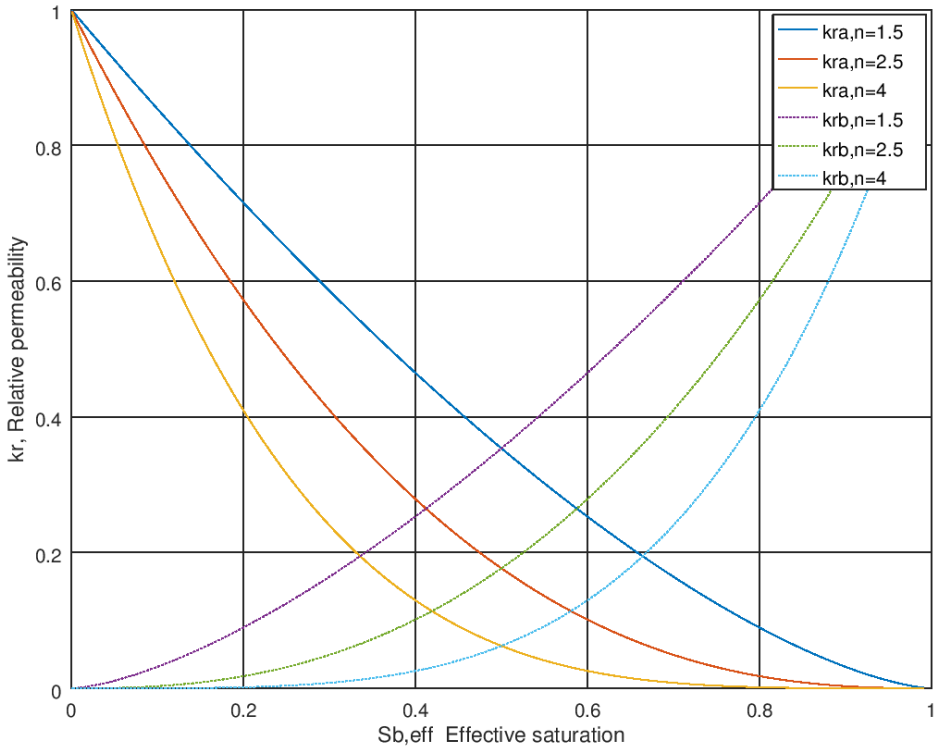

Figure 9 Relative permeability model - Brooks and Corey model

As it is shown in the graph, with the increase of power coefficient n, the relative permeability of phase b goes down at the same effective saturation phase b, vice versa.

Van Genuchten Model:

$$k_{ra} = K_{ra,max} * (1 - S_{b,eff})^{1/2}(1 - (S_{b,eff})^{1/n})^{2n} \quad (2\text{-}21)$$

$$k_{rb} = K_{rb,max} * S_{b.eff}^{1/2}(1 - (1 - S_{b.eff}^{1/n})^{n})^{2} \quad (2\text{-}22)$$

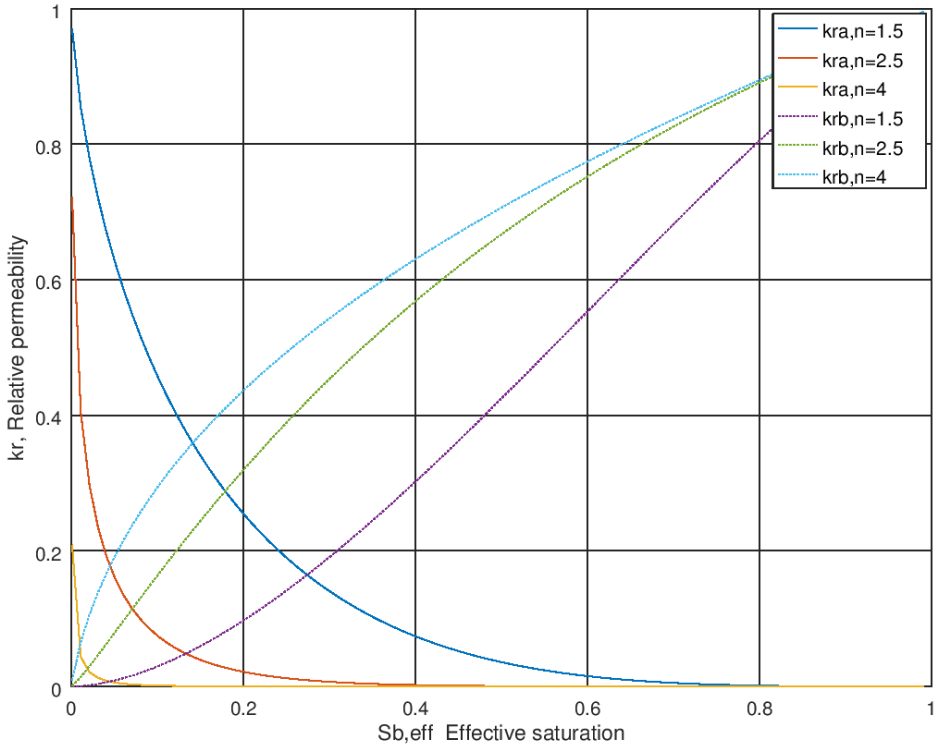

Figure 10 Relative permeability model - Van Genuchten model

It is indicated in the graph that the increase of power coefficient n leads to higher relative permeability of phase *b* at the same effective saturation, which is contrary to Brooks and Corey model.

Both capillary pressure model and relative permeability model depend on the materials, indicating that those models are able to be obtained through doing corresponding experiments on different materials.

2.4 Equations to be solved

The summary of equations that need to be solved is listed below.

$$\varepsilon \frac{\partial S_i}{\partial t} + \nabla \cdot \boldsymbol{U}_i = q_i \quad (2\text{-}23)$$

$$\boldsymbol{U}_i = -\frac{\boldsymbol{K}_i}{\mu_i}(\nabla p_i - \rho_i \boldsymbol{g}) \quad (2\text{-}24)$$

$$K_i = K k_{ri}(S_i) \quad (2\text{-}25)$$

$$p_c(S_i) = p_a - p_i \quad (2\text{-}26)$$

Table 1 gives a summary of parameters in the equations.

Table 1 A summary of parameters in the equations

Parameters shown in the equation	Definition	Input
ε	Porosity of materials	Material property – obtained from experiments
q_i	Injection or extraction	Set zero value in our case
μ_i	Viscosity	Fluid property – constant at the same temperature and pressure
ρ_i	Density	Fluid property – constant at the same temperature and pressure
g	Gravity	Constant
K	Permeability of materials	Material property – obtained from experiments
$k_{ri}(S_i), p_c(S_i)$	Relative permeability model and capillary pressure model	Experiments (since it will be complex to perform experiments and default values are used or adjusted according to different cases)

3 The package of OpenFoam

The structure of OpenFoam is composed of solvers, libraries, and boundary conditions, constant, controlDict. They are placed in different files, requiring calling different functions.

Gravity, mesh, transport properties and wellbore properties (that are source term only considered in evaporation chapter) are included in the constant. They use applications to run different solvers. Due to connections of functions and models, models can be applied in different dictionaries.

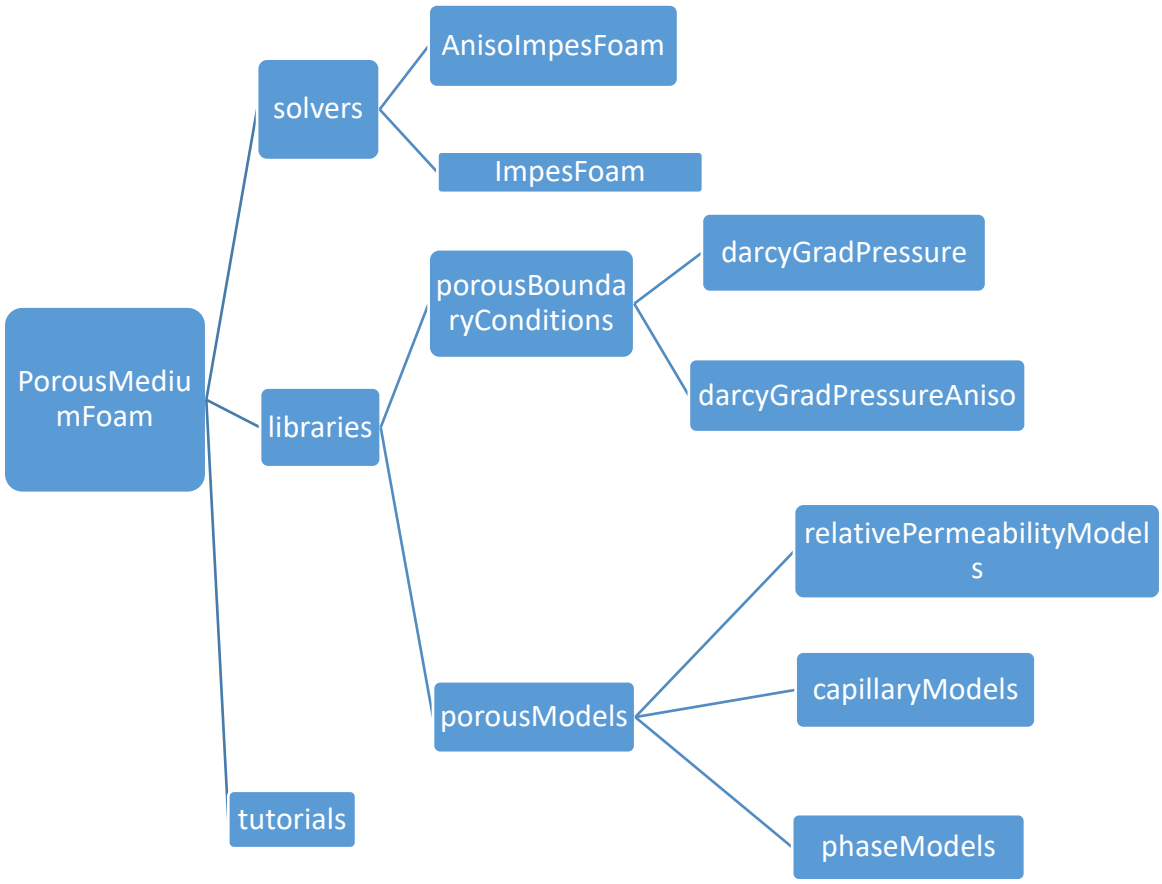

Figure 11 The main structure of the package

Besides the fundamental solvers and libraries in OpenFoam, there are some solvers and models available in the porousMultiphaseFoam package. In absorbing materials modelling, only a part of the package need to be looked into and modified. The file of solvers contains anisoImpesFoam, darcyFoam, groundwaterFoam, impesFoam, porousScalarTransportFoam. There are two models in the libraries, porousBoundaryConditions and porousModels. Also, several tutorials included are based on applications of different solvers and models. (Horgue, P., Soulaine, C., Franc, J., Guibert, R., & Debenest, G, 2015)

ImpesFoam and AnisoImpesFoam are the main solvers used in this thesis. Brooks and Corey model and VanGenuchten model are available in the package. The main difference between ImpesFoam and AnisoImpesFoam is permeability. The former one is scalar, another being tensor. Those two solvers create fields for various parameters and provide adjustable time step. Then, saturation equation and pressure equation are solved. There is a type of pressure boundary condition - Darcy gradient pressure, which is to illustrate Darcy velocity on the considered boundary. The verification and validation also are studied to test the durability of the model.

Modifications of the package are adapted to develop solvers and models. All case studies are based on capillaryValidation files (one of folders in tutorial folders) only including capillary forces and gravity, no diffusion modelled. Investigation of the Brooks-Corey model and Van Genuchten model will be conducted. Furthermore, more models and changes can later be implemented.

There was a fault in anisoImpesFoam that was corrected in this work, codes shown in the appendix.

The numerical method is using default values, which are using first order upwind scheme. Courant number (CFL) is known as a comparison of time scales. In general, the courant number should be below one, meaning that fluid particles move from one cell to another cell within one-time step. Otherwise they will move through more than one cell at each time step, which could affect convergence negatively (Andersson, B., Andersson, R., Håkansson, L., Mortensen, M., Sudiyo, R., & Van Wachem, B, 2011).

In this package, the courant numbers are provided by different solvers; isotropy with three available courant numbers, which are coats, courant and Tod, and anisotropy with two available courant number that are coats and courant. All of them are tied in simulations. The courant number, called courant in the files, in impesFoam is the same as the one in anisoImpesFoam calculated by flux, time step and cells and can adjust time step. Coats in impesFoam is using scalar field which is different from the one in anisoImpesFoam using tensor field instead. However, the function and parameters need are the same, which include time step, pressure, saturation, permeability and others. Tod can only be applied in impesFoam, affected by time step, saturation and others, which is simplified Coats. The courant number is vital when it comes to the convergence and stability. They limit time step and adjust time step.

Wellbores model is the model adding injection and extraction which is reflected in the source term of mass conservation equation.

4 Simulation cases and results

All the cases account for gravity. The governing equations only consider the effects of capillary forces no diffusion modelled. Based on the basic case shown below and as a start, relative permeability model is chosen as Brooks and Corey model and capillary pressure model is Van Genuchten model. The fluids are air and water. The properties of the two phases air and water are constant, therefore remaining the same in all following simulations. The performance of models in those simulations is various, therefore, investigation of models is taken into account. Some power coefficients of models are tested, which showed that the results were sensitive to the values of the coefficients so that they need to be taken care of, which could be a challenge. However, the adjustment of those parameters to fit into experiments are necessary when it comes to validation by comparing with experiments.

All the results shown are transient results. The properties of porous medium are changed according to the base case given by the tutorial files in the package, whose conditions are illustrated below. The effective saturation in relative permeability model is calculated by minimum saturation and maximum saturation. The effective saturation in capillary pressure model is obtained by minimum saturation and maximum saturation in capillary pressure model. In fact, there will not be much differences between minimum saturation and minimum saturation in capillary pressure model.

As it is concluded in last part of chapter 2, the parameters except properties of fluids are material specific and tests are required in order to determine theses parameters.

Table 2 A summary of parameters in simulations

Porosity	0.5	
Minimum saturation	0.001	
Maximum saturation	0.999	
Density of water (kg/m3)	1e3	Liquid at room temperature and pressure
Dynamic viscosity of water (kg/(m*s))	1e-3	Liquid at room temperature and pressure
Density of air (kg/m3)	1	Gas at room temperature and pressure
Dynamic viscosity of air (kg/(m*s))	1.76e-5	Gas at room temperature and pressure
Relative permeability model	Brooks and Corey model	
Power coefficient of Relative permeability model	3	
Capillarity pressure model	Van Genuchten model	
Power coefficient of Capillarity pressure model	0.5	
Air entry pressure (pa)	100	

Minimum saturation in capillary pressure model	0	
Maximum saturation in capillary pressure model	0.999	
solver	ImpesFoam (isotropy)	

4.1 Boundary conditions

Boundary conditions are designed depending on real situations where absorbing materials absorb liquids. The area contacting with liquids has almost fully saturated condition, called the bottom (named as outlet in OpenFoam files) which will be mentioned in the simulations as one of crucial boundary conditions. The opposite side of absorbing materials is connected to the air, called the top (named as inlet in OpenFoam files) which could have boundary conditions of air. However, it also depends on other factors, for instance, whether evaporation is considered. Those factors will be discussed in this chapter. The faces between the bottom and the top are set as empty, meaning that no solution is required for the plane when it is normal to 3rd (and 2nd) dimension, in most situations to simplify the simulations, called front and back – four faces in this work (named as front and back in OpenFoam files).

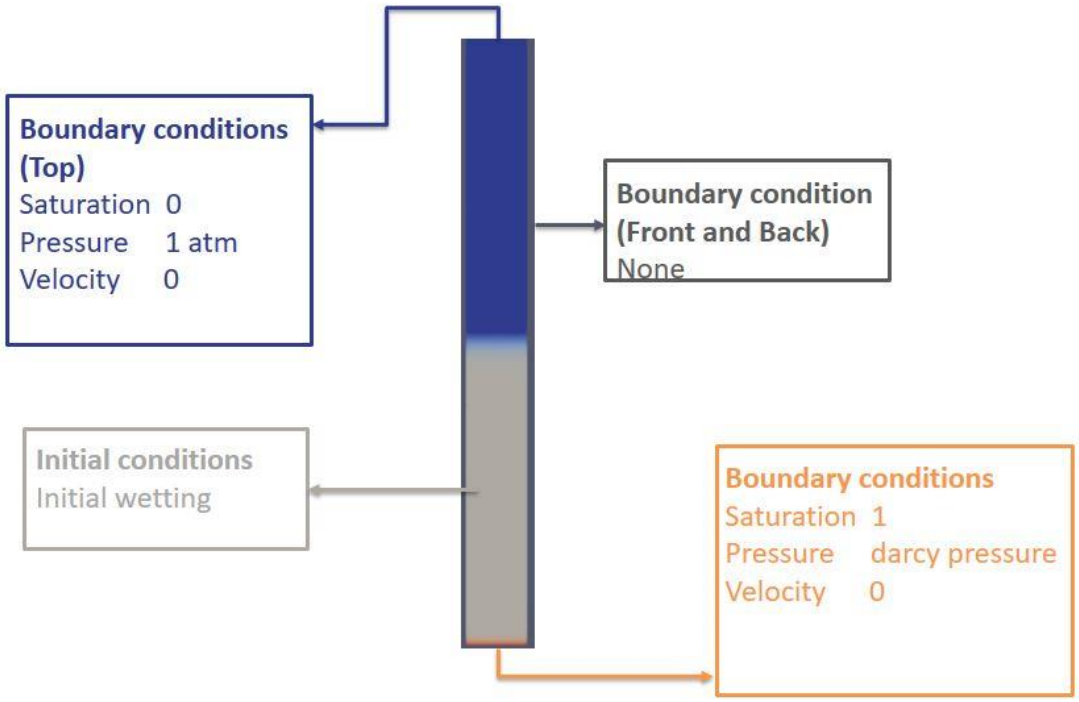

Figure 12 Boundary conditions

Besides those conditions, the fluids are modelled as infinite reservoirs of water and air, expressed by fixed saturation value, called source in the following simulations. Due to multiple ways for liquids and absorbing materials to contact, line source (contacting area is like a line) and point source (contacting area is like a point) are studied to test durability of the model.

Except 3D case study and boundary condition study, other investigations are based on the geometry shown above.

4.2 Initial case:

Besides the conditions illustrated in the table above, this first case was simulated based on the isotropy and initial wetting (half of the sample) with saturation 0.5. The saturation boundary condition of bottom is 0.99 in case 1. The total number of cells is 1000 with the geometry 0.1cm*0.1cm*1cm.

A summary of two cases' conditions:

Table 3 A summary of boundary conditions

		Basic case	Case 2
The size of region(cm^3)		0.1×0.1×1	0.1×0.1×1
Boundary conditions	K permeability	Scalar (1e-11) isotropic	Scalar (1e-11) isotropic
	Sb (Saturation of water)	Inlet fixedValue 0.005 Outlet fixedValue 0.99 Front and back empty	Inlet fixedValue 0.005 Outlet fixedValue 0.99 Front and back empty
	Velocity (water phase and air phase)	Inlet fixedValue 0 Outlet zeroGradient Front and back empty	Inlet fixedValue 0 Outlet zeroGradient Front and back empty
	Pressure	Inlet fixedValue 0 Outlet darcyGradPressure Front and back empty	Inlet fixedValue 0 Outlet darcyGradPressure Front and back empty
Direction of gravity		Negative y direction (towards skin)	Negative y direction
Saturation box		Half of geometry with saturation 0.5	N/A
Time step		1e-5	1e-5
CFL		Todd/Coats	Todd/coats

It shows that the saturation decreased on the top of pre-wetting part, while the saturation increased near the bottom part. There are several possible reasons to explain the rising of saturation on the bottom and saturation decrease on the top of wetting part, such as the accumulation of fluid due to gravity, the drive of capillary pressure. More simulations are required to understand this phenomenon and illustrate the existence of capillary forces.

The graph shows initial conditions of the sample and transient result at 2000s.

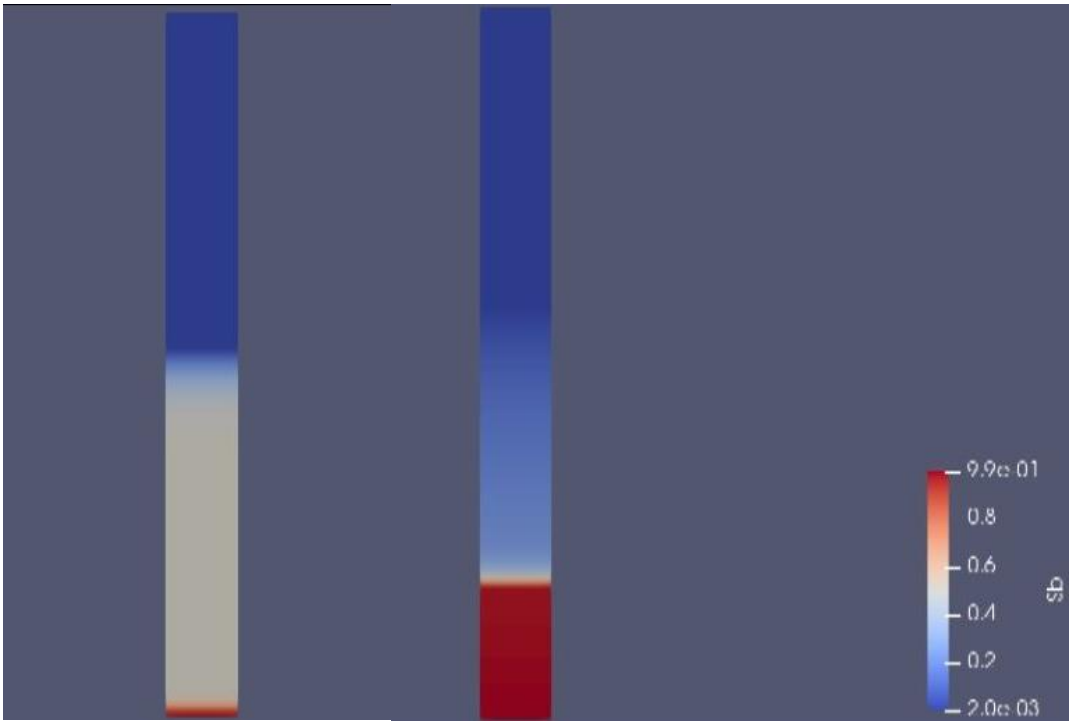

Figure 13 Initial condition and result at 2000s

Nevertheless, it is not apparent that absorption is caused by capillary forces in the example case given by the package. Therefore, another crucial change was made in the boundary condition of velocity fields to perform the simulation. The boundary conditions were adjusted that the saturation of bottom is set fixed value 0.99 and boundary condition of velocity is zero gradient. The initial saturation condition of domain is 0.005. This case was modelled to prove the existence of capillary forces, which turned out that saturation was increasing vertically against gravity due to the acting of capillary forces.

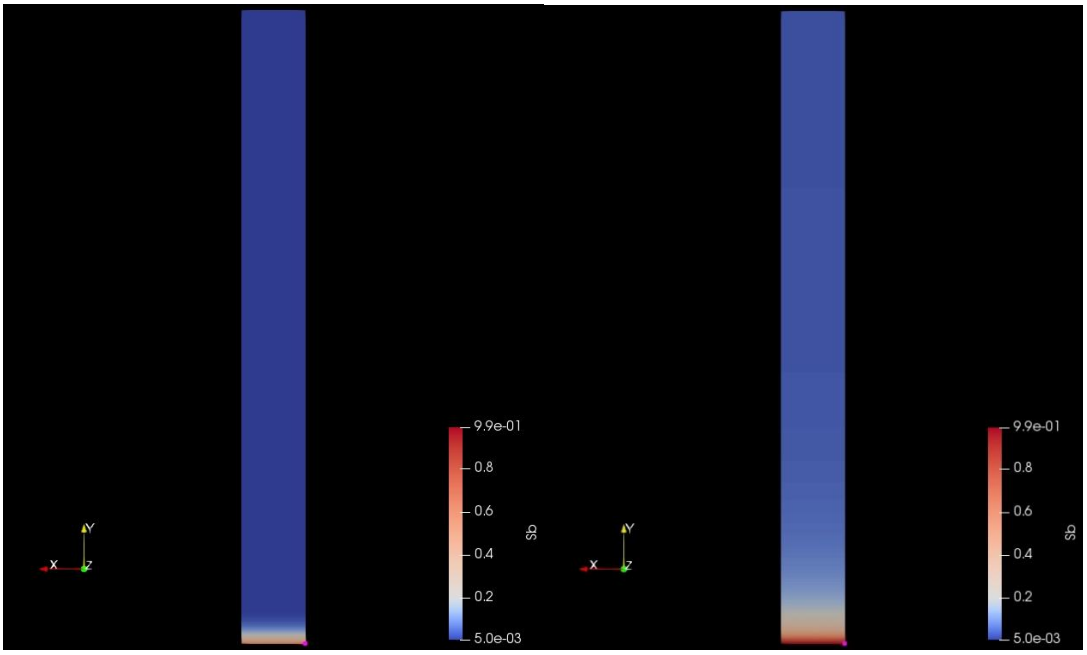

Figure 14 Initial condition and result at 2000s

4.3 3D case study

Another two situations are performed. Suppose there is an infinite reservoir acting as line source and point source in the bottom with velocity zero gradient. The top is connected to air. The front and back conditions are empty. The geometry was constructed as a cube with dimension 1 cm in all three directions. The number of mesh cells is 25000. The geometry and mesh were generated in Beta CAE Ansa (17.1.3).

In addition, extracting conditions from reality are the cornerstone of simulations, for example, that those important boundary conditions are set according to the situation when wound dressing is put on the wound. The partial area of bottom (indicated by red color) is contacting part with fluid almost fully saturated. The front and back area is empty, no specific requirements for conditions so far, which might be implemented in the further research with more information. The top of cube is connected with air. Other conditions according to the basic case.

4.3.1 Line source

The case below shows a line source, which is the initial condition of domain. Since the mesh is coarse in order to reduce computational time and keep simulations stable, the fluid front is not as sharp as it might be with a denser mesh.

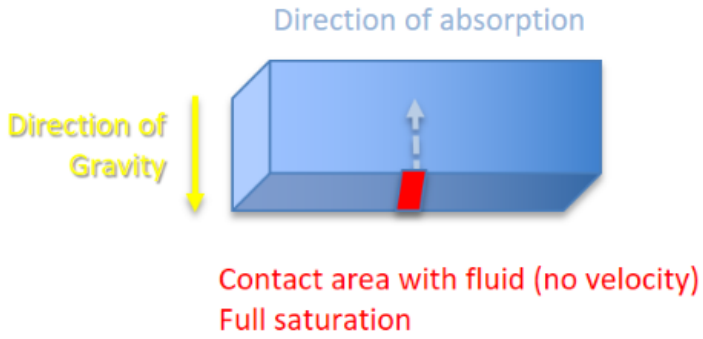

Figure 15 Initial case of line source

It started to transport horizontally and vertically. The transportation of flow is caused by capillary forces due to only capillary forces modelled. Also, gravity is acting towards capillary forces, resulting in the contour shown below, more fluid transport in the bottom.

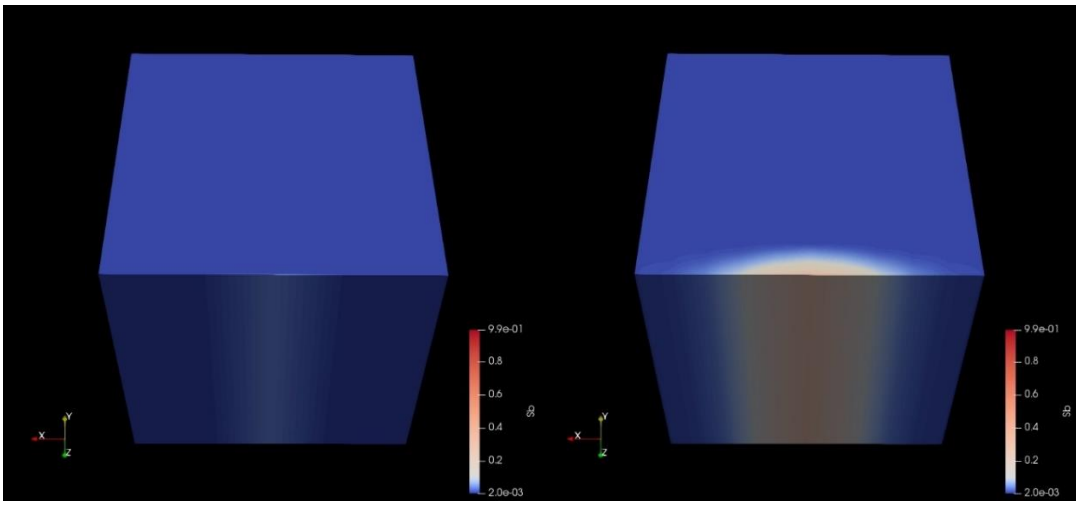

Figure 16 Cube at 0s and 20000s

4.3.2 Point source

This case shows a point source. It performs similar to the case with line source. But line source transports in two directions, point source transporting in three directions.

Figure 17 Initial case of point source

The initial condition and simulation result of saturation at 11000 seconds at distant 0.001cm from bottom are represented below respectively.

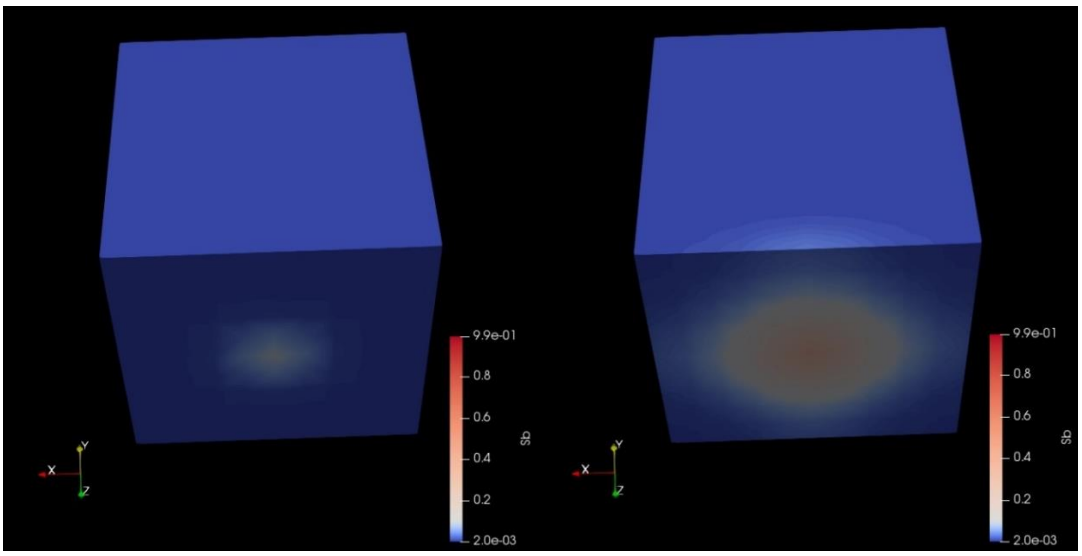

Figure 18 Cube at 0s and 11000s

Both the results of line source and point source show that the horizontal transport and vertical transport of flow are driven by capillary forces. From the point source, it is obvious to find out same fluid transports at two other directions which are perpendicular to gravity direction, due to its isotropy that permeability is the same in all different orientations.

4.3.3 Anisotropy

To further study what have been presented above, one can collect data from literature. Porosity is set as default value 0.5 and due to unknown properties. The parameters of models are set as default values as well due to unknown materials. The permeability (of a foam) is set to a tensor (4.474e-10, 0, 0; 0, 1.654e-10, 0; 0, 0, 0.545e-10) (Di Fratta, C., Klunker, F., Trochu, F., & Ermanni, P., 2015). For anisotropy, due to various permeability in different orientations, the horizontal transport in two directions performs differentially, one direction transporting more fluid than another direction. It can be seen from the contour shown below. The result of simulation shows the different saturation distribution compared to isotropic case (point source). Although the mesh and geometry of anisotropic case and isotropic case, the anisotropic case took much longer time and larger computational power compared to isotropic case.

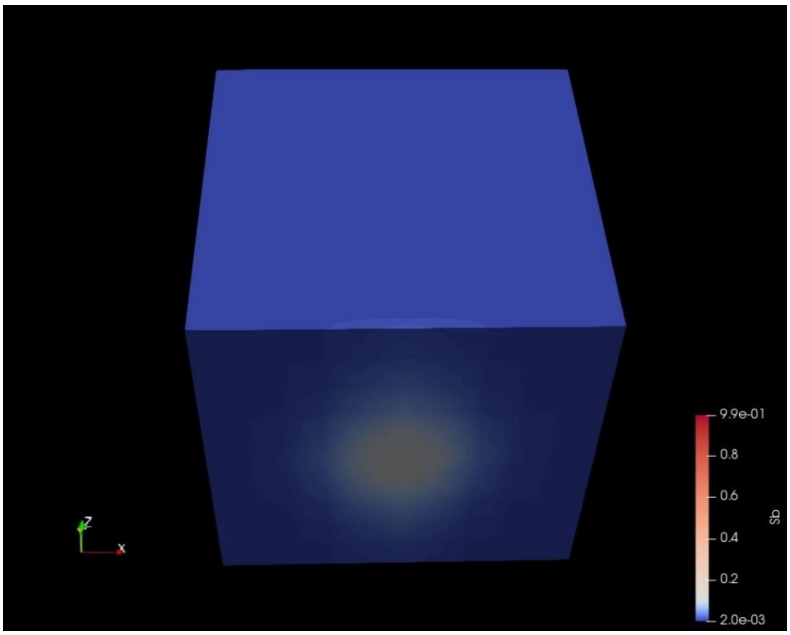

Figure 19 Result at 11000s

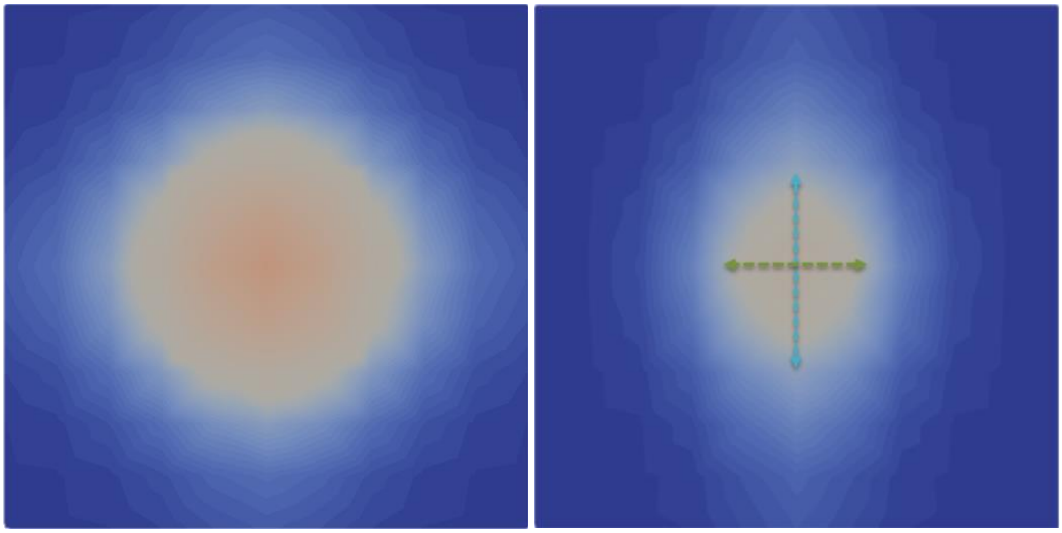

Figure 20 Comparison of isotropy case and anisotropy case

4.3.4 The effects of gravity

The wound in the arm sometimes is vertical, extracting conditions shown below.

Figure 21 Initial case of the effects of gravity

This case is investigated to study the effects of gravity. All the conditions are the same as point source case, except the direction of gravity. It is shown below that gravity has quite large impact on saturation distribution through showing higher saturation at bottom part and lower saturation at top part. The transportation of fluid in three directions is supposed to be same without gravity. What is shown below can give a clear thought about effects of gravity.

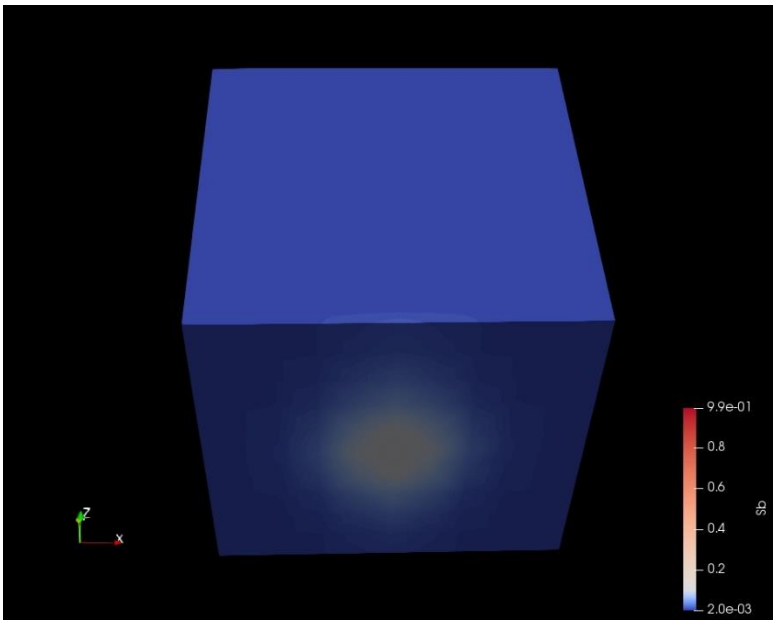

Figure 22 Cube at 11000s

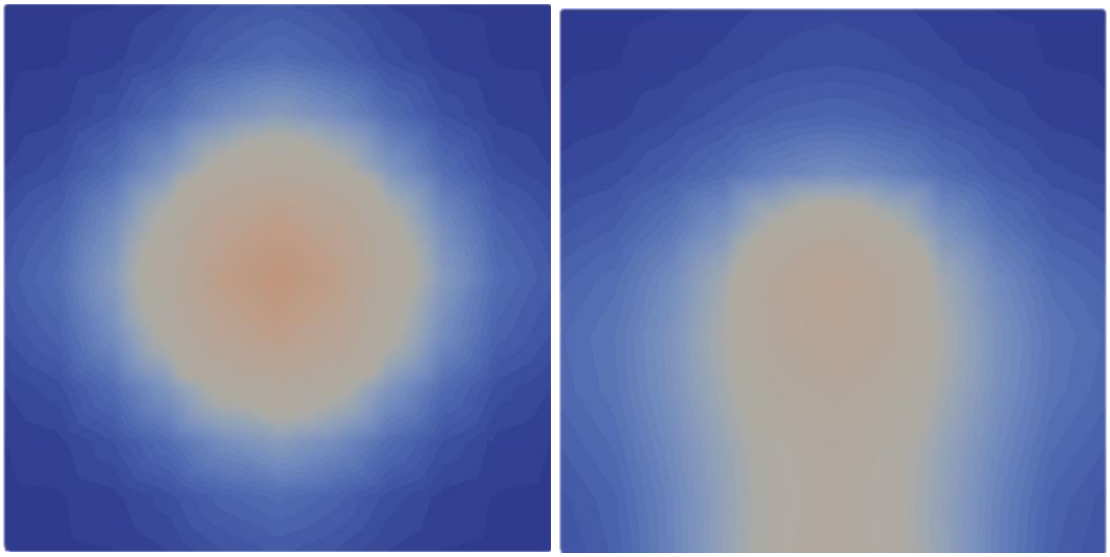

Figure 23 Comparison of cases with gravity acting in different directions

Comparing the results, one can see an obvious effect of gravity on fluid transportation.

4.3.5 The change of porosity

Each parameter plays a crucial role in the equations. One of the parameters, porosity is changed from 0.5 to 0.7 to investigate on the impact. Comparing the results at the same step (10000 seconds), it turned to be that higher porosity leads to more fluid transport to fill in to reach the same saturation. Generally speaking, the change of porosity will only influence the saturation level at each point not the way of fluid transportation.

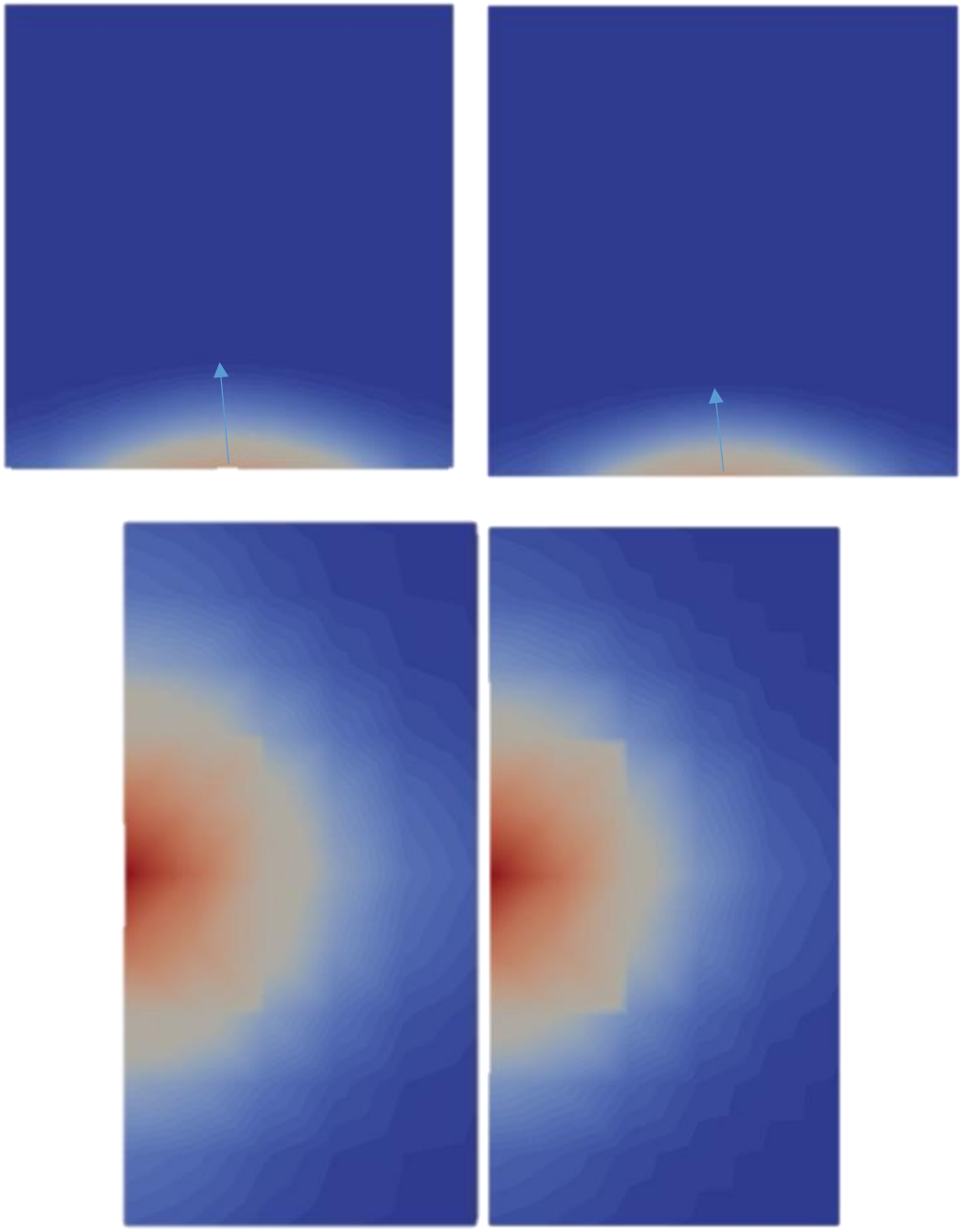

Figure 24 Comparison of porosity 0.5 and 0.7 respectively

Higher porosity it is, the less saturation it will be at the same point and time.

The form below shows the cases studied in this section:

Table 4 A summary of boundary conditions

		Line source	Point source	Anisotropy	Gravity	Porosity change
The size of region(cm^3)		1×1×1	1×1×1	1×1×1	1×1×1	1×1×1
Boundary conditions	K permeability	Scalar (1e-10) isotropic	Scalar (1e-10) isotropic	Tensor anisotropic	Scalar (1e-10) isotropic	Scalar (1e-10) isotropic
	Sb (Saturation of water)	Inlet fixedValue 0.005 Outlet fixedValue 0.99 Front and back empty	Same	Same	Same	Same
	Velocity (water phase and air phase)	Inlet fixedValue 0 Outlet zeroGradient Front and back empty	Same	Same	Same	Same
	Pressure	Inlet fixedValue 0 Outlet darcyGradPressure Front and back empty	Same	Same	Same	Same
Direction of gravity		Negative y direction	Negative y direction	Negative y direction	Negative z direction (parallel to the skin)	Negative y direction
Saturation box		N/A	N/A	N/A	N/A	N/A
Time step		1e-5	1e-5	1e-5	1e-5	1e-5
CFL		Coats	Coats	Coats	Coats	Coats

4.4 Simulations with different boundary conditions

Since the absorbing materials applied in daily life have a low thickness (typically millimeters) compared to their width (typically decimeters), geometry is constructed to be closer to them, whose domain is 1×1×1, shown in the figure 25. The boundary condition of saturation is studied. There are two situations, one with fixed value about 0.005 at inlet, one with zero gradient at inlet. The fixed value models infinitely fast evaporation. The boundary condition of zero gradient models that the rate evaporation can be neglected comparing to rate of fluid transport, therefore, the saturation of inlet can be as high as possible.

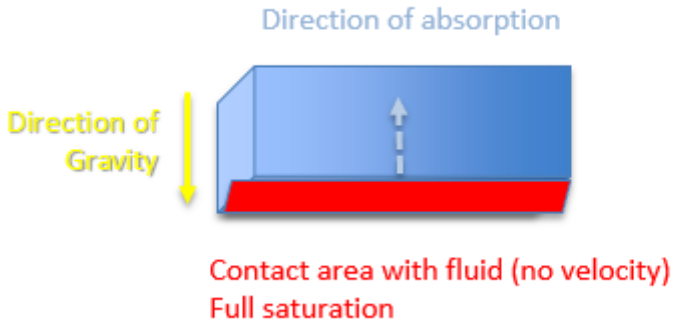

Figure 25 Initial case with different boundary conditions

The one with fixed saturation reveals that the distribution of saturation remains the same at a certain time, showing the equilibrium. This is mainly due to that the fixed value of inlet constrains the fluid saturation. The saturation level remains the same when it reaches equilibrium. For the one with zero gradient, the saturation at the surface is increasing as time increases, which would be utilized to compare with when evaporation is included. However, in reality, the evaporation is between those two states. The case with fixed inlet saturation reached equilibrium in a shorter time than the case with zero gradient.

Fixed saturation at the top boundary:

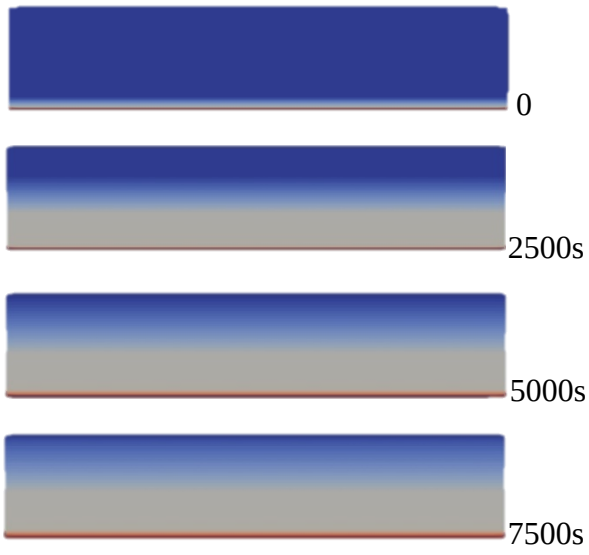

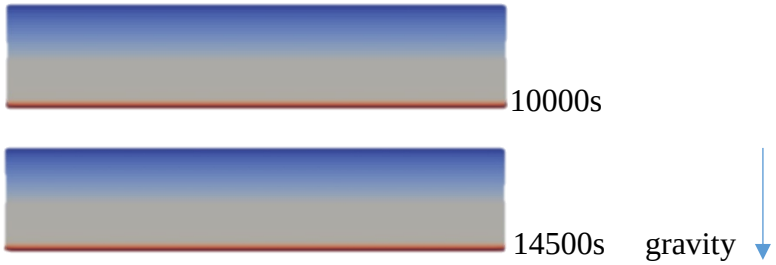

Zero saturation gradient at the top boundary:

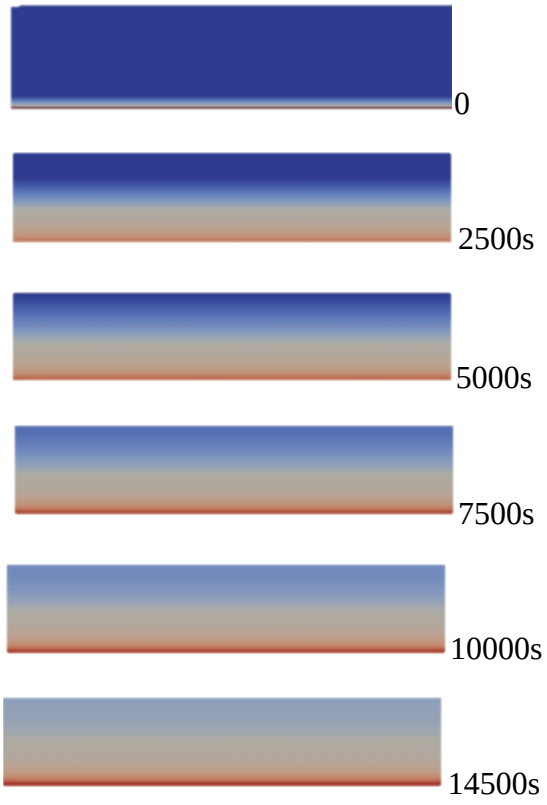

Figure 26 Comparison of two boundary conditions

4.5 Investigation of different models

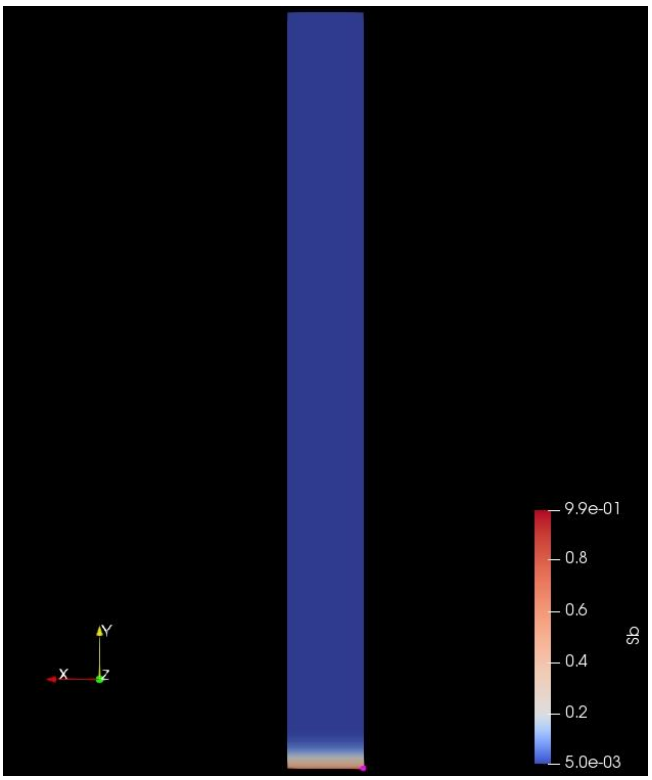

Figure 27 Initial conditions and geometry

The study of different models in this chapter has the same initial conditions and geometry as it is shown in the Figure 27. In order to understand more about different models, the simulations are compared by using different models and parameters.

4.5.1 Capillary pressure model _ Brooks and Corey model

In this section, not only is the power coefficient of Brooks and Corey model (capillary pressure model) investigated, but Brooks and Corey model will be taken as an example to study the impact of entry pressure, minimum saturation and maximum saturation. Due to its time-consumption and requirement of computer memory, the equilibrium cannot be reached. Instead, the same simulation time 200,000s would be the stop time for the cases shown below.

Table 5 Different parameters study

Capillary pressure model	B&C 1	B&C 2	B&C 3	B&C 4	B&C 5
Power coefficient	2	3	2	2	2
Entry pressure	1000	1000	100	1000	1000

Maximum saturation	0.999	0.999	0.999	0.95	0.999
Minimum saturation	0	0	0	0	0.01

Other settings are according to the basic case shown above with simple geometry whose relative permeability model is Brooks and Corey model. The capillary pressure model was changed to Brooks and Corey model.

Those are the results of five cases listed in the table at 200,000s.

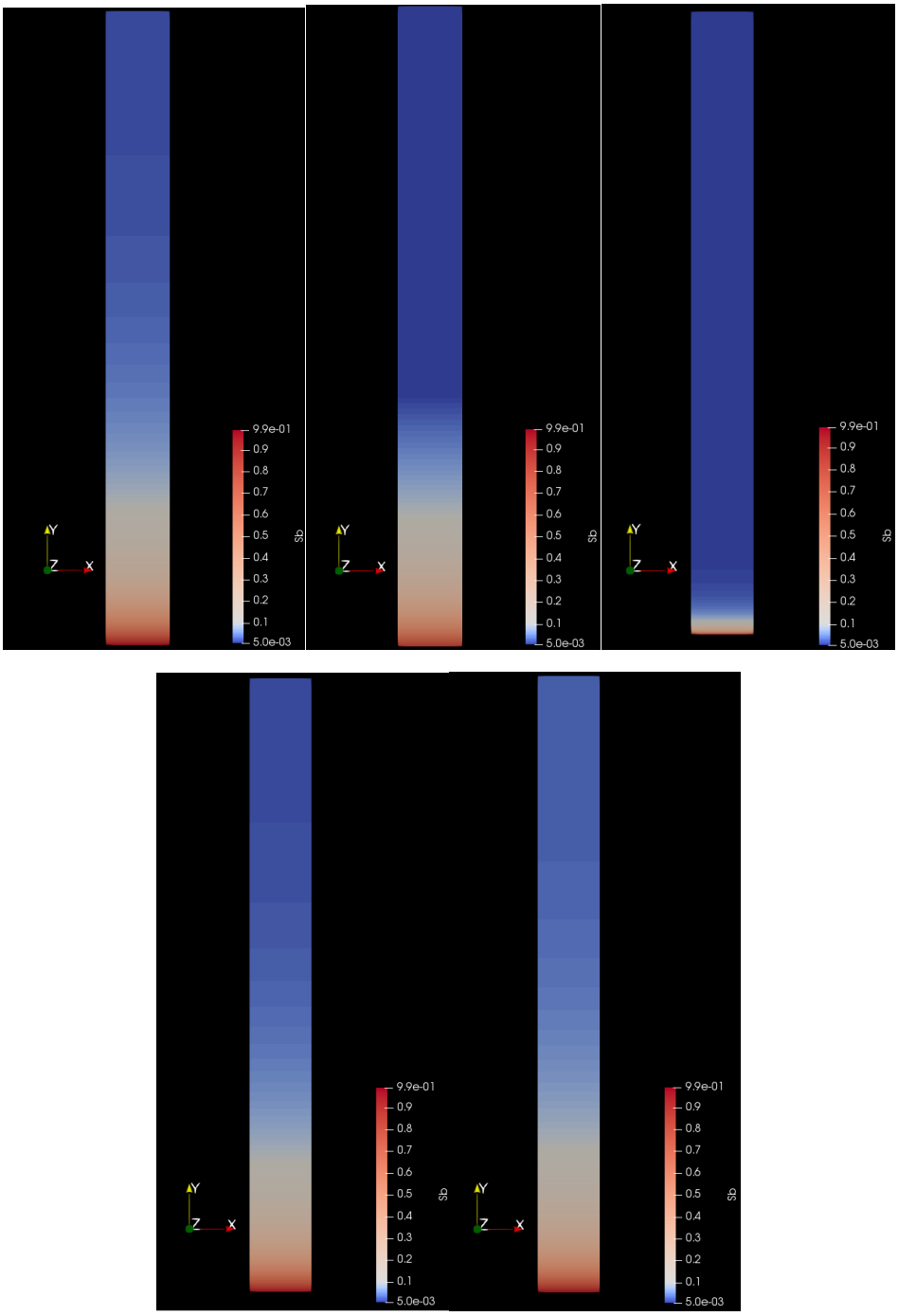

Figure 28 B&C1 to B&C5 respectively at 200,000s from left to right

An observation point is selected at the distance 0.01 cm. The graph Figure 29 shows how the saturation of phase b changed with the increase of time at different cases.

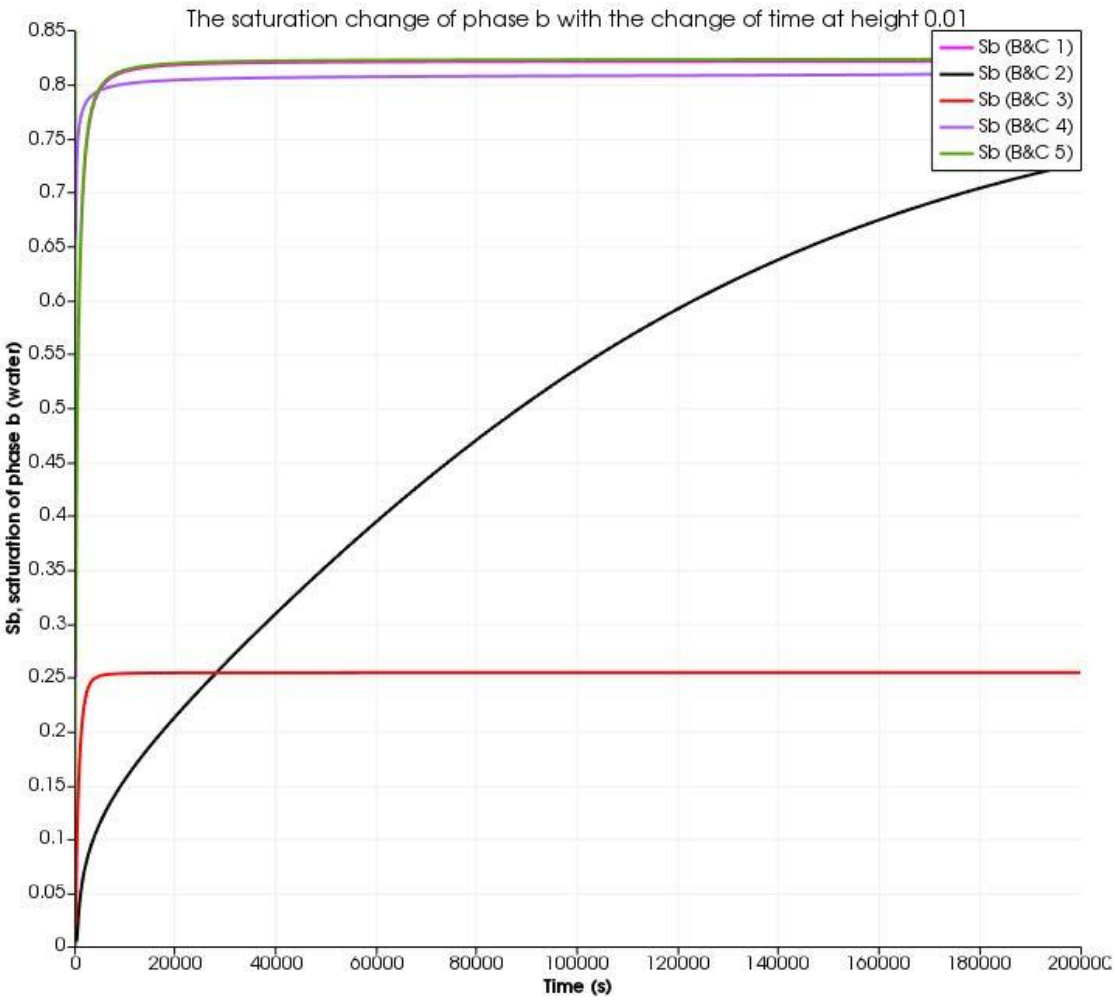

Figure 29 Saturation change over time

The saturation increases rapidly at the beginning with low saturation and reach equilibrium at a certain time within 20,000s except case 2. Case 2 has higher power coefficient that leads to lower capillary pressure, which is consistent with the analysis of different models mathematically (chapter 2). Case 3 with lower entry pressure results in lowest saturation. Although Case 1,4 and 5 are very close to each other, lower maximum saturation could lead to consuming less time to reach equilibrium and higher minimum saturation could reach higher saturation at equilibrium.

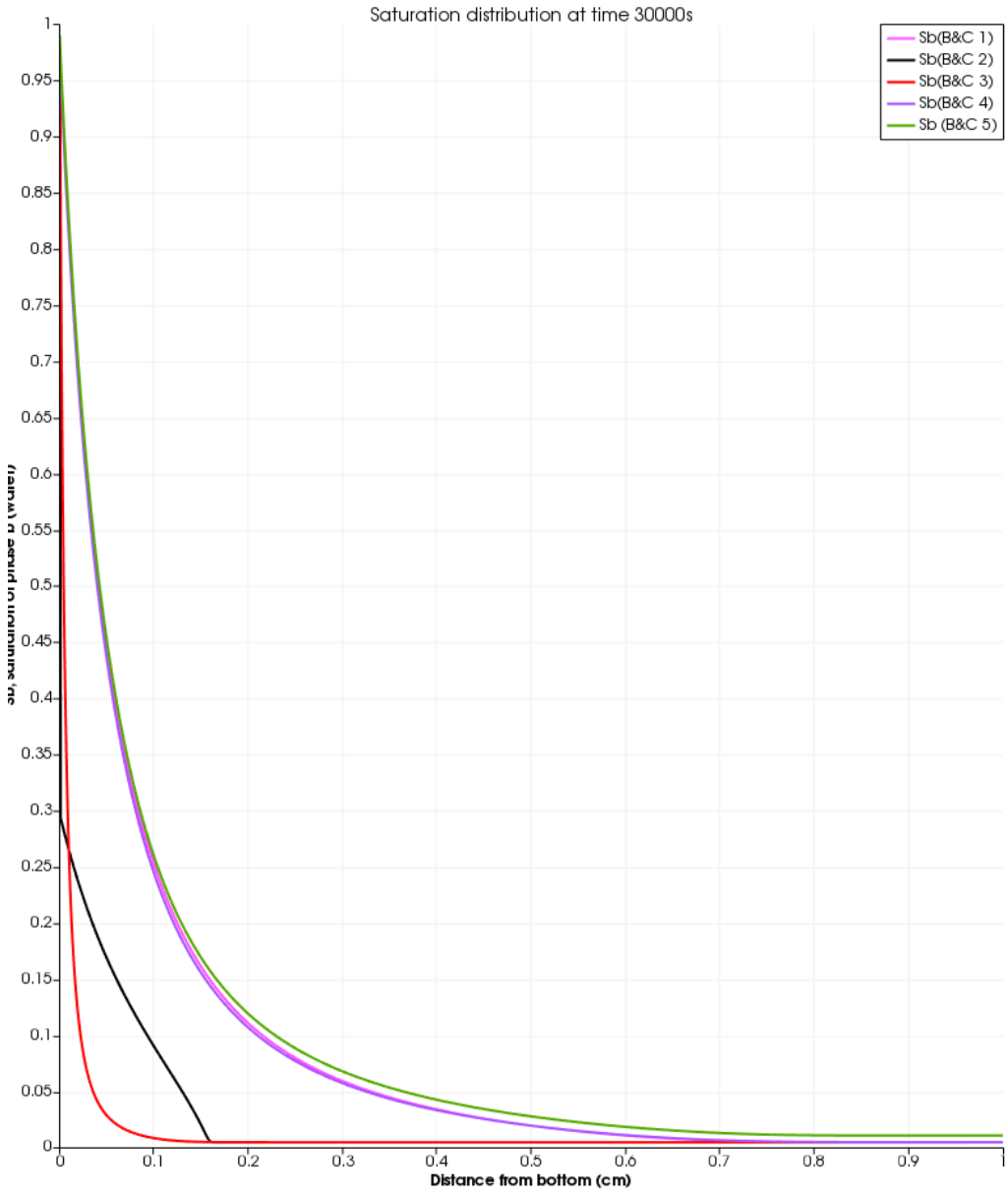
Saturation distribution at time 30000s
Sb(B&C 1)
Sb(B&C 2)
Sb(B&C 3)
Sb(B&C 4)
Sb (B&C 5)
Distance from bottom (cm)

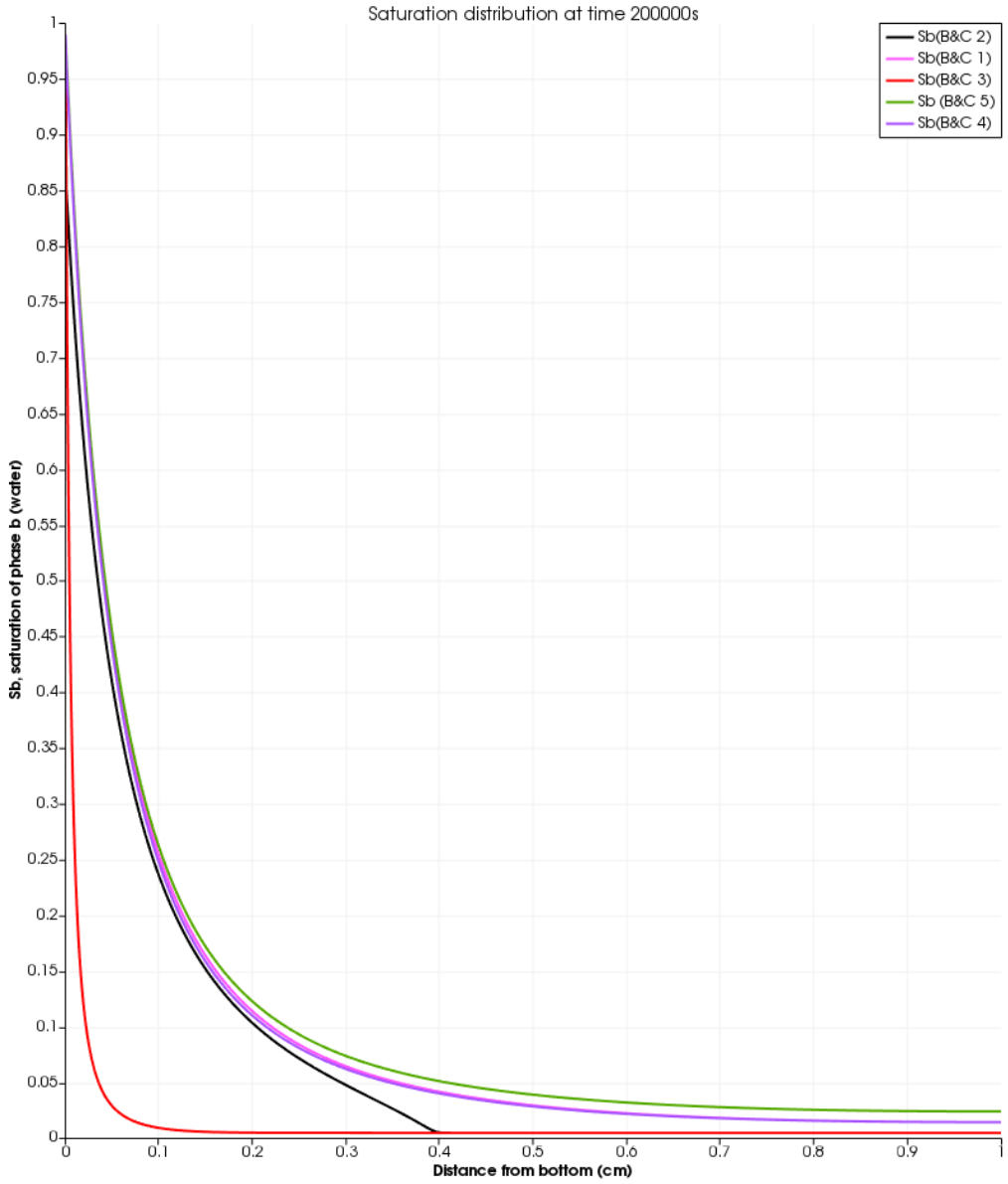

Figure 30 Saturation distribution at 30,000s and 200,000s respectively

The graphs, Figure 29 and Figure 30, show the saturation distribution along the direction of absorption at 30000s and 200000s respectively.

Case 1, case 4 and case 5 present higher saturation level than other cases. Case 2 and case 3 reveal that higher power coefficient and lower entry pressure could result in lower saturation level at the same time.

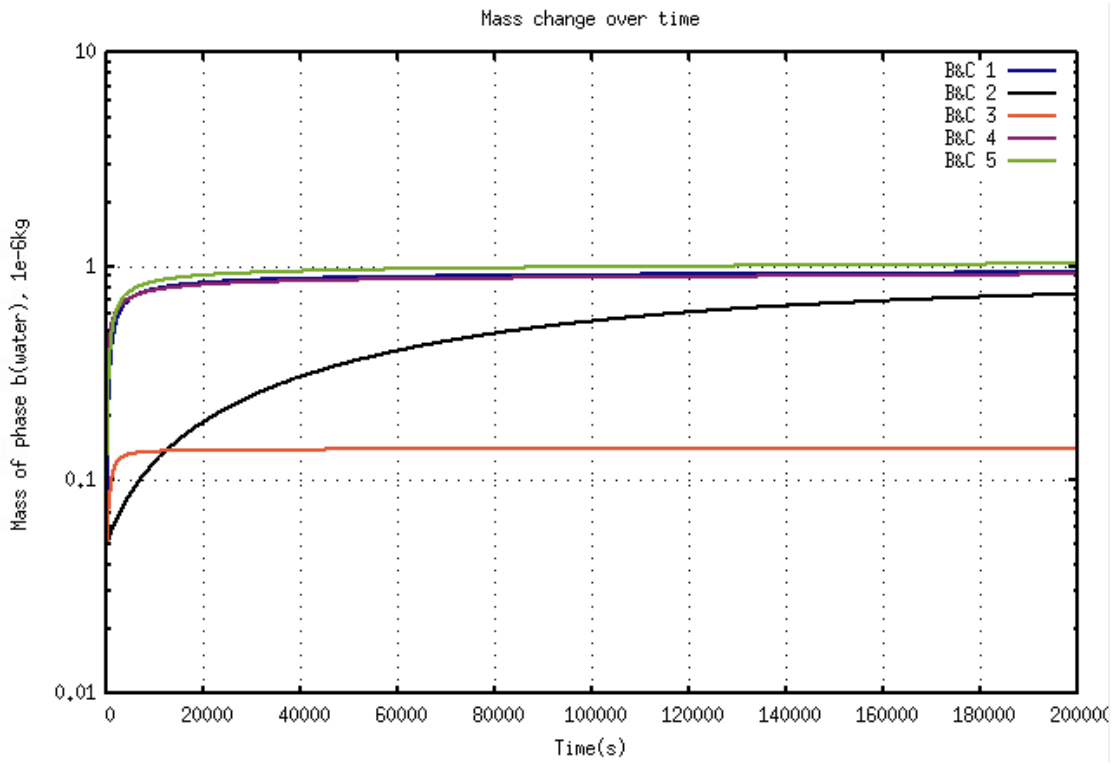

Figure 31 Mass change over time

This graph shows the mass change over time. The case 5 gains most weight compared to other cases. The case 3 has the least mass among five cases. The higher entry pressure, higher minimum saturation and lower power coefficient it is, the more mass it will absorb.

4.5.2 Capillary pressure model _ Van Genuchten model

Other settings are remained consistence with the basic case shown above with simple geometry. The impact of power coefficient in Van Genuchten model is studied.

Table 6 Parameter study

Capillary pressure model	Van Genuchten 1	Van Genuchten 2
Power coefficient	0.4	0.7
Pc0	100	100

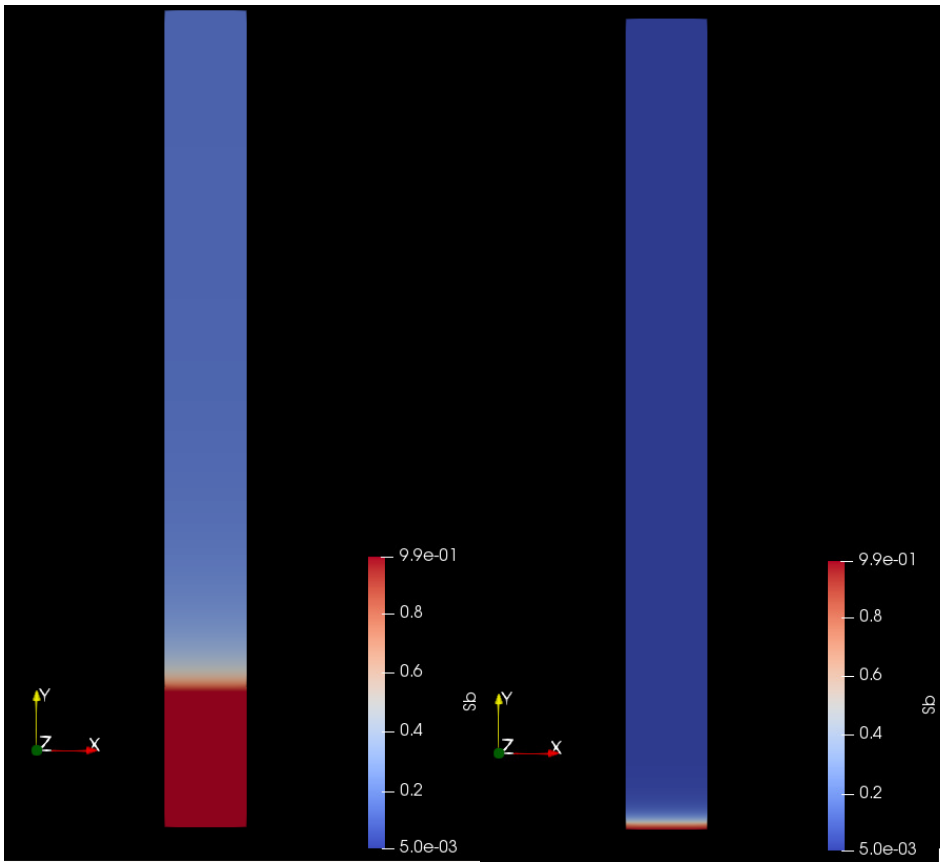

Figure 32 Case 1 and case 2 at 200,000s respectively

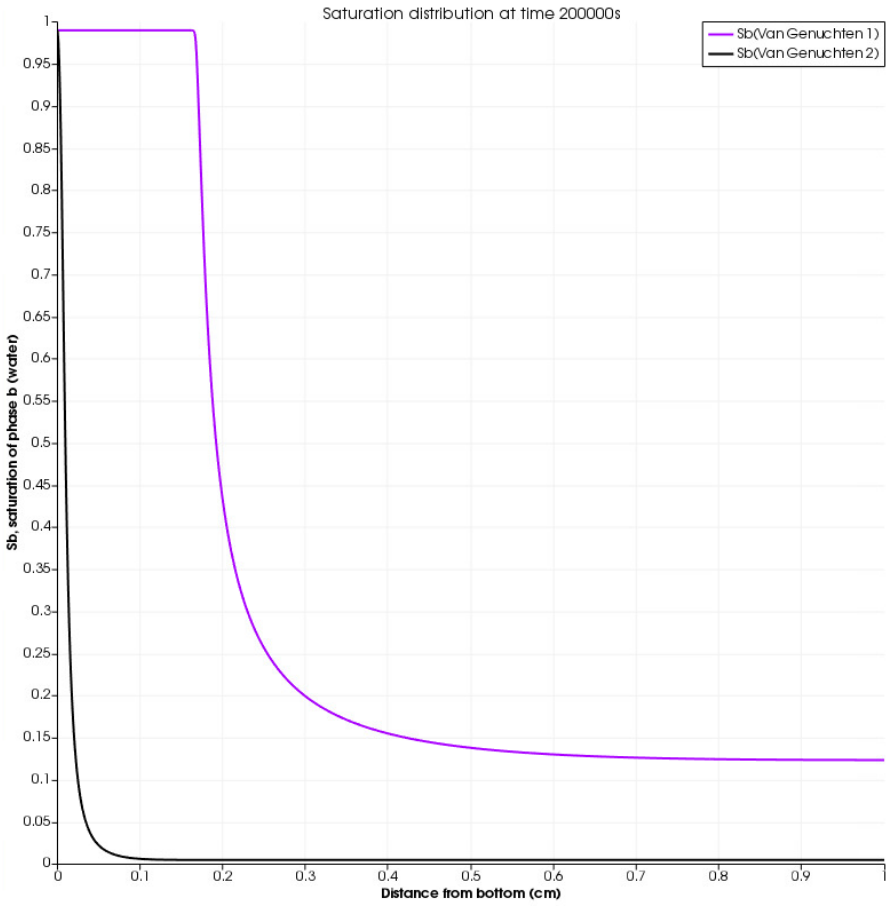

Figure 33 Saturation distribution at 200,000s

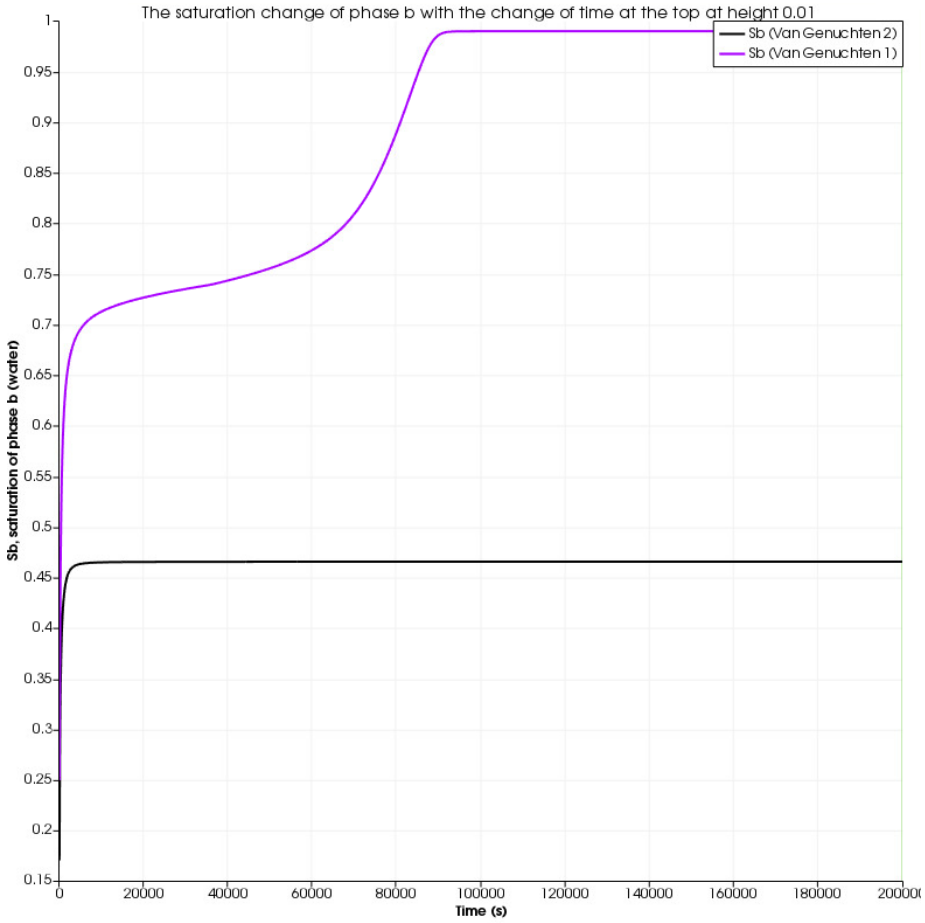

Figure 34 Saturation change over time

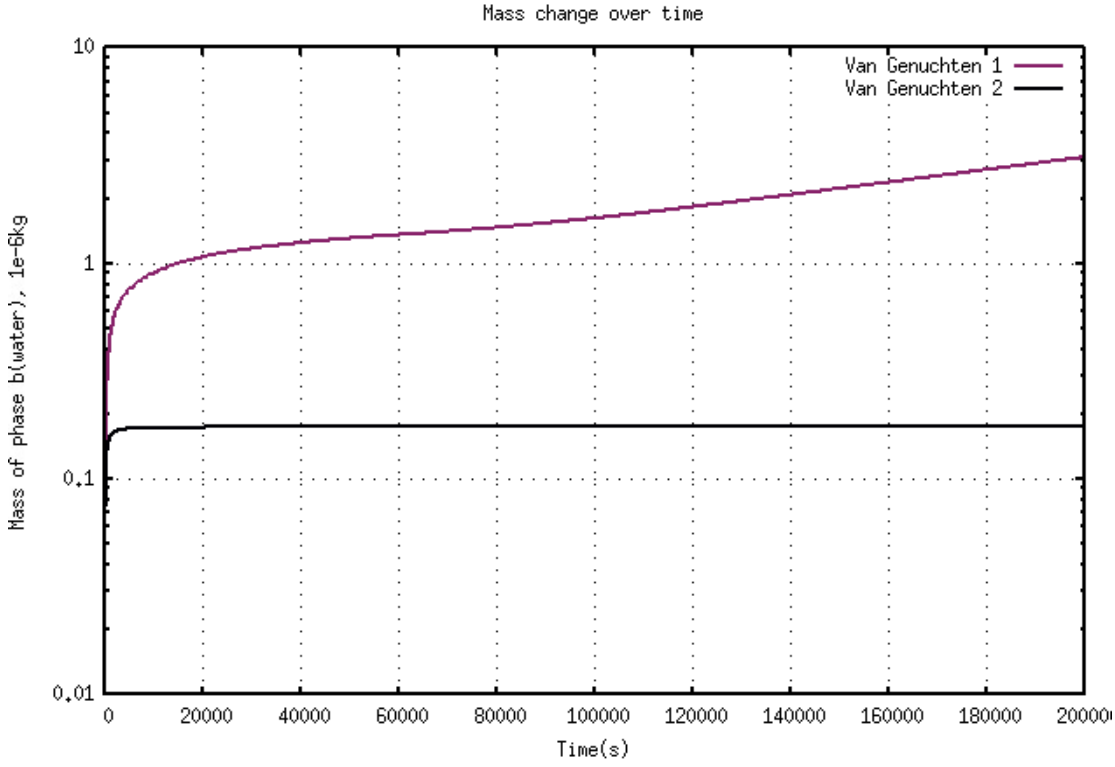

Figure 35 Mass change over time

Lower power coefficient led to higher saturation level, which also took longer time to reach equilibrium and took longer computational time. Case 1 shows fully saturation at the bottom and sharp interface with twice rapid increase during absorption (at the observation point). Case 2 reach equilibrium fast at low saturation level.

4.5.3 Capillary pressure model _ linear model

Other settings remain constant with the basic case shown above with simple geometry. The capillary pressure model was changed to linear model. The relative information of linear model is given below. Different maximum capillary pressures are used in different cases to compare.

Table 7 Parameter study

Capillary pressure model	Linear model 1	Linear model 2
Sbminpc	0.001	0.001
Sbmaxpc	0.999	0.999
pc0	0	0
pcMax	19620	29620

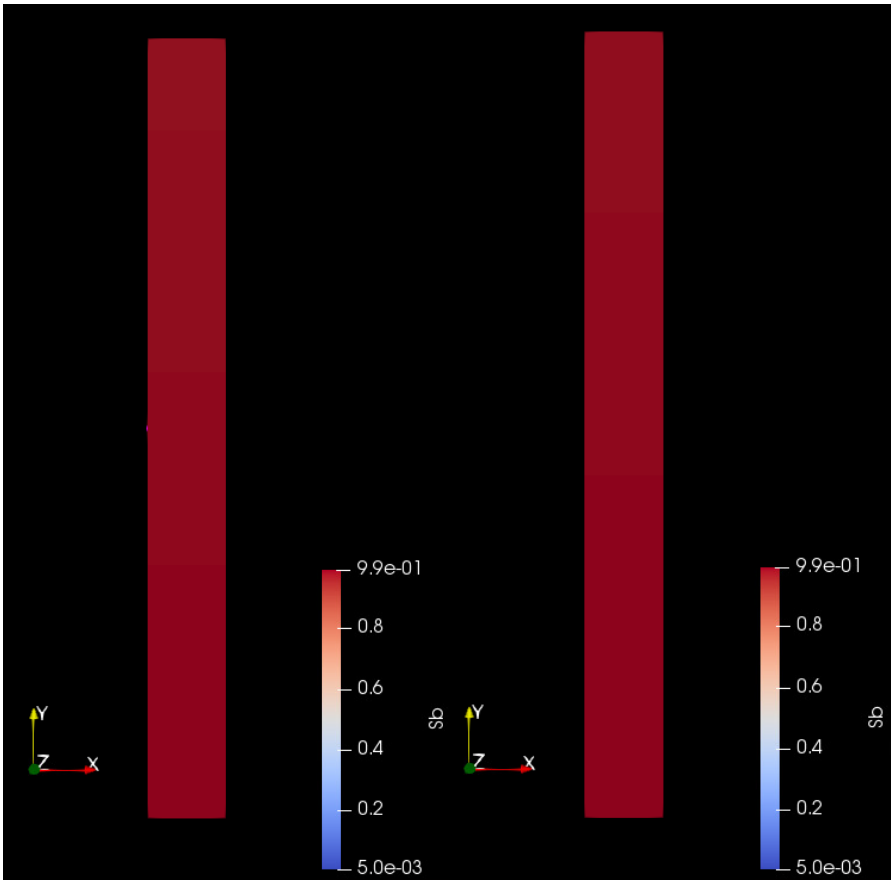

Figure 36 Linear model 1 and 2 at 120,000s respectively

The result is shown in the Figure 36, illustrating that all of them are fully saturated after a certain time.

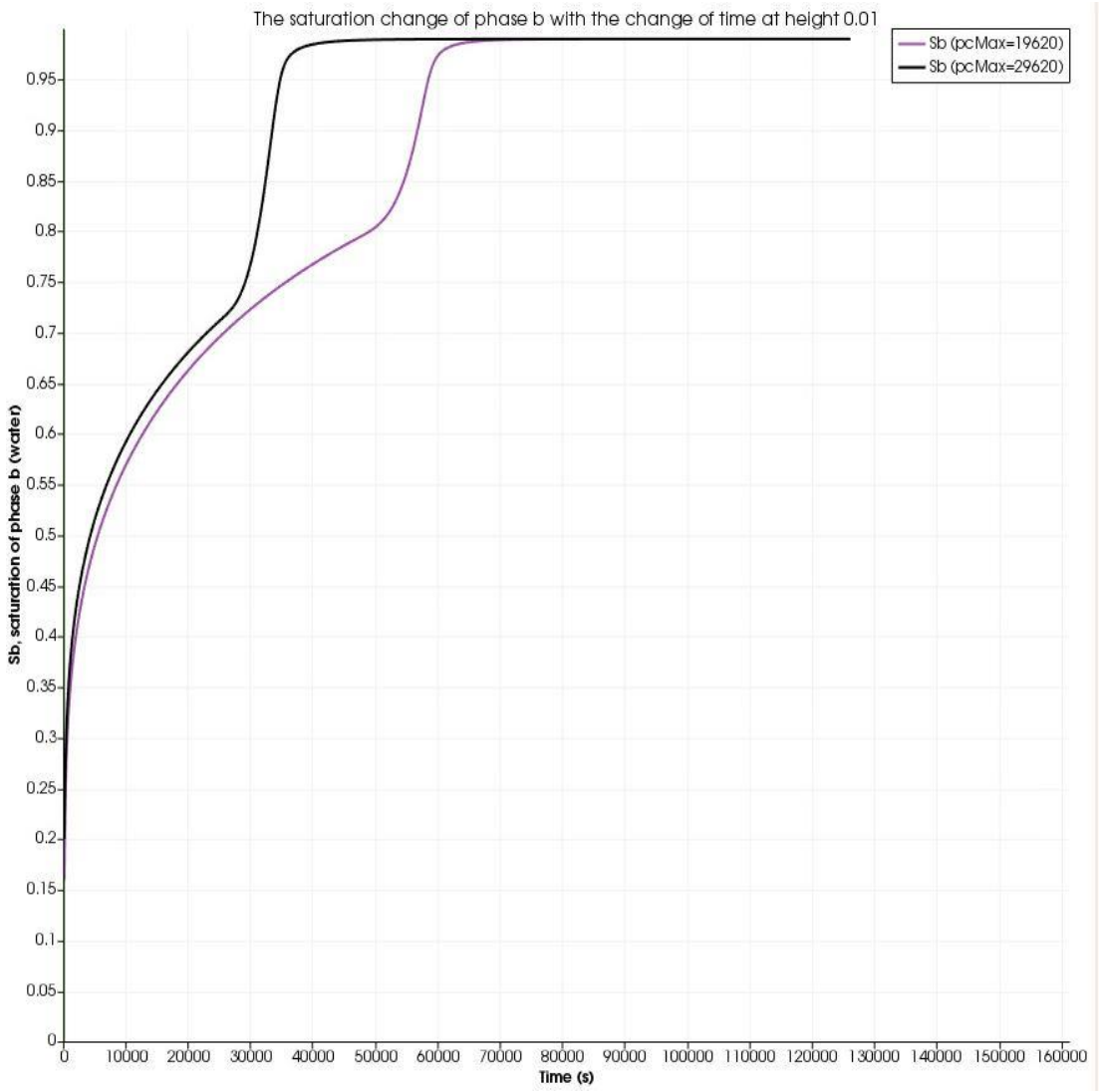

Figure 37 Saturation change over time

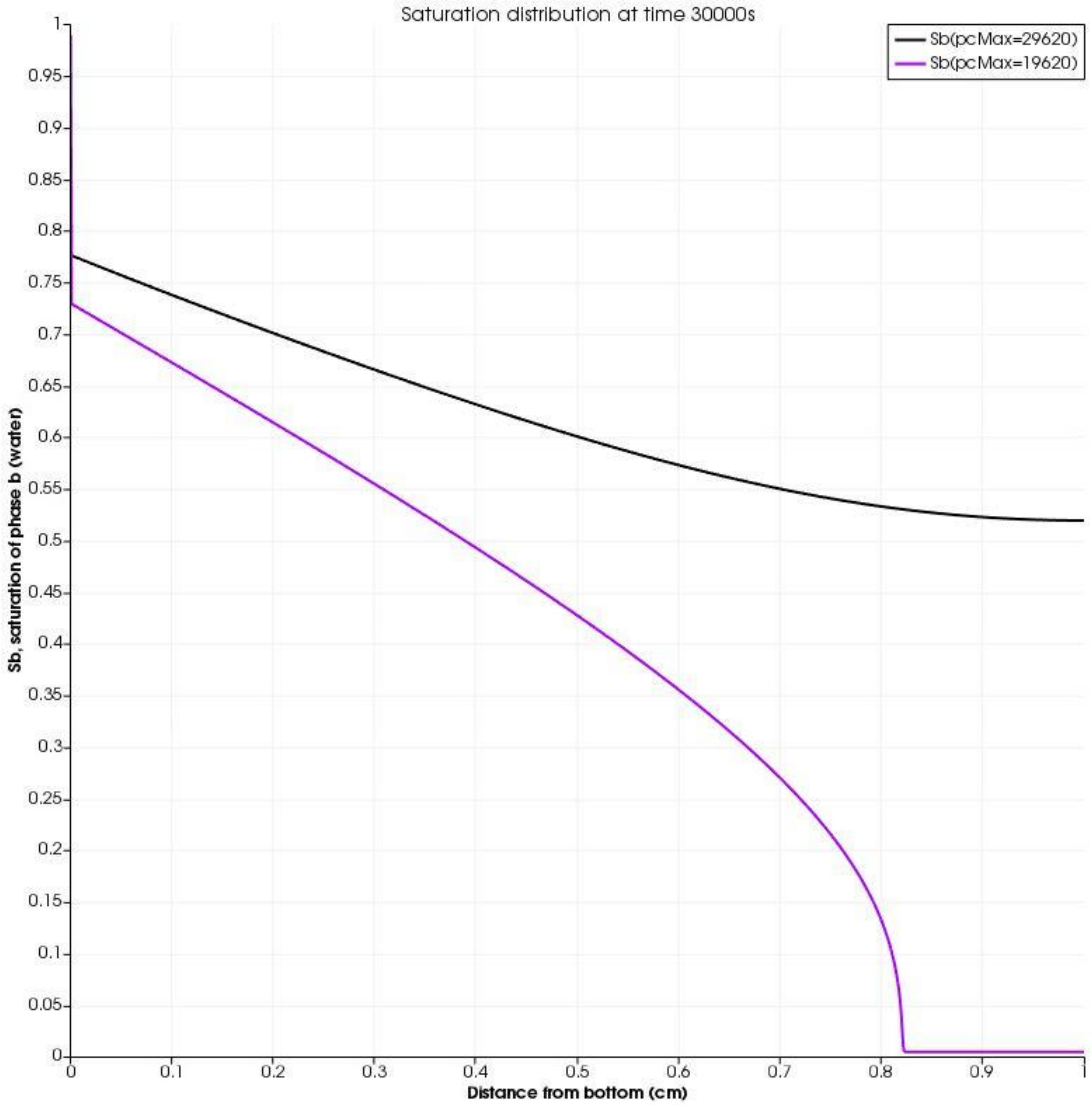

Figure 38 Saturation distribution at 30,000s

It can be seen higher maximum capillary pressure can make it reach almost fully saturation at earlier time and higher saturation level at the same time. Both of them have two stages where the saturation increased rapidly. This model will lead to sharper fluid front compared to other models, indicated by the graph shown in the Figure 38.

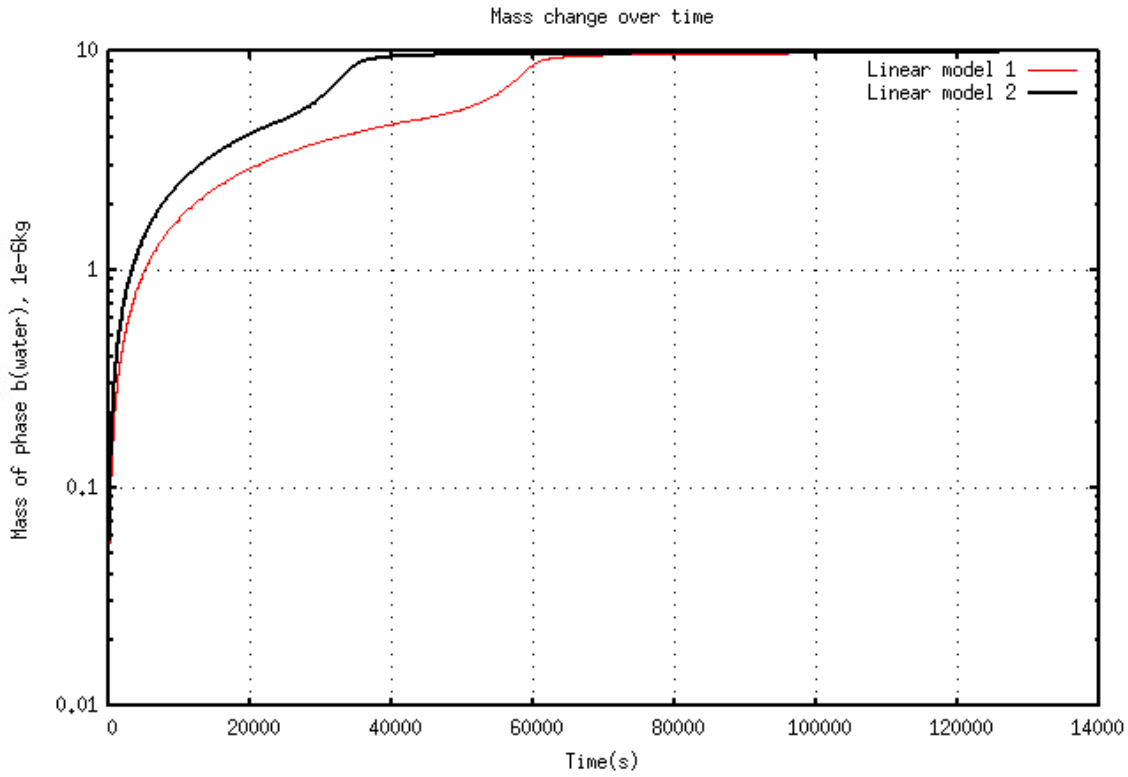

Figure 39 Mass change over time

The plot shows the change of mass over time. The Linear model 2 reaches equilibrium faster than Linear model 1 and they are all saturated in the end.

4.5.4 Relative permeability model_ Van Genuchten model

Other settings are remained the same as the basic case except relative permeability model and capillary pressure model. The relative permeability model is changed to Van Genuchten model and capillary pressure model is changed to Brooks and Corey model.

Table 8 Parameter study

Relative permeability model	Van Genuchten 1	Van Genuchten 2
Power coefficient	1.5	4
Pc0	100	100

It shows the saturation distribution along vertical direction of cylinder.

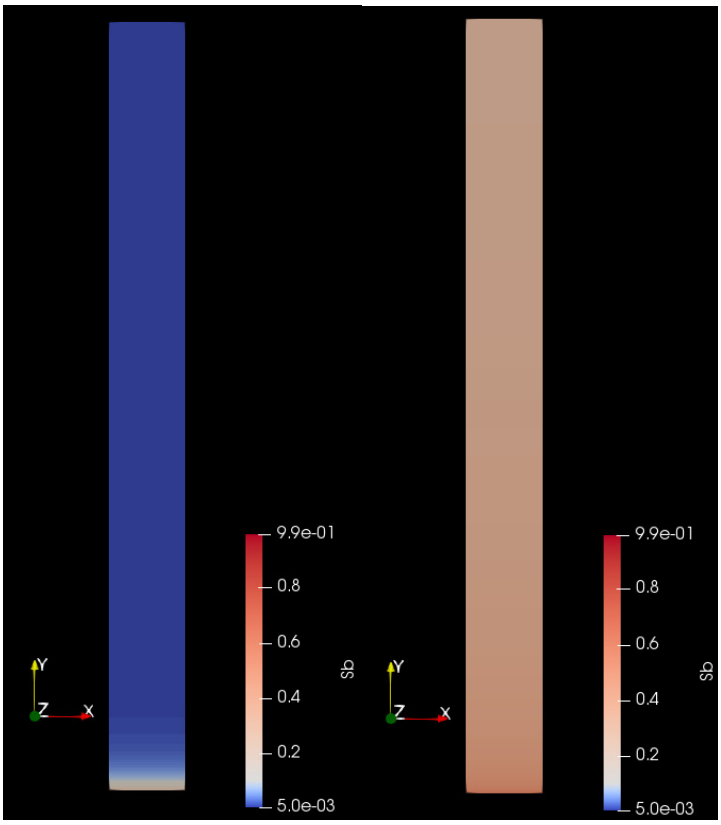

Figure 40 Van Genuchten 1 and 2 respectively at 200,000s

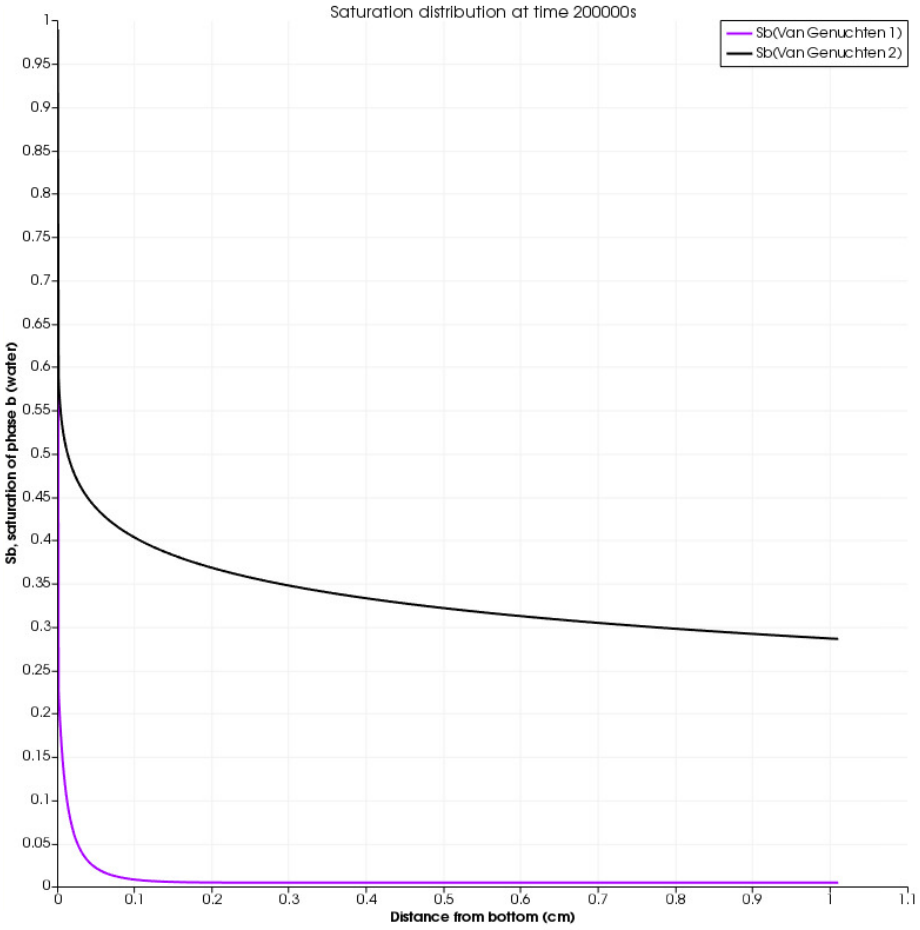

Figure 41 Saturation distribution at 200,000s

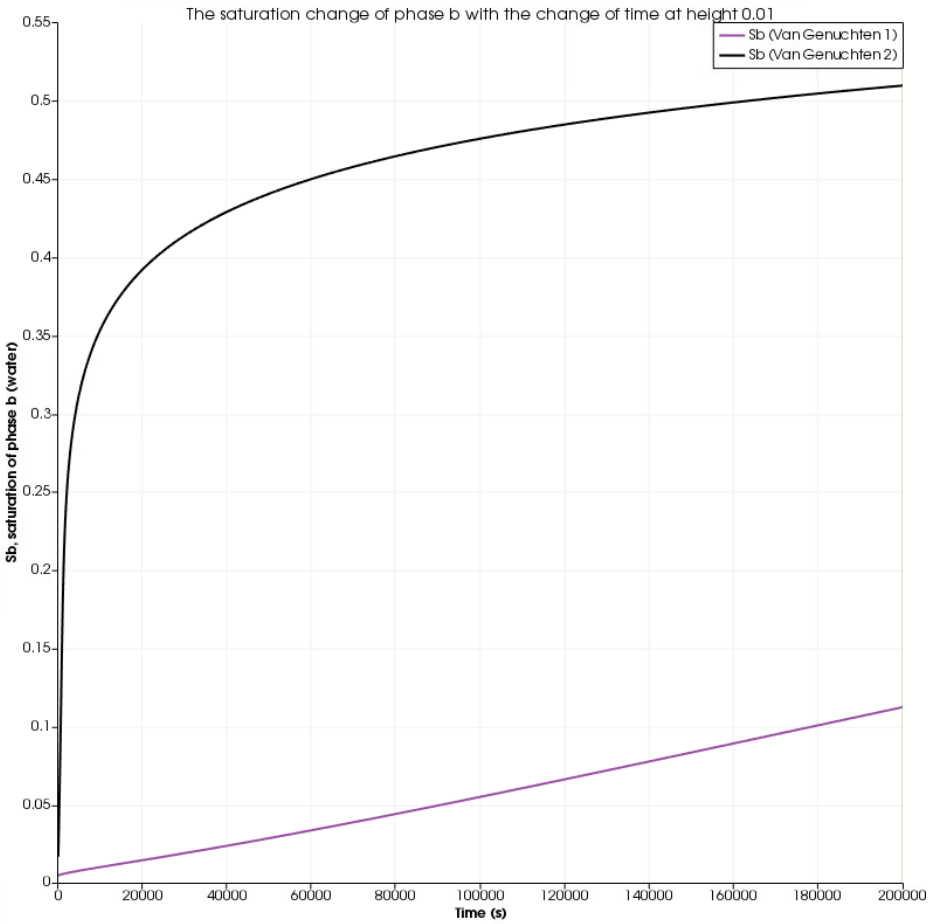

Figure 42 Saturation change over time

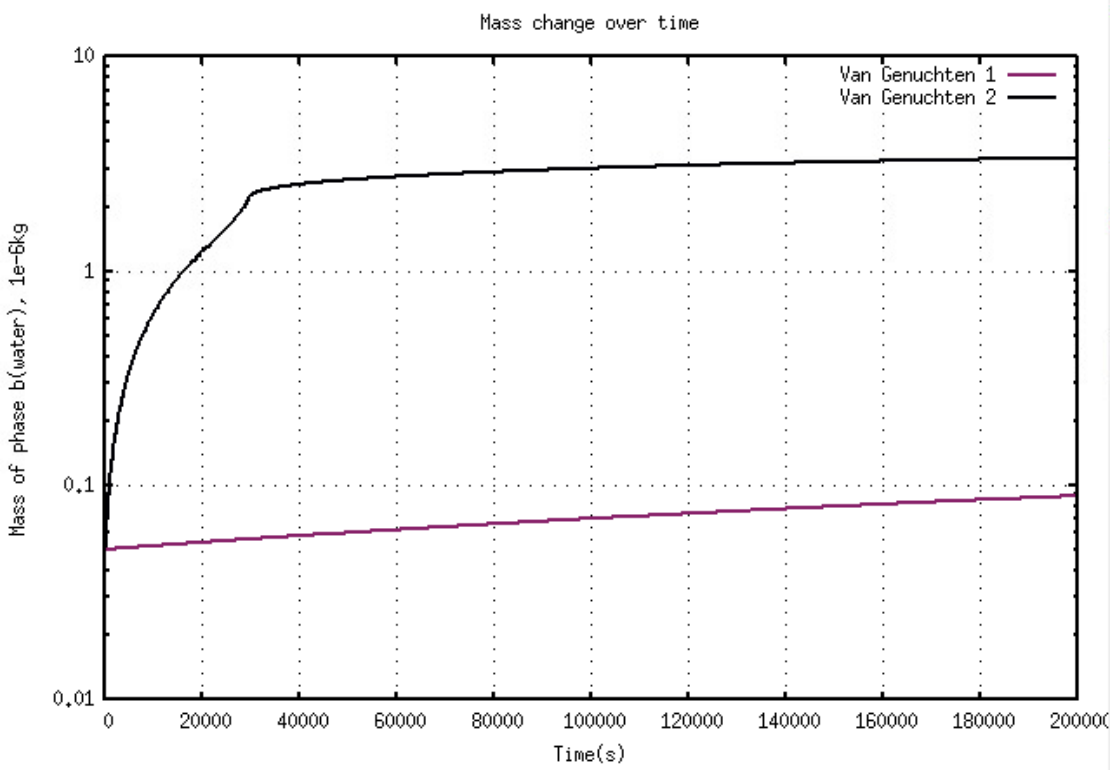

Figure 43 Mass change over time

The power coefficient of Van Genuchten model has quite large impact on saturation level and distribution. As it can be seen from the graphs, higher power coefficient, indicating higher permeability, leads to higher saturation level at the same time and less time consumption to reach equilibrium. The saturation distribution of both of two cases have similarities - small saturation gradient.

4.5.5 Relative permeability model_ Brooks and Corey model

The conditions are remained the same as the basic case. Although relative permeability model is Brooks and Corey model, the power coefficient would be investigated in order to understand how it influences Brooks and Corey model (Power coefficient m=2 and 3).

Table 9 Parameter study

Relative permeability model	Brooks and Corey 1	Brooks and Corey 2
Power coefficient	2	3
Pc0	100	100

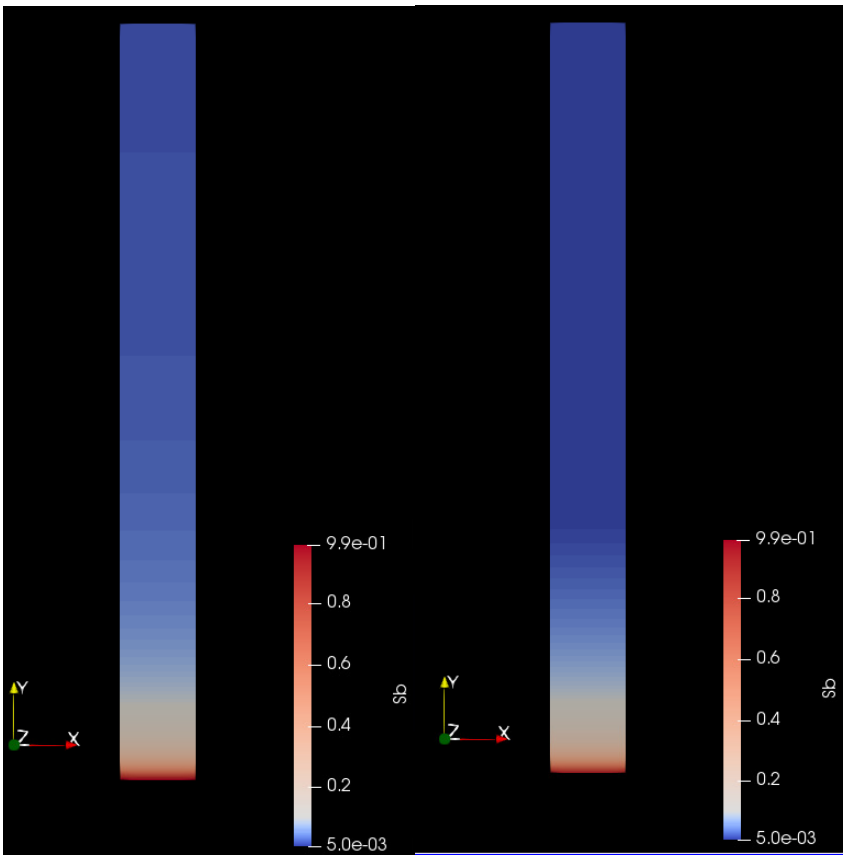

Figure 44 Brooks and Corey 1 and 2 respectively at 200,000s

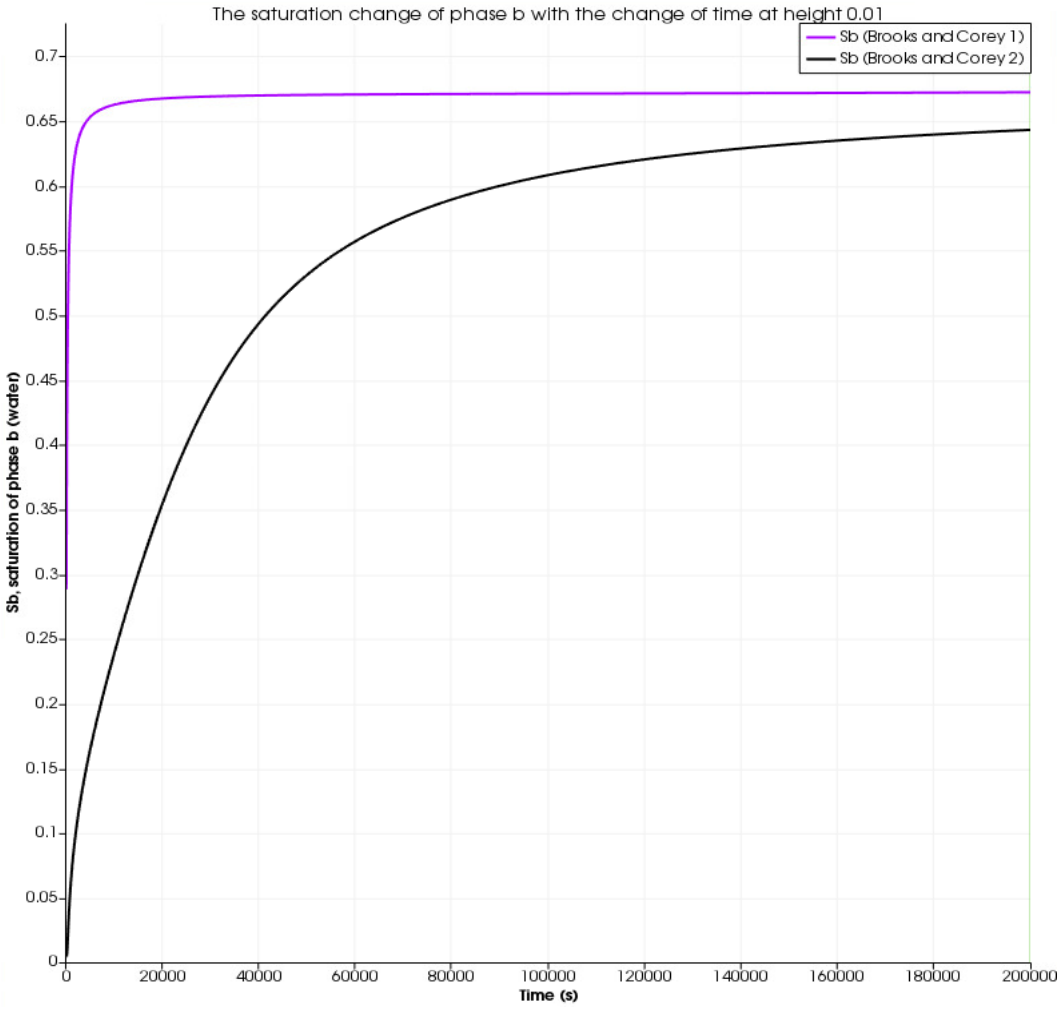

Figure 45 Saturation change over time

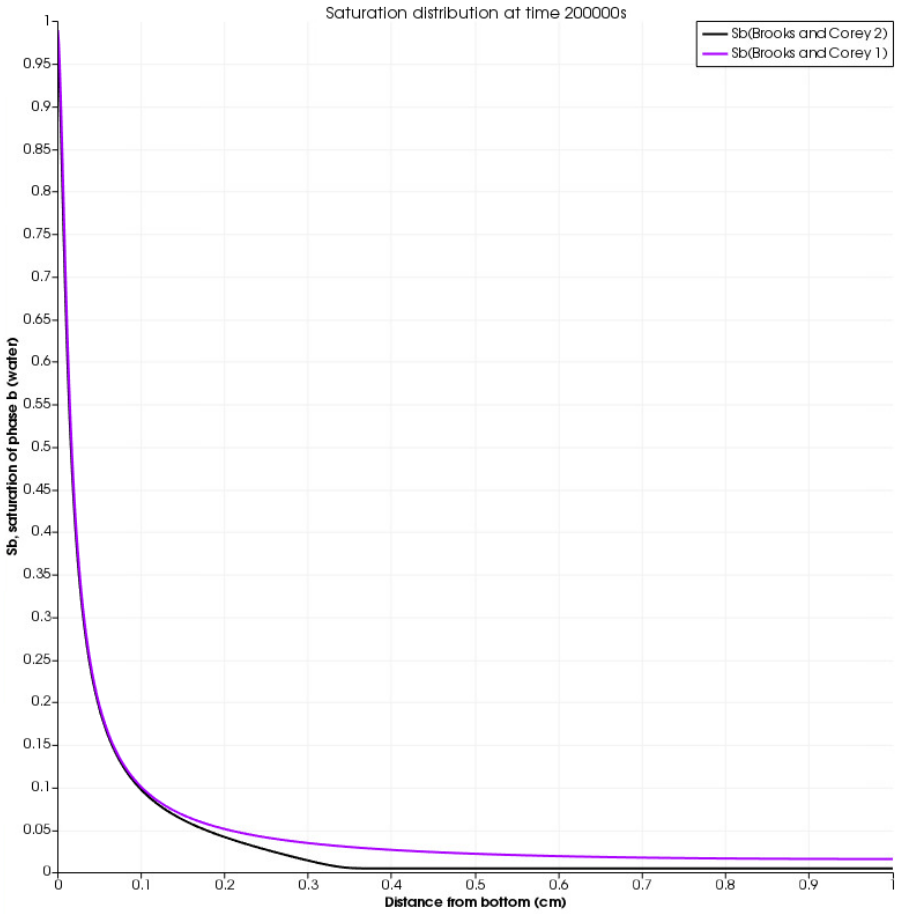

Figure 46 Saturation distribution at 200,000s

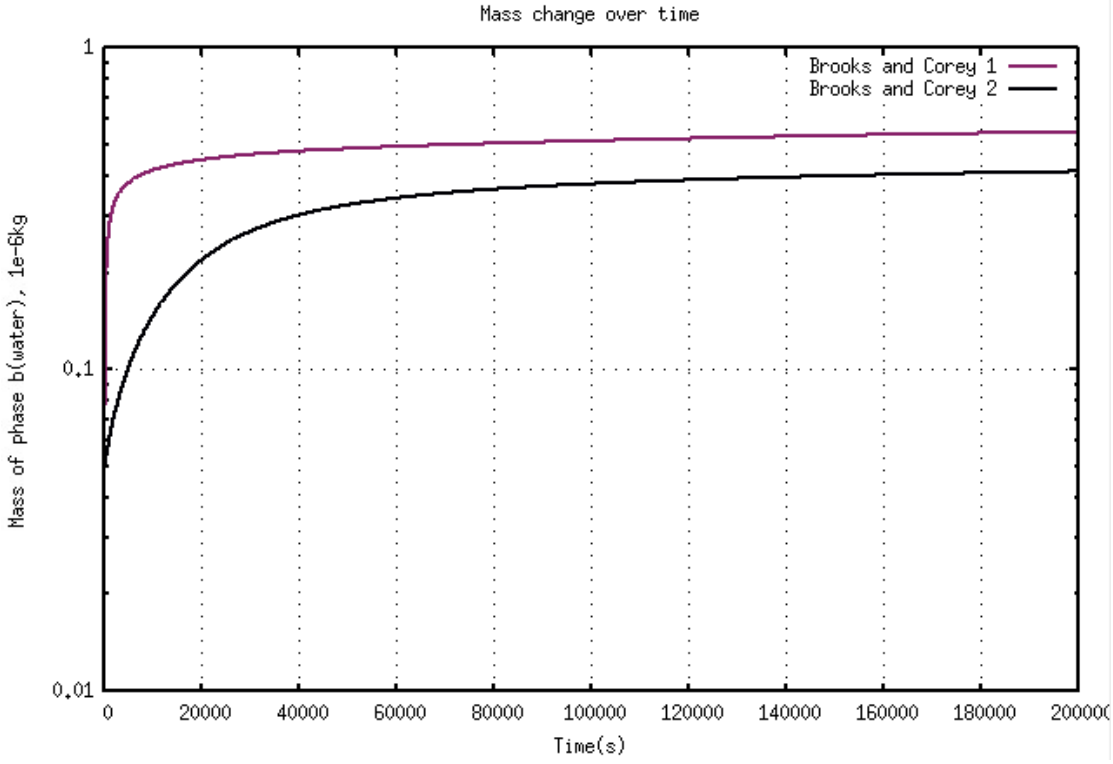

Figure 47 Mass change over time

The power coefficient of Brooks and Corey model affects saturation level and distribution quite much. It is shown that, lower power coefficient, indicating higher permeability, leads to higher saturation level at the same time and less time consumption to reach equilibrium. Both of two cases have large saturation gradient.

4.5.6 Summary

For capillary pressure model, linear model shows a sharp fluid front and takes less time to reach equilibrium. Linear model also has higher saturation level among other capillary pressure models. Van Genuchten model will be more sensitive to power coefficient of the model compared to other models. Brooks and Corey model is also sensitive to power coefficient.

Moreover, higher entry pressure can lead to higher saturation level at the same given time. Minimum and maximum saturation also have impact on the saturation level and distribution, however they are not evident compared to other parameters.

For relative permeability model, the impact of power coefficient in Van Genuchten model is quite large. The power coefficient of Brooks and Corey model influences the results as well.

5 Experiments:

Experiments are performed to validate the models and provide models with some referring parameters. Within the limited time and instruments, two parameters of materials are tested, which are porosity and permeability. The testing materials are denoted “material 1” and “material 2” and are typical absorbing materials used in medical dressings.

5.1 Introduction

Most absorbing materials have usually non-uniform structure, which makes it complicated to measure the pore size that varies quite much. Experiments are performed preferably in macro scale instead of micro scale, due to that modelling is based on Darcy scale (macro scale). Micro scale measurements require more advanced instruments and evaluating the results to find macro-scale parameters is not straightforward.

Several methods including direct method, optical method, imbibition method, mercury injection, gas expansion and density method, are available to measure porosity.

1. Direct method: Bulk volume of a sample is measured through approximately measuring length ($\boldsymbol{L}$), width ($\boldsymbol{W}$), height ($\boldsymbol{h}$). Then all the voids are destroyed to measure the volume of only the solids through compressing the material to a certain shape and measuring length ($\boldsymbol{L'}$), width ($\boldsymbol{W'}$), height ($\boldsymbol{h'}$). Calculating porosity through equation $\boldsymbol{\varepsilon = \frac{L' * W' * h'}{L * W * h}}$.
2. Optical method: By using optical instruments, the images of porous media can be taken to obtain the pore structure. Impregnating pores with some materials, such as plastic, is very necessary in order to make the structure visible. Due to irregular distribution of pore space, the porosity observed in images might vary a lot.
3. Imbibition method: The porous sample is immersed in a wetting fluid under vacuum (it can be partially vacuum through suction air by injectors). Weighting sample before ($\boldsymbol{m}$) and after imbibition ($\boldsymbol{m'}$) using weight instrument. Calculating pore volume by using fluid density ($\boldsymbol{\rho}$) and weight. Calculating porosity through equation $\boldsymbol{\varepsilon = \left[\frac{(m'-m)}{\rho}\right] / (L * W * h)}$.
4. Mercury injection method: The sample is immersed in mercury, because most materials are not wetted by mercury. High pressure need to be provided to ensure that mercury will enter pore space. It is the same principle as imbibition method but with different fluid.
5. Gas expansion method: Gas expansion method is to measure the effective porosity. The bulk volume is determined. Then a container enclosing a sample with known volume under known gas pressure is connected with evacuated container of known volume. Gas will expand into evacuated container and gas pressure decrease. Through pressure and bulk volume of the sample, porosity can be calculated.

6. Density methods: The bulk density ($\boldsymbol{\rho_B}$) of the sample and the density of the solids ($\boldsymbol{\rho_S}$) are determined in the sample. It can be possible to find the density of the solids (for example, fibers) through literatures. Calculating porosity through equation $\boldsymbol{\varepsilon = 1 - \frac{\rho_B}{\rho_S}}$.

A summary of porosity measurements is listed below (Dullien, 1992).

Table 10 A summary of porosity measurements

Experimental methods	Advantages	Disadvantages
Direct method	Easy performed, low cost	
Optical methods	Help understand the structure of the sample	Instruments required, porosities may differ significantly due to pore structure provided randomly
Imbibition method	Easy performed, cheap, possible to obtain best values of porosity	Sufficient care required, swelling might influence results
Mercury injection method	Easy performed, cheap, possible to obtain best values of porosity	High pressure needed, which may cause changes in the pore structure
Gas expansion method	Low cost	Not easy to control
Density method	Easy performed, cheap	Not accurate

Comparing all the methods and considering time and complexity, imbibition method and direct method are selected to determine porosity of material, which are simple and efficient to obtain results. Mercury injection method is also alternative of porous media measurement, which doesn't wet most materials. (Dullien, 1992)

Since some methods mentioned above are not difficult to perform, it can be better to perform different methods and compare the results in order to validate some values of porosity. Some data from literatures are also comparable.

Permeability is also regarded as an important property of materials to measure, which is determined by pore structure. In general, the value of permeability varies in different direction of porous medium that is composed of non-uniform structure, mentioned as anisotropy.

$$Q = (\frac{kA}{\mu})(\Delta p/L) \quad (5\text{-}1)$$

Which is defined based on Darcy's law and can be calculated in macroscopic aspect. The constant flow rate is injected into porous medium to fill in pore space and flow through it. To obtain approximate value of permeability, various flow rates or fluids should be used to repeat the experiments.

This experiment of permeability shown in the Figure 48 is simple to start with but not accurate enough for future development of materials, due to many errors analyzed later. Calibration is needed in such a case with known permeability of materials. Pressure difference between two faces of the sample is supposed to decrease gradually as flow progresses across the sample. The instrument needs calibration with samples of known properties, permeability and porosity to test its accuracy.

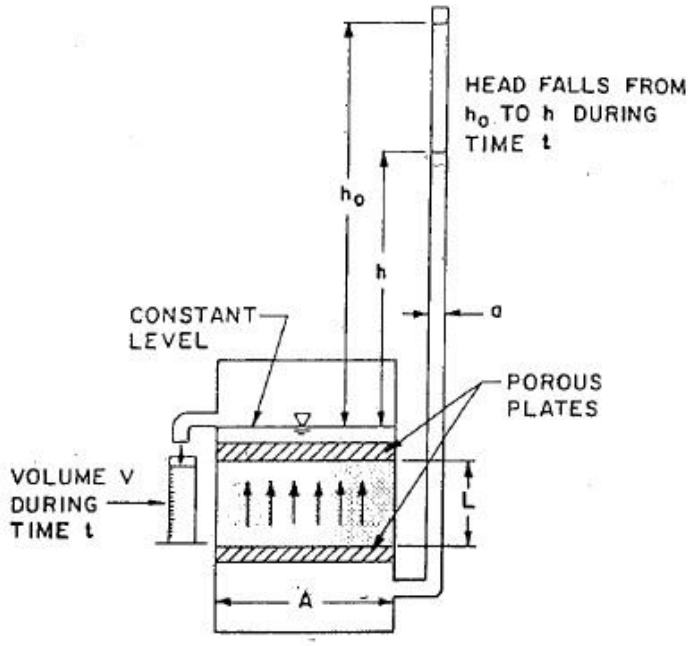

(Dullien, 1992)

Figure 48 Experiment of permeability

The permeability can be calculated below:

$$k = \left(\frac{aL\mu}{At\rho g}\right) ln(h_0/h_1) \quad (5\text{-}2)$$

This equation comes from the Darcy's equation and is formulated according to the experiment.

An alternative experiment method requires to use fabric and taking images of flow front, which is advanced and complex compared to simpler ones. (Di Fratta, C.,

Klunker, F., Trochu, F., & Ermanni, P., 2015)It can be utilized in the future. Pressure difference is measured through sensors, one being injection pressure and another front pressure during time t.

$$K_s = \frac{\mu \emptyset}{2\Delta p} \frac{(x_s - x_{in})^2}{t_s} \quad (5\text{-}3)$$

Where μ is fluid viscosity, $\emptyset$ is porosity, x_s, x_{in} are the positions of cavity sensor and inlet respectively.

The picture below shows the experiment.

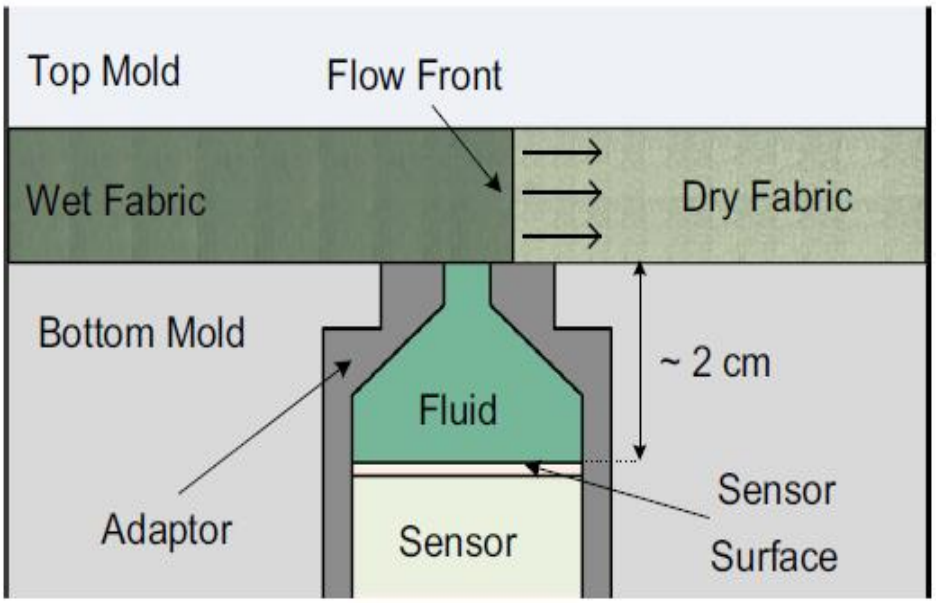

Figure 49 Experiment of permeability by measuring flow front

The permeability can be also described in micro scale as a function of radius of pore structure. (Nishiyama, N., & Yokoyama, T, 2017)

$$k = c\emptyset r^2 \quad (5\text{-}4)$$

Where r is radius of pore structure which are determined through different methods, c is the factor related to pore structure, $\emptyset$ is the porosity. It is described in a microscopic scale. This picture from literature illustrates the typical radius that is the smallest pore size when gas flows through and bubble appears.

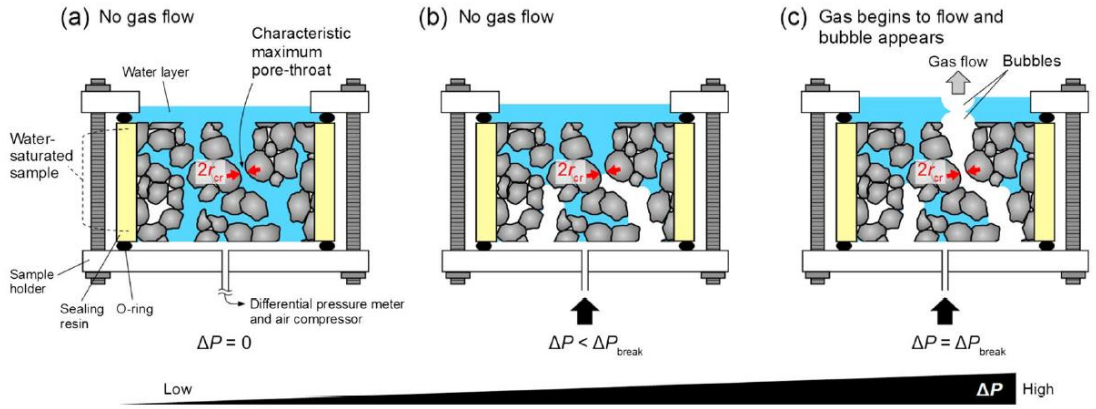

Figure 50 Permeability experiment by measuring radius

Air entry pressure, pore size and other parameters can be obtained by using this method.

Other parameters of materials need to be determined approximately through experiments, for instance, the minimum and maximum saturation of the material. In different models, including Brooks and Corey model, Van Genuchten model and so on, the parameters of each model are obtained through getting relationship between saturation and capillary pressure by experiments. Due to various materials, those models mentioned above might not be fitted. But according to experimental data, one can establish corresponding models for different materials.

More advanced instruments can improve the quality of experiments and reduce errors. There are some examples. Sensors are used to measure the pressure and flow rate. High speed camera is applied to record the process to improve understanding of absorption. X-ray and MRI are more likely to significantly improve the experiments, due to more accurate measurements.

MRI (magnetic resonance imaging) are mostly used in medical area, human bodies. The main principle of MRI is to create signals due to hydrogen atoms. MRI can create a large magnetic field, resulting in aligning of many free hydrogen nuclei with the direction of the magnetic field. To obtain an image of an object, the object is placed in a uniform magnetic field 0.7T (0.5-1.5 Tesla). The object's hydrogen nuclei align with the magnetic field and create a net magnetic moment. A radio-frequency (RF) pulse is applied perpendicular to magnetic field created by hydrogen nuclei. This pulse, with a frequency equal to the Larmor frequency, causes magnetic moment to tilt away from magnetic field. FID response signal can be obtained when RF signal is removed and the nuclei lose energy by emitting their own RF signal.

MRI could offer an opportunity to characterize the pore size distribution and the flow of the fluid within the pores.

5.2 Performing experiments

In the experiments, it will involve in porosity measurement, permeability measurement and some simple experiments to validate the models.

5.2.1 Porosity measurement

The porosity is tested by several simple measurements that mainly are direct method and imbibition method. Due to the characteristics of materials, both of material 1 and material 2 are swelling quite much in the experiments, which could affect the results of experiments. Comparing with different methods, advantages and disadvantages are discussed to provide approximate values from experiments.

Direct method is a simple method that the materials are cut into pieces and compressed (air will be compressed out as much as possible until it cannot be compressed more by human force). The initial volume was calculated through measuring different dimensions of different orientations by the Vernier caliper (mm), read by human eyes. The 10 ml measuring cylinder is used in the experiments to obtain the volume of compressed materials.

The results from direct method are shown in the table below, which is measured in dry condition. Each experiment was performed three times. The values shown in Table 11 have been multiplied by a constant in order to keep the properties of the material used confidential.

Table 11 The result of porosity using direct method

Materials		Volume before compression (cm^3)	Volume after compression (cm^3)	Average volume after compression	Porosity
Material 1	1	8	1,44	1,29	0,84
	2	8	1,26		
	3	8	1,17		
Material 2	1	18	4,68	4,68	0,74
	2	18	4,5		
	3	18	4,86		

The porosity of material 1 from experiments is in the range of the value given by literature (Gunashekar, S., Pillai, K., Church, B., & Abu-Zahra, N., 2015) .

Imbibition method is basically injecting water to materials until it is saturated which can be indicated by water coming out of materials. Considering about limited resources, it won't be performed in vacuum. The samples are cut into three different sizes 2cm×2cm, 4cm×4cm, 6cm×6cm and three samples for each size. The electronic scale (g) is to weigh materials when they are dry and fully saturated. The problem of this method is that the swelling of materials that could absorb more water results in unrealistic value above one. To be able to calculate the porosity, it is obtained through calculating the volume of materials after fully wetting, reflected by water coming out of materials that could cause an error, and the weight gained from the process of

injecting water. As the size of samples increases, the porosity calculated from each set of data went up a little bit due to increasing area of surface. It might stick more fluid on the surface which cannot be found by eyes that could cause variations. The values shown in Table 12 have been multiplied by a constant in order to keep the properties of the material used confidential.

Table 12 The result of porosity using imbibition method

Materials		Times	Dry weight (g)	Fully wet weight (g)	Weight of water (g)	Average volume of water (cm^3)	wetting Length (cm)	wetting width (cm)	wetting height (cm)	wetting volume (cm^3)	Volume fraction	Porosity
Material 1	size 1	1	0,014	0,261	0,247	0,261	1,26	1,26	0,20	0,323907648	0,804859	0,9018
		2	0,016	0,279	0,263							
		3	0,015	0,288	0,273							
	size 2	1	0,131	2,888	2,758	2,618	3,63	3,63	0,20	2,68088202	0,97647	
		2	0,122	2,705	2,582							
		3	0,114	2,628	2,514							
	size 3	1	0,304	6,941	6,637	6,525	5,89	5,89	0,20	7,061742538	0,923993	
		2	0,290	6,687	6,397							
		3	0,284	6,825	6,541							
Material 2	size 1	1	0,023	0,589	0,565	0,568	1,10	1,10	0,53	0,640965685	0,885539	0,8980
		2	0,027	0,611	0,584							
		3	0,025	0,579	0,554							
	size 2	1	0,198	4,924	4,726	4,761	3,14	3,14	0,53	5,269481847	0,903561	
		2	0,208	5,003	4,795							
		3	0,201	4,964	4,763							

	size 3	1	0,563	13,504	12,941	12,952	5,18	5,18	0,53	14,31398001	0,904864	
		2	0,563	13,801	13,237							
		3	0,544	13,222	12,678							

Comparing two methods, one in dry condition and another being wet, for material 1, the results are similar. As for material 2, those results differ a little bit, that the porosity measured by using direct method is much lower than the one measured by imbibition method. (It might be elastane of each material that caused the difference.)

5.2.2 Permeability measurement

The permeability measurement was performed based on Darcy law. A simple experiment was set up to get some approximate values. A sample was fitted into a measuring cylinder with two openings as shown below. The water will be provided from top open and flows through the samples in cylinder. Materials are cut or rolled to fit into cylinder and try to avoid any space between materials and cylinder. Due to the limitations of facilities, many factors could have an impact on the results, such as, the time to read the value and the size of those samples, the constriction of the measuring cylinder which can affect the swelling of materials. Although many changeable and unstable factors exist in experiments, the approaches are based on fundamental principles and obey the rules of experiments, leading to an acceptable range of values by comparing partial data with literatures. (Gun15)

This is the simple build-up instrument to measure permeability.

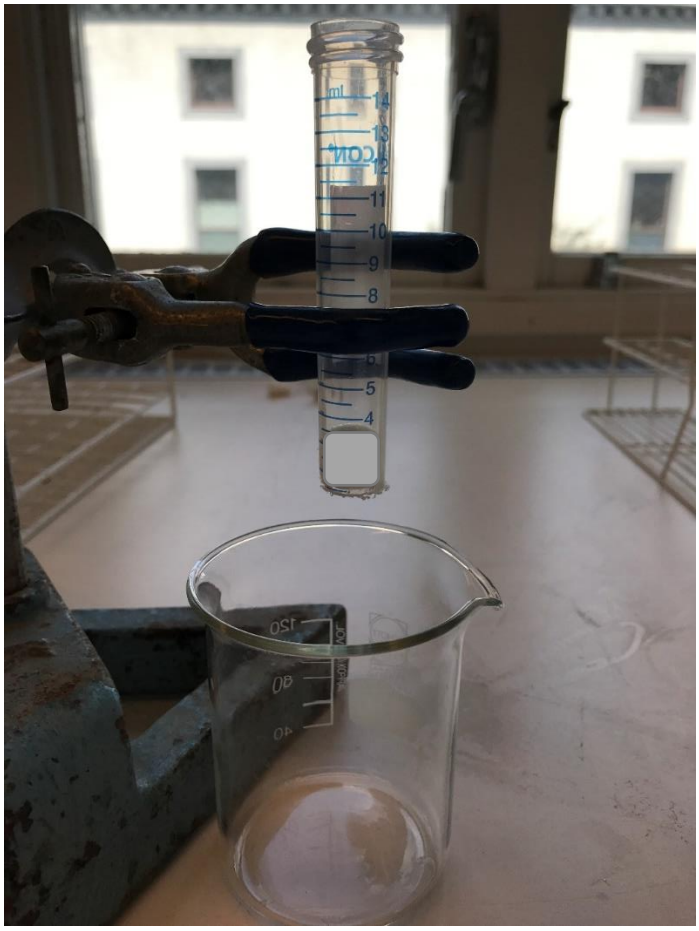

Figure 51 Instrument and set-up of permeability measurement

Figure 52 Different directions of measuring

Table 13 The result of permeability measurement

Materials	direction		Length of materials at flow direction (cm)	Start height (cm)	Record height (cm)	Time (s)	Permeability	average permeability
Material 1	x direction	1	2,79	7,5	4,5	61,41	2,35E-11	1,82E-11

		2	2,61	7,5	4,5	84,55	1,6E-11	
		3	3,24	7,5	4,5	109,47	1,53E-11	
	y direction	1	2,61	7,5	4,5	35,60	3,79E-11	2,79E-11
		2	2,43	7,5	4,5	48,95	2,56E-11	
		3	2,79	7,5	4,5	71,20	2,02E-11	
	z direction	1	0,81	7,5	1,85	8,37	1,38E-10	1,78E-10
		2	0,54	7,5	1,85	5,07	1,51E-10	
		3	0,72	7,5	1,85	4,17	2,46E-10	
Material 2	x direction	1	3,15	7,5	4,5	682,63	2,38E-12	3,42E-12
		2	4,14	7,5	5,2	433,43	3,53E-12	
		3	3,6	7,5	5,2	305,27	4,35E-12	
	y direction	1	3,6	7,5	5,2	549,13	2,42E-12	2,07E-12
		2	3,6	7,5	5,2	712,00	1,87E-12	
		3	3,51	7,5	5,2	677,29	1,91E-12	
	z direction	1	0,315	7,5	4,5	15,75	1,03E-11	1,54E-11
		2	0,315	7,5	4,5	10,43	1,56E-11	
		3	0,315	7,5	4,5	8,08	2,01E-11	

The values shown in Table 13 have been multiplied by a constant in order to keep the properties of the material used confidential.

As it can be seen from the table, the permeability of material 1 and material 2 is quite different. The permeability of material 1 is much larger than material 2.

The limitations of permeability measurement: 1. whether there is any leak between materials and measuring instrument is not certain; 2. the values are read by eyes, which may occur errors 3. The way of placing materials also has an impact on results; 4. The time is not so accurate, due to time differences when performing different parts; 5. Materials are seized manually, resulting in variations as well. 6. Materials are heterogeneous so that smaller samples might not be representative. 7. The material is

compressed to an unknown degree. All in all, the values obtained shall be regarded as estimates of the material properties.

5.2.3 Verification

There are several measurements that have been performed to verify the model. The simulation models are not built on specific kind of material, which could make results from simulations and results from experiments not corresponded. Therefore, the validation would not prove the exact same phenomenon, but how fluid behaves in the porous medium and observation of the fluid front.

Simple experiments were performed through putting materials into different directions. The material 1 and material 2 are put into water respectively and recorded in the process of absorbing water.

The process of material 1 is quite fast and fluid front is sharp. After a while, it reached equilibrium by eye observations.

The observation of material 2 is not easy due to its diffusive fluid front. It took longer time to achieve the same height as material 1. No equilibrium state was found for one hour, which means more diverse and advanced experiments can be performed to observe the equilibrium of material 2. The approximate fluid distribution is that the higher part is wet but appears low saturation and the bottom part has much higher saturation.

Since all the observations are based on transparent of fluid, they are not reliable enough but can input some information. For material 1, the symptoms of water absorption have some similarities with capillary pressure model – linear model, which both have sharp fluid front and transport fluid very fast. However, material 1 reached equilibrium very fast, linear model not. The difference among wetting part is not so apparent, relative permeability model – Brooks and Corey model could work in such a case. For material 2, capillary pressure model – Van Genuchten model might have some similarities to the process of absorption, which is diffusive fluid front.

Those models can be developed to fit into different absorbing materials. The way of fluid transport in the modelling is corresponding to the absorption experiments. It can be interpreted the behaviors of fluids from experiments and simulations are similar.

The simulation of material 1:

Table 14 Model selection of material 1

Relative permeability model	Brooks and Corey
Brooks and Corey coefficient	3
Capillary pressure model	Linear model
Entry pressure	0

Maximum capillary pressure	29620
Height (cm)	9.5

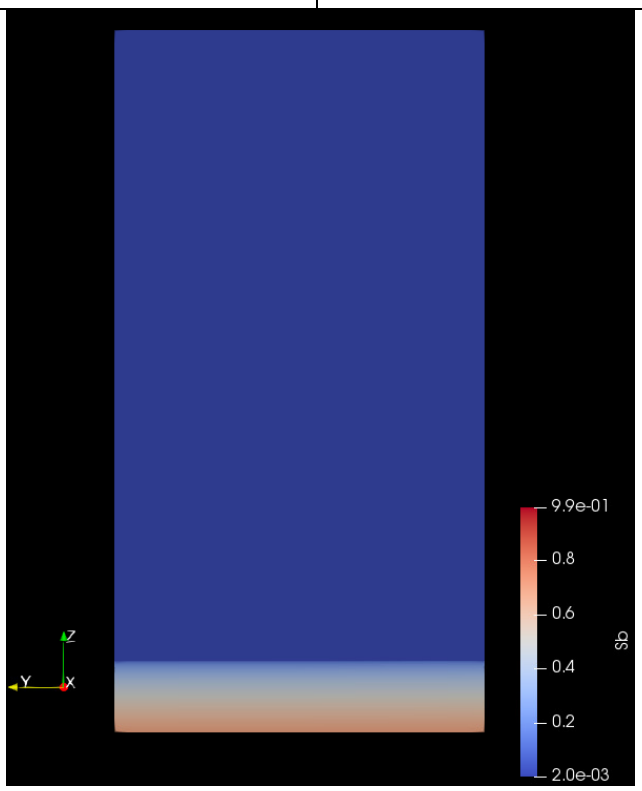

Figure 53 Material 1 at 5000s

It shows a sharp fluid front in the simulation, same as the experiment. But it took longer time to reach the same level as the experiment, which should be investigated in the future work.

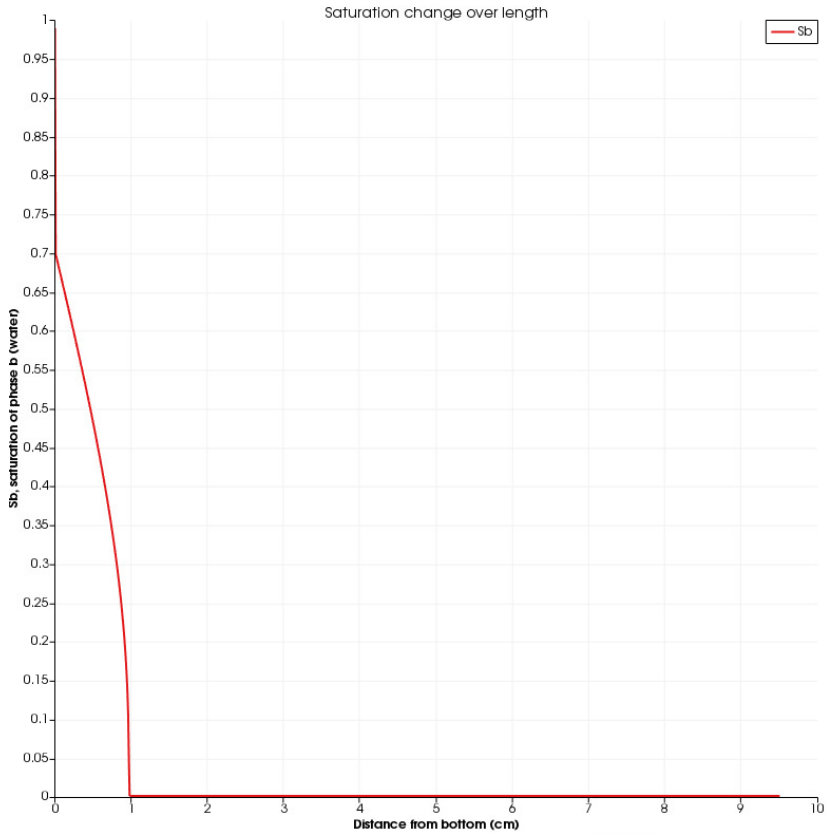

Figure 54 Saturation change over the length at 5000s

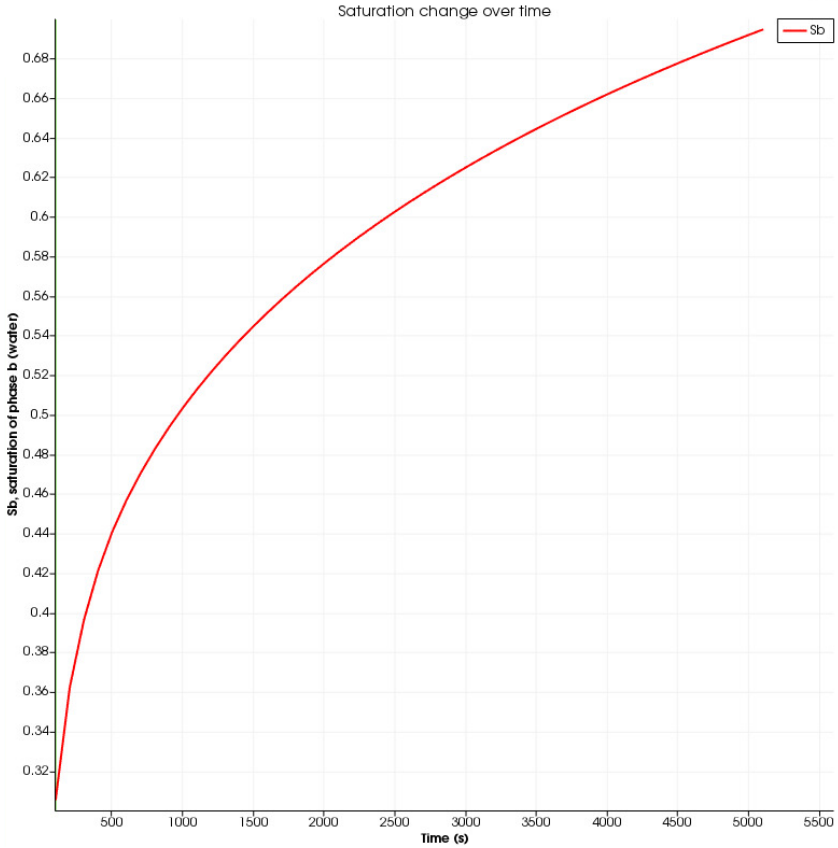

Figure 55 Saturation change over time at height 0.02

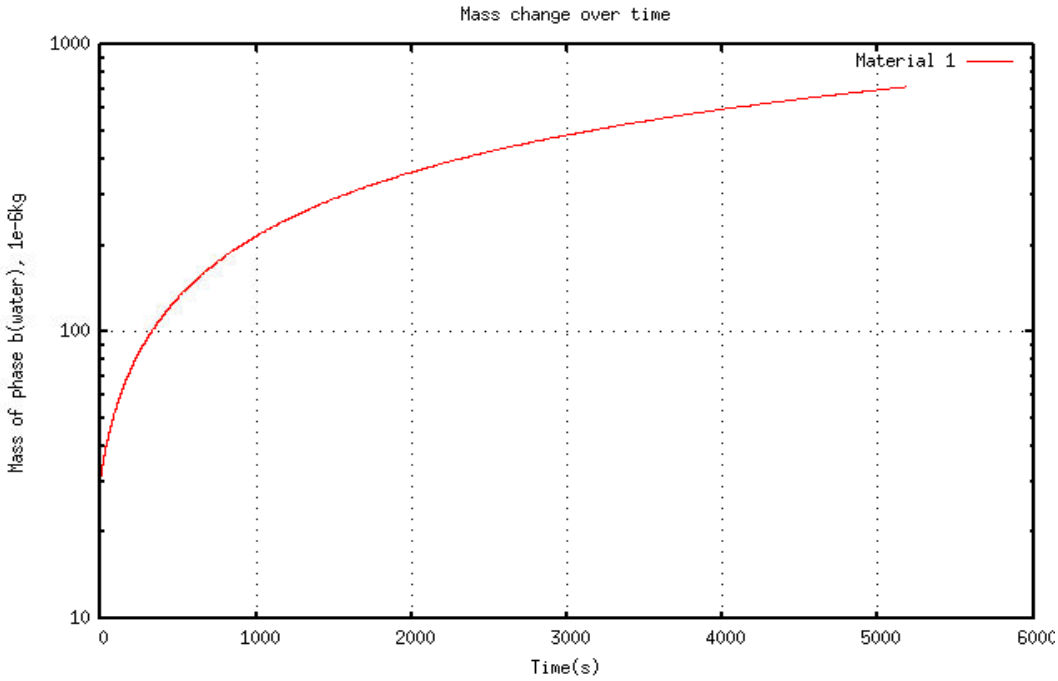

Figure 56 Mass change over time

The simulation of material 2:

Table 15 Model selection of material 2

Relative permeability model	Brooks and Corey
Brooks and corey coefficient	2
Capillary pressure model	Van Genuchten model
Entry pressure	1000
Van Genuchten coefficient	0.4
Height (cm)	8.8

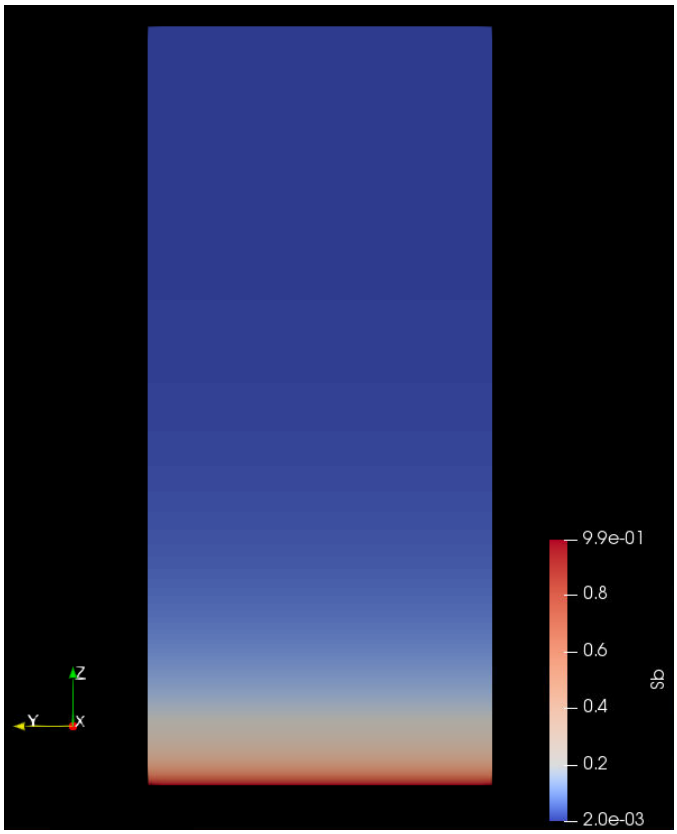

Figure 57 Material 2 at 13500s

It shows diffusive fluid front, same as the experiment. But it took much longer time to reach the same level as the experiment.

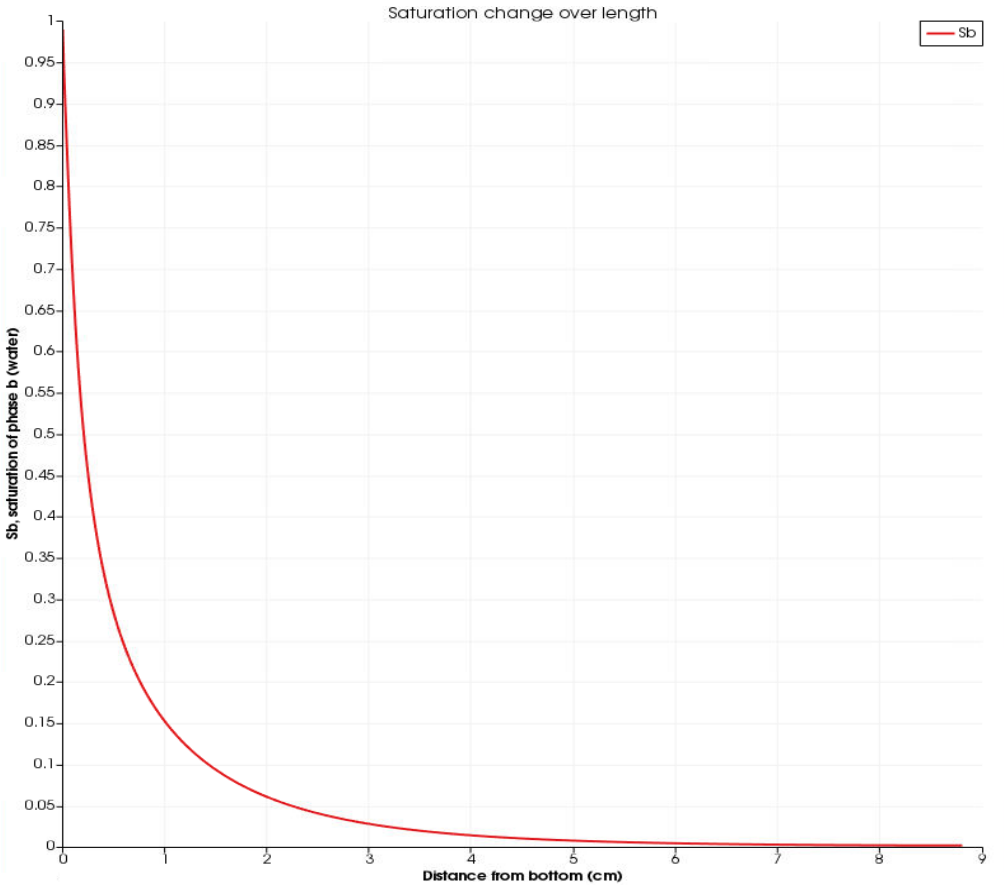

Figure 58 Saturation change over the length at 13500s

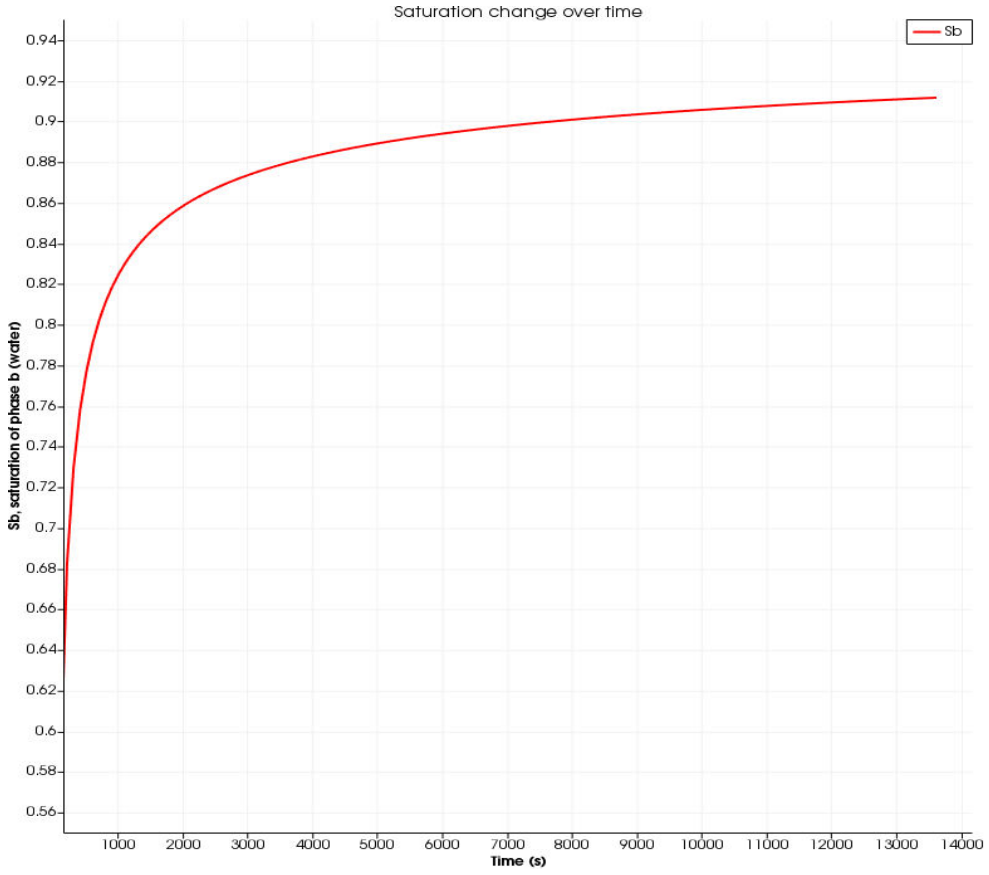

Figure 59 Saturation change over time

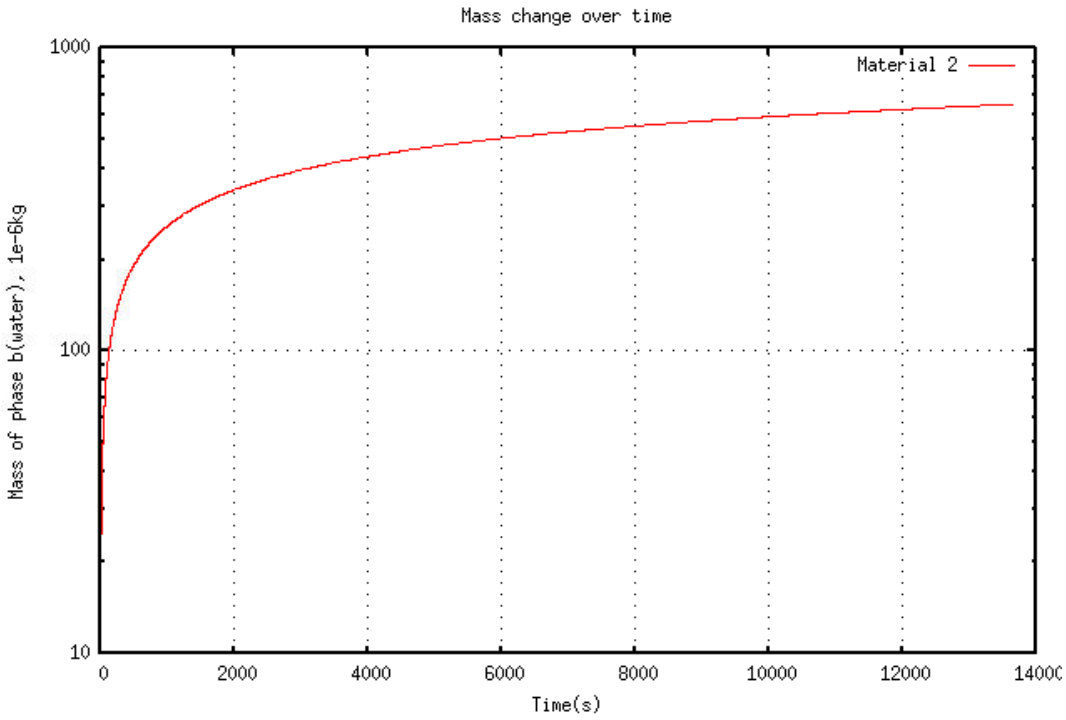

Figure 60 Mass change over time

6 Evaporation

Evaporation in porous materials is caused by the vapor pressure in the liquid and is limited by the vapor present in the gas phase, mass transfer, and heat transfer, or by a combination of the three. The temperature of wound is usually higher than the temperature of environment, indicating the influence of evaporation. Since evaporation modelling is complicated, a pre-study of evaporation has been performed.

Since there is no clear evidence showing when evaporation starts in the material, also depending on the relative humidity and temperature of the surrounding fluid, some assumptions are made to simplify the problem that evaporation doesn't occur in the material but the surface of material, and constant temperature in this case. In order to simplify it, the theory shown below is to be used at the boundary.

Capillary theory of drying - this theory is to explain the movement of moisture in the bed during surface drying. (Richardson, J. F., Harker, J. H., & Backhurst, J. R., 2002)

Drying of a granular material according to the capillary theory is illustrated in the equation (6.1). If a bed of uniform spheres, initially saturated, is to be surface dried in a current of air of constant temperature, velocity and humidity, then the rate of drying is

$$\frac{dw}{dt} = k_G A(P_{w0} - P_w) \tag{6-1}$$

Where P_{w0} is saturation partial pressure of water vapour at the wet bulb temperature of the air, P_w is the partial pressure of the water vapor in the air stream, A is the area for heat transfer or evaporation, k_G is mass transfer coefficient, w is total moisture.

Depending on different saturations at different parts of absorbing materials, the evaporation loss rate varies in porous mediums. Some pore spaces can limit molecular motion, which affects the evaporation rate. The evaporation rate inside a porous medium is lower than the case with open environment. (Pillai, 2009;2008)

Evaporation can be sufficiently slow so that thermal effects can be ignored in the simulation. The energy equation can be included in the future to investigate on temperature distribution.

It can be assumed that the effects of evaporation inside can be ignored when the samples have small thickness. A pre-study of evaporation loss can be done through some assumptions. Evaporation will only happen on the surface of samples and other parts remain the same.

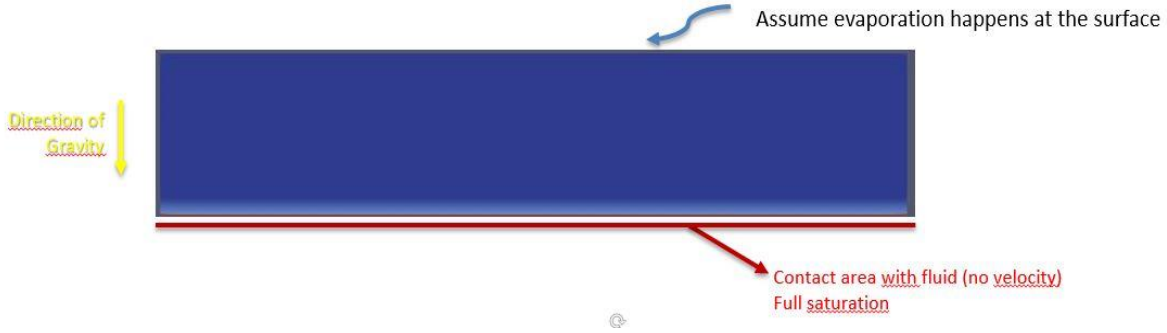

Figure 61 The simplified model of evaporation

According to engineering tool books (ToolBox, 2004), the evaporation of water surface at ambient temperature can be illustrated as

$$\dot{m} = D * A * (x_s - x) \tag{6-2}$$

Where **D** is the evaporation coefficiency obtained from experiments, $\boldsymbol{x_s}$ is maximum humidity ratio of saturated air at the same temperature as the water surface (kg water in kg dry air), $\boldsymbol{x}$ is humidity ratio air (kg water in kg dry air).

$$D = (25 + 19v) \tag{6-3}$$

Where v is the air velocity

$$A = A_t * \varepsilon * S_b \tag{6-4}$$

Where A is effective area, A_t is the total area of surface of porous medium

The area of water surface at the surface of porous medium is approximately determined by porosity and saturation. In order to implement the evaporation loss in OpenFoam, a simplified method is applied to change the boundary condition of velocity. The boundary condition of water's velocity is expressed as

$$u_a = \frac{D*A*(x_s - x)}{\rho_b * A_t} \tag{6-5}$$

It requires extension package of OpenFoam to implement boundary condition. Wellbore model is used to extract liquid from surface with value expression.

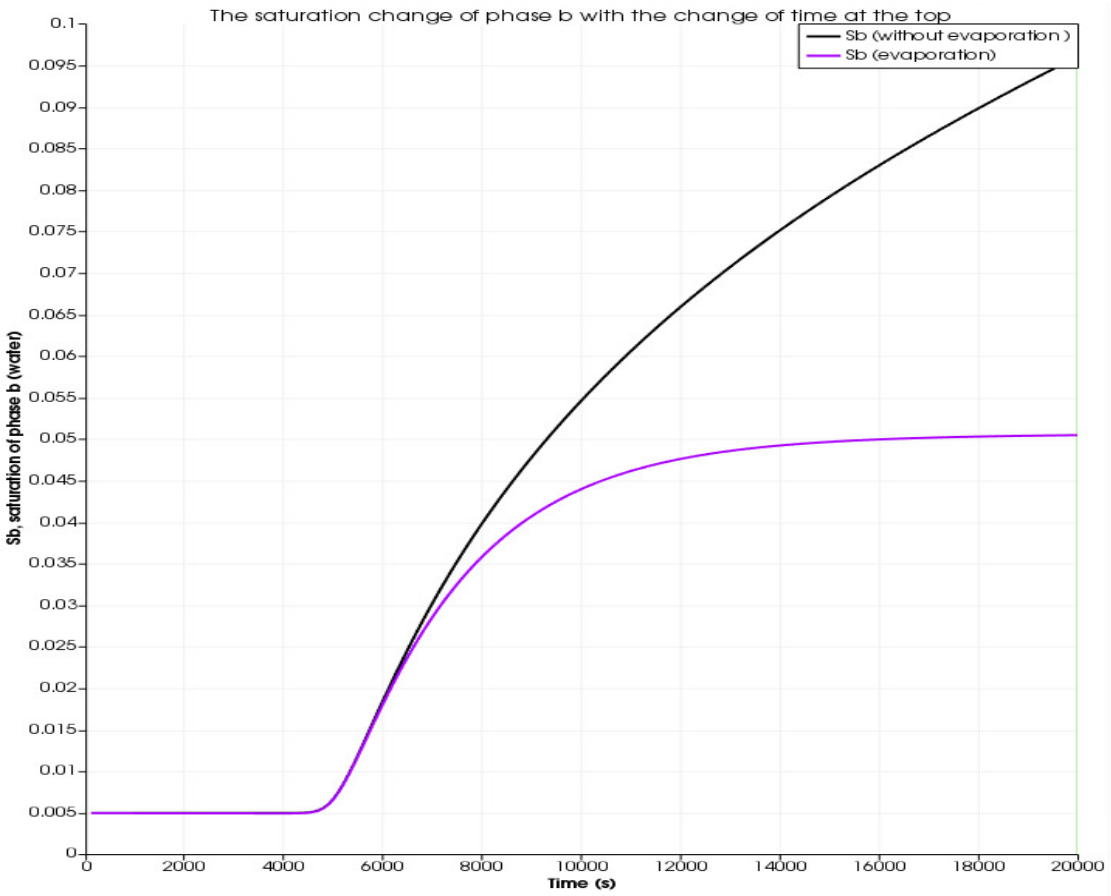

Figure 62 Saturation change over time

It is just a simple case which might not be enough for reality that temperature will be involved. But it can bring the thought how to model evaporation. As it is indicated in the model, the saturation on the surface will reach equilibrium at early stage.

7 Conclusion

The models of absorbing materials in OpenFoam were investigated with different capillary pressure models, relative permeability models, the effects of gravity in different directions and comparison between anisotropic and isotropic materials. Some experiments were performed to obtain porosity and permeability. The method was validated by comparing CFD simulation and experiments. A simplified model of evaporation was implemented in the model.

The qualitative results of simulation give a view of models and parameters. The gravity, capillary forces and anisotropy act in the simulations, and the behavior is intuitively correct. Capillary pressure models, such as linear model, Brooks and Corey model, and Van Genuchten model, were studied. Linear model results in sharp fluid front and fast fluid transport. Brooks and Corey model and Van Genuchten model are inclined to have diffusive fluid front and fast fluid transport at the beginning. The gradient of diffusive fluid front is decided by power coefficients of models. Relative permeability models, including Brooks and Corey model and Van Genuchten model, show the change of relative permeability as a function of saturation. In Brooks and Corey model, the relative permeability of two phases is symmetric. In Van Genuchten model, the relative permeability of phase a (gas phase) decreases rapidly with phase b (liquid phase) saturation, whereas the one of phase b (liquid phase) increases almost proportionally.

The boundary conditions were investigated. The boundary condition of the top saturation of water can influence the distribution of saturation and the equilibrium.

The investigation of different parameters is done. Higher entry pressure and lower power coefficient of Brooks and Corey model (capillary pressure model) could increase the saturation level. The increase of minimum saturation could enhance the saturation level. The decrease of maximum saturation could reduce the saturation level and the time to reach equilibrium. The linear model (capillary pressure model) could be influenced by maximum capillary pressure higher value of which can increase saturation level.

When it comes to relative permeability model, higher power coefficient of Van Genuchten model and lower power coefficient of Brooks and Corey model will lead to higher permeability, meaning higher saturation level.

For isotropy, only two methods of calculating courant number are stable and reliable with simple set-up. For anisotropy, only one is stable and durable with simple set-up.

Todd, as one of methods to calculate courant number will be efficient in simple cases only involving simple mesh and boundary conditions. Coat is used most often in the following simulations, which is durable compared to other methods to calculate adjustable time step.

Moreover, the quantitative results depend on input data. Only approximate values are available, due to the limited scope of the present work. The properties of absorbing materials, for instance, porosity and permeability, are obtained from experiments approximately. Porosity measurement: Material 1and Material 2 have reasonable

results. Permeability measurement: Different directions have different permeability. Verification is to show the ways of fluid transport behave similar in experiments and simulations. However, they are basic simplified model, which are difficult to get the same results from experiments and simulations.

Evaporation modelling is recommended for further investigation. A pre-study is done by implementing boundary condition of top extraction whose results illustrate the effects of evaporation of surface.

8 Limitations and future investigation:

The modelling and experimental results in the present work has resulted in several suggestions for further research.

The continuum models have an obvious obstacle concerning averaging. The discrete models don't have those limitations, for example, Lattice, but requiring computational effort. In the further research, the discrete models can be developed to adapt to porous medium. More precise experiments should be performed.

Multilayer simulation of absorbing materials can be further researched based on the one-layer simulation made in this work.

The energy equation should be implemented to implement evaporation model by introducing the temperature distribution in the fluids, the porous material, and possibly the human skin.

Liquid should be changed to different liquids to test the model and study the influence of the liquid in the model in order to develop it, such as plasma.

Swelling cannot be neglected in reality, which makes it necessary to study on swelling. Not only do the materials using in the experiments swell quite much, but most of absorbing materials are capable of swelling to absorb more liquid. It could be possible if a simple scaling model could be developed to account for swelling.

9 References

Clark, G. L., & Liu, C. H. (1957). Quantitative Determination of Porosity by X-Ray Absorption. *Analytical Chemistry*, 29(10), 1539-1541.

Di Fratta, C., Klunker, F., Trochu, F., & Ermanni, P. (2015). Characterization of textile permeability as a function of fiber volume content with a single unidirectional injection experiment. *Composites Part A: Applied Science and Manufacturing*, 77, 238-247.

Dullien, F. A. (1992). *Porous media: Fluid transport and pore structure (2nd ed.).* San Diego: Academic Press.

Gunashekar, S., Pillai, K., Church, B., & Abu-Zahra, N. (2015). Liquid flow in polyurethane foams for filtration applications: a study on their characterization and permeability estimation. *Journal Of Porous Materials*, 22(3), 749.

Horgue, P., Soulaine, C., Franc, J., Guibert, R., & Debenest, G. (2015). An open-source toolbox for multiphase flow in porous media. *Computer Physics Communications*, 187, 217-226.

Kissa, E. (1996). Wetting and wicking. *Textile Research Journal*, 66(10), 660-668.

LANDERYOU, M. E. (2005). Infiltration into inclined fibrous sheets. *Journal of Fluid Mechanics*, 529, 173-193.

Landeryou, M., Eames, I., Frampton, A., & Cottenden, A. (2004). Modelling strategies for liquid spreading in medical absorbents. *International Journal of Clothing Science and Technology*, 16(1/2), 163-172.

Leverett, M. (1941). Capillary behavior in porous solids. *Transactions of the AIME*, 142(01), 152-169.

Nishiyama, N., & Yokoyama, T. (2017). Permeability of porous media: Role of the critical pore size. *Journal of Geophysical Research: Solid Earth*, 122(9), 6955-6971.

Pillai, K. P. (2009;2008). *A study on slow evaporation of liquids in a dual-porosity porous medium using square network model.* M: International Journal of Heat and Mass Transfer,.

Sahimi, M. (2011). *Flow and transport in porous media and fractured rock: from classical methods to modern approaches.* John Wiley & Sons.

Skjaeveland, S.M., Siqveland, L.M., Kjosavik, A., Hammervold Thomas,W.L., Virnovsky, G.A. (2000). Capillary Pressure Correlation for Mixed-Wet Reservoirs. *SPE Reservoir Eval. & Eng.*, 3. (1).

Szymkiewicz, A., & SpringerLink (e-book collection). (2013). *Modelling water flow in unsaturated porous media: Accounting for nonlinear permeability and material heterogeneity.* New York: Springer.

10 Appendix

The codes of anisotropyfoam in coatsNo.H

```
if(activateCapillarity)
{
    volTensorField CFLCoatsnew(
    "CFLCoatsnew",
    (runTime.deltaT()/eps)*2*mag(pcModel->dpcdS())*fvc::surfaceSum(Kf*mesh.magSf()/mag(mesh.delta()))*(kra*krb/(mub*kra+mua*krb))
);
    CFLCoats.ref() += CFLCoatsnew/mesh.V();
}
```

The boundary conditions of point source:

```
/*--------------------------------*- C++ -*----------------------------------*\
| =========                 |                                                 |
| \\      /  F ield         | OpenFOAM: The Open Source CFD Toolbox           |
|  \\    /   O peration     | Version:  4.1                                   |
|   \\  /    A nd           | Web:      www.OpenFOAM.org                      |
|    \\/     M anipulation  |                                                 |
\*---------------------------------------------------------------------------*/
FoamFile
{
    version     2.0;
    format      ascii;
    class       volScalarField;
    location    "0";
    object      K;
}
// * * * * * * * * * * * * * * * * * * * * * * * * * * * * * * * * * * * * * * * //

dimensions      [0  2  0 0 0 0 0];

internalField   uniform 1e-10;

boundaryField
{
    Inlet
    {
        type            zeroGradient;
    }
    Outlet
    {
        type            zeroGradient;
    }

    FrontAndBack
    {
        type            empty;
    }
    Outlet_wall
    {
        type            zeroGradient;
    }
}


// ************************************************************************* //
```

```
/*--------------------------------*- C++ -*----------------------------------*\
| =========                 |                                                 |
| \\      /  F ield         | OpenFOAM: The Open Source CFD Toolbox           |
|  \\    /   O peration     | Version:  4.1                                   |
|   \\  /    A nd           | Web:      www.OpenFOAM.com                      |
|    \\/     M anipulation  |                                                 |
\*---------------------------------------------------------------------------*/
FoamFile
{
    version     2.0;
    format      ascii;
    class       volScalarField;
    object      p;
}
// * * * * * * * * * * * * * * * * * * * * * * * * * * * * * * * * * * * * * * * //

dimensions      [1 -1 -2 0 0 0 0];

internalField   uniform 0.0;

boundaryField
{
    Outlet_wall
    {
        type            darcyGradPressure;
        value           uniform 0;
    }

    Inlet
    {
        type            fixedValue;
        value           uniform 0;
    }

    FrontAndBack
    {
        type            empty;
    }
    Outlet
    {
        type            zeroGradient;
    }

}

// ************************************************************************* //
```

```
/*--------------------------------*- C++ -*----------------------------------*\
| =========                 |                                                 |
| \\      /  F ield         | OpenFOAM: The Open Source CFD Toolbox           |
|  \\    /   O peration     | Version:  4.1                                   |
|   \\  /    A nd           | Web:      www.OpenFOAM.org                      |
|    \\/     M anipulation  |                                                 |
\*---------------------------------------------------------------------------*/
FoamFile
{
    version     2.0;
    format      ascii;
    class       volScalarField;
    location    "0";
    object      Sb;
}
// * * * * * * * * * * * * * * * * * * * * * * * * * * * * * * * * * * * * * * * * * * * * //

dimensions      [0 0 0 0 0 0 0];

internalField   uniform 2e-4;

boundaryField
{
    Inlet
    {
        type            fixedValue;
        value           uniform 0.005;
    }
    Outlet
    {
        type            zeroGradient;
    }
    FrontAndBack
    {
        type            empty;
    }
    Outlet_wall
    {
        type            fixedValue;
        value           uniform 0.99;
    }
}


// ************************************************************************* //
```

```
/*--------------------------------*- C++ -*----------------------------------*\
| =========                 |                                                 |
| \\      /  F ield         | OpenFOAM: The Open Source CFD Toolbox           |
|  \\    /   O peration     | Version:  4.1                                   |
|   \\  /    A nd           | Web:      www.OpenFOAM.com                      |
|    \\/     M anipulation  |                                                 |
\*---------------------------------------------------------------------------*/
FoamFile
{
    version     2.0;
    format      ascii;
    class       volVectorField;
    location    "0";
    object      Ua;
}
// * * * * * * * * * * * * * * * * * * * * * * * * * * * * * * * * * * * * * * * * * * * * //

dimensions      [0 1 -1 0 0 0 0];

internalField   uniform (0 0 0);

boundaryField
{
    Outlet
    {
        type            fixedValue;
        value           uniform (0 0 0);
    }
    Inlet
    {
        type            zeroGradient;
    }

    FrontAndBack
    {
        type            empty;
    }
    Outlet_wall
    {
        type            zeroGradient;
    }
}


// ************************************************************************* //
```

```
/*--------------------------------*- C++ -*----------------------------------*\
| =========                 |                                                 |
| \\      /  F ield         | OpenFOAM: The Open Source CFD Toolbox           |
|  \\    /   O peration     | Version:  5.x-version-5.0                       |
|   \\  /    A nd           | Web:      www.OpenFOAM.org                      |
|    \\/     M anipulation  |                                                 |
\*---------------------------------------------------------------------------*/
FoamFile
{
    version     2.0;
    format      ascii;
    class       volScalarField;
    location    "0";
    object      Winj;
}
// * * * * * * * * * * * * * * * * * * * * * * * * * * * * * * * * * * * * * * * * * * * * //

dimensions      [0 0 0 0 0 0 0];

internalField   uniform 0;

boundaryField
{
    FrontAndBack
    {
        type            empty;
    }
    Inlet
    {
        type            zeroGradient;
    }
    Outlet
    {
        type            fixedValue;
        value           uniform 0;
    }
    Outlet_wall
    {
        type            zeroGradient;
    }
}


// ************************************************************************* //
```

```
/*--------------------------------*- C++ -*----------------------------------*\
| =========                 |                                                 |
| \\      /  F ield         | OpenFOAM: The Open Source CFD Toolbox           |
|  \\    /   O peration     | Version:  5.x-version-5.0                       |
|   \\  /    A nd           | Web:      www.OpenFOAM.org                      |
|    \\/     M anipulation  |                                                 |
\*---------------------------------------------------------------------------*/
FoamFile
{
    version     2.0;
    format      ascii;
    class       volScalarField;
    location    "0";
    object      Winj;
}
// * * * * * * * * * * * * * * * * * * * * * * * * * * * * * * * * * * * * * * * * //

dimensions      [0 0 0 0 0 0 0];

internalField   uniform 0;

boundaryField
{
    FrontAndBack
    {
        type            empty;
    }
    Inlet
    {
        type            zeroGradient;
    }
    Outlet
    {
        type            fixedValue;
        value           uniform 0;
    }
    Outlet_wall
    {
        type            zeroGradient;
    }
}


// ************************************************************************* //
```

```
/*--------------------------------*- C++ -*----------------------------------*\
| =========                 |                                                 |
| \\      /  F ield         | OpenFOAM: The Open Source CFD Toolbox           |
|  \\    /   O peration     | Version:  5.x-version-5.0                       |
|   \\  /    A nd           | Web:      www.OpenFOAM.org                      |
|    \\/     M anipulation  |                                                 |
\*---------------------------------------------------------------------------*/
FoamFile
{
    version     2.0;
    format      ascii;
    class       volScalarField;
    location    "0";
    object      Wext;
}
// * * * * * * * * * * * * * * * * * * * * * * * * * * * * * * * * * * * * * * * * //

dimensions      [0 0 0 0 0 0 0];

internalField   uniform 0;

boundaryField
{
    FrontAndBack
    {
        type            empty;
    }
    Inlet
    {
        type            zeroGradient;
    }
    Outlet
    {
        type            fixedValue;
        value           uniform 0;
    }
    Outlet_wall
    {
        type            zeroGradient;
    }
}


// ************************************************************************* //
```

The boundary condition of evaporation:

```
/*--------------------------------*- C++ -*----------------------------------*\
| =========                 |                                                 |
| \\      /  F ield         | OpenFOAM: The Open Source CFD Toolbox           |
|  \\    /   O peration     | Version:  5.x-version-5.0                       |
|   \\  /    A nd           | Web:      www.OpenFOAM.org                      |
|    \\/     M anipulation  |                                                 |
\*---------------------------------------------------------------------------*/
FoamFile
{
    version     2.0;
    format      ascii;
    class       volScalarField;
    location    "0";
    object      Wext;
}
// * * * * * * * * * * * * * * * * * * * * * * * * * * * * * * * * * * * * * * * * * * * * //

dimensions      [0 0 0 0 0 0 0];

internalField   uniform 0;

boundaryField
{
    FrontAndBack
    {
        type            empty;
    }
    Outlet
    {
        type            fixedValue;
        value           uniform 0;
    }
    Inlet
    {
        type            groovyBC;
        refValue        uniform 0;
        refGradient     uniform 0;
        valueFraction   uniform 1;
        value           uniform 0;
        valueExpression "(25+19*0.25)*(0.015-0.004)/(3600*rhob)*eps*a";
        gradientExpression "0";
        fractionExpression "1";
        evaluateDuringConstruction 0;
        variables       "a{Inlet}=vector(0,0,Sb);";
        timelines       (
);
        lookuptables    (
);
        lookuptables2D  (
);
    }
}
```